

1970

The isothermal transformation of austenite at temperatures near Ms.

Robert H. Edwards
Wollongong University College

Follow this and additional works at: <https://ro.uow.edu.au/theses>

University of Wollongong

Copyright Warning

You may print or download ONE copy of this document for the purpose of your own research or study. The University does not authorise you to copy, communicate or otherwise make available electronically to any other person any copyright material contained on this site.

You are reminded of the following: This work is copyright. Apart from any use permitted under the Copyright Act 1968, no part of this work may be reproduced by any process, nor may any other exclusive right be exercised, without the permission of the author. Copyright owners are entitled to take legal action against persons who infringe their copyright. A reproduction of material that is protected by copyright may be a copyright infringement. A court may impose penalties and award damages in relation to offences and infringements relating to copyright material.

Higher penalties may apply, and higher damages may be awarded, for offences and infringements involving the conversion of material into digital or electronic form.

Unless otherwise indicated, the views expressed in this thesis are those of the author and do not necessarily represent the views of the University of Wollongong.

Recommended Citation

Edwards, Robert H., The isothermal transformation of austenite at temperatures near Ms., thesis, , University of Wollongong, 1970. <https://ro.uow.edu.au/theses/3008>

NOTE

This online version of the thesis may have different page formatting and pagination from the paper copy held in the University of Wollongong Library.

UNIVERSITY OF WOLLONGONG

COPYRIGHT WARNING

You may print or download ONE copy of this document for the purpose of your own research or study. The University does not authorise you to copy, communicate or otherwise make available electronically to any other person any copyright material contained on this site. You are reminded of the following:

Copyright owners are entitled to take legal action against persons who infringe their copyright. A reproduction of material that is protected by copyright may be a copyright infringement. A court may impose penalties and award damages in relation to offences and infringements relating to copyright material. Higher penalties may apply, and higher damages may be awarded, for offences and infringements involving the conversion of material into digital or electronic form.

UNIVERSITY OF NEW SOUTH WALES
WOLLONGONG UNIVERSITY COLLEGE
DEPARTMENT OF METALLURGY

THE ISOTHERMAL TRANSFORMATION OF AUSTENITE
AT TEMPERATURES NEAR M_s .

A THESIS SUBMITTED FOR THE DEGREE OF
MASTER OF SCIENCE

by

Robert H. Edwards, BSc. (Tech).

July 1970

ACKNOWLEDGEMENTS

The author wishes to thank Prof. G. Brinson for use of the laboratory facilities and Dr. N. Kennon for invaluable help and guidance in the preparation of this thesis. The author also wishes to thank Dr. P. McDougall for suggestion of techniques. Gratitude is extended to the Wiltshire File Company for supplying the steel used in the experimental work and to Australian Iron and Steel Pty. Ltd., for carrying out the analysis of the steel and for the use of the electron microscope.

Robert H. Edwards

SUMMARY

The investigation described in this thesis is concerned with the identification of the products of isothermal transformation of austenite containing 1.44% C, at temperatures just above and just below the M_s temperature, and determination of the isothermal transformation diagram for this range of temperatures.

In part A of the thesis, the literature relevant to the martensite and lowerbainite transformations is reviewed, with particular emphasis being placed on those features of each transformation which may possibly be used to identify the product. It is concluded that habit plane measurements offer the most suitable experimental means for identification of the products. In part B the experimental techniques of quantitative metallography, for habit plane measurements, and optical and electron microscopy, for study of the morphology and internal inhomogeneities of the products, are described.

It is demonstrated that austenite transforms isothermally to two different products, at temperatures both above and below M_s , and that the results of habit plane measurements enable unequivocal identification of the products as isothermal martensite and lower bainite.

It is further shown that the observed morphological features of the products are consistent with this identification. The identification of the products and the results of the kinetic studies of the transformations then provides a detailed specification of the isothermal transformation diagram for the range of temperatures examined.

TABLE OF CONTENTS

<u>PART A</u>	<u>LITERATURE SURVEY</u>	<u>PAGE</u>
1	INTRODUCTION	1
2	THE SUBCRITICAL TRANSFORMATION OF AUSTENITE	3
3	THE MARTENSITE TRANSFORMATION	6
3.1	Morphology of Martensite	6
3.2	Transformation Kinetics	11
3.3	Crystallography	13
3.31	Crystallographic Properties	13
3.32	Crystallographic Theory	16
3.4	Nucleation and Transformation Mechanism	19
3.5	The Isothermal Transformation	25
3.51	Transformation Kinetics	26
3.52	Effect of Austenite Grain Size	28
3.53	Effect of Composition	29
3.6	Thermodynamics of the Martensite Transformation	30
4	THE BAINITE TRANSFORMATION	33
4.1	Morphology of Bainite	33
4.2	Thermodynamics of the Bainite Transformation	35
4.3	Transformation Kinetics	37
4.4	Crystallography	40
4.41	Crystallographic Properties	40

<u>PART A</u>	<u>LITERATURE SURVEY</u>	<u>PAGE</u>
4.42	Crystallographic Theory	42
4.5	Factors which Influence the Transformation	44
4.51	Austenite Grain Size	44
4.52	Austenitising Temperature	45
4.53	Composition of Austenite	47
4.54	Influence of other Transformations	47
4.55	Influence of Stress	49
4.6	Mechanism of Transformation	50
4.61	The Hultgren Mechanism	51
4.62	The Cottrell and Ko Mechanism	51
4.63	Comments on the Mechanisms	52
4.64	Nucleation	53
5	STABILISATION OF AUSTENITE	55
6	ISOTHERMAL TRANSFORMATION JUST ABOVE M_s	58
7	ISOTHERMAL TRANSFORMATION JUST BELOW M_s	60
8	EXPERIMENTAL PROCEDURES FOR DISTINGUISHING BETWEEN MARTENSITE AND BAINITE	62
<u>PART B</u>	<u>EXPERIMENTAL WORK</u>	
9	INTRODUCTION	66
10	MATERIALS AND TECHNIQUES	68
10.1	Material	68
10.2	Heat Treatment	68

<u>PART B</u>	<u>EXPERIMENTAL WORK</u>	<u>PAGE</u>
10.21	Austenitisation	68
10.22	Determination of the Ms Temperature	70
10.23	Quenching and Isothermal Transformation	71
10.3	Metallographic Technique	71
10.31	Optical Metallography	71
10.32	Habit Plane Analysis	72
10.33	Electron Metallography	74
11	RESULTS	75
11.1	The Ms Temperature	75
11.2	Products of Isothermal Transformation Above Ms	76
11.3	Products of Isothermal Transformation Below Ms	76
11.4	Transformation Kinetics	77
11.5	Morphology of Transformation Products	78
11.6	Electron Diffraction	81
11.7	Habit Planes	83
12	DISCUSSION	85
12.1	Habit Planes	85
12.2	Morphology	87
12.3	Surface Relief	90
12.4	Transformation Kinetics	92
13	CONCLUSIONS	97
14	APPENDICES	99
15	REFERENCES	104

PART A

LITERATURE SURVEY

1. INTRODUCTION

It is generally accepted that austenite transforms isothermally at temperatures just above M_s but the identity of the transformation product, or products, has not been satisfactorily established. At temperatures below the M_s temperature the occurrence of an isothermal transformation, and the nature and mode of formation of the product, have for many years been subject to considerable controversy. In 1940 a form of isothermal transformation diagram,⁽¹⁾ which attempted to reconcile the established isothermal characteristics of the bainite transformation with the athermal nature of the martensite transformation, was proposed. The diagram received support from metallographic⁽²⁾ and dilatometric studies^(3,4) but the techniques employed were not capable of unequivocally identifying the products of isothermal transformation of austenite.

Since the work of Cohen,⁽¹⁾ very few investigations of isothermal transformation near M_s have been reported, and consequently the isothermal transformation diagram, at temperatures near M_s , has not been established.

It is therefore apparent that a detailed study of the isothermal transformation of austenite, at temperatures near M_s , is needed to resolve the controversy. This thesis provides such a study.

Part A of the thesis consists of a review of the factors relevant to the transformation of austenite at temperatures near M_s and the characteristic properties of the transformation, which possibly may be used to identify the products. In Part B the experimental techniques of quantitative metallography, optical and electron microscopy and kinetic studies, used to investigate the isothermal transformation, and the results obtained, are described. The characteristic properties reviewed in Part A are then used to identify the products of transformation at temperatures near M_s and thereby provide detailed information concerning the isothermal transformation diagram in this range of temperature.

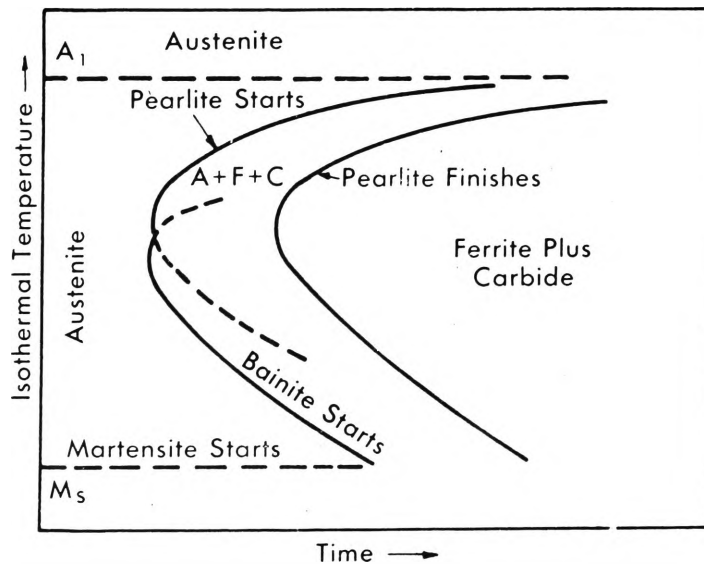


FIG.1 Isothermal transformation diagram of a plain carbon steel of eutectoid composition.

(Hehemann and Troiano.⁽¹²⁶⁾)

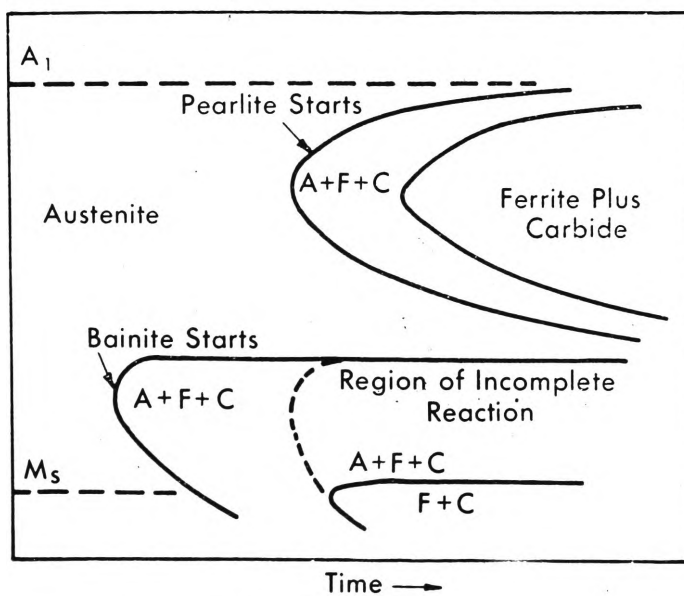


FIG.2 Isothermal transformation diagram of an alloy steel showing the separated pearlite and bainite transformations.

(Hehemann and Troiano.⁽¹²⁶⁾)

2. THE SUBCRITICAL TRANSFORMATION OF AUSTENITE

The properties of annealed and normalised steels are determined by the structures formed by transformation of austenite. These structures are governed by the rates of transformation at the temperatures of formation of the micro-constituents and the consequent morphological development of the product phases. Since mechanical properties depend principally on micro-structure, the rates of transformation, and the nature of the product phases, have been studied extensively. Davenport and Bain ⁽⁵⁾ first investigated the isothermal transformation characteristics of a wide range of carbon and alloy steels and presented their results in the form of isothermal transformation diagrams. (TTT curves).

The principal feature of these diagrams is that, for plain carbon steels, they consist of a single C-curve (Fig. 1), whereas for alloy steels the diagrams consist of two C-curves which, depending on the composition of the austenite, may or may not overlap (Fig. 2).

Ignoring the formation of pro-eutectoid ferrite or cementite, slow cooling or isothermal transformation results in the transformation of austenite (interstitial solid solution of carbon in f.c.c. iron) to a mixture of ferrite (interstitial solid solution of carbon in b.c.c. iron) and cementite (orthorhombic compound Fe_3C). At

temperatures between the eutectoid and nose of the TTT diagram the ferrite-cementite aggregate forms as the micro-constituent pearlite. Pearlite is nucleated by a crystal of cementite, usually located at an austenite grain boundary. Depletion of the surrounding austenite in carbon, by growth of the cementite crystal, results in formation of a ferrite lamellae. Growth of the pearlite then proceeds by the formation of alternate ferrite and cementite lamellae and by simultaneous edgewise propagation of the lamellae. The characteristics of the transformation of austenite to pearlite have been critically reviewed elsewhere^(6,7,8) and will not be considered further in this thesis.

At temperatures between the nose of the transformation diagram and the M_s temperature, austenite transforms to a ferrite-carbide aggregate (bainite), which differs from pearlite in that it is probably nucleated by ferrite and, consequently, has a different morphology. The product of isothermal transformation, at temperatures just below the nose of the TTT curve, is termed "upper bainite" and is characterised by a feathery appearance (Fig. 6), while at lower transformation temperatures the product, termed "lower bainite", has an acicular appearance in polished and etched sections (Fig. 6). These

transformations will be considered in detail in section 4.

The transformation of austenite to both pearlite and bainite are processes occurring by migration of iron atoms to accomplish the structural change, and by long range diffusional migration of carbon atoms to provide the required changes in composition. Rapid cooling suppresses these atom movements and an essentially diffusionless transformation occurs at a lower temperature. The product, martensite, has an acicular appearance in polished and etched sections and, when tempered, is dark etching closely resembling lower bainite (Fig. 3). The characteristics of the martensite transformation, which starts at a temperature M_s and is complete at a temperature M_f , will be considered in section 3. For convenience, the product of transformation will be referred to as "athermal" martensite. Isothermal transformation below M_s results in transformation to a product which has not yet been satisfactorily identified. This transformation will be considered in section 7.

3. THE MARTENSITE TRANSFORMATION

The term martensite was proposed by F. Osmond in honour of the German Metallurgist A. Martens, to designate the "constituent or structure" found in hardened steel. It later became apparent that transformations producing martensite occurred in other alloy systems and also in some pure metals, and consequently, the term martensite is now used to designate the product of the transformation.

In this section those properties which may characterise the martensite transformation will be considered and the factors and conditions which influence the properties or progress of the transformation will be reviewed. In particular, the formation of martensite during isothermal transformation will be considered in detail.

3.1 Morphology of Martensite

The morphological features of martensite have been studied extensively since the "acicular" constituent" was first recognised in hardened steel by Osmond in 1895. Photomicrographs of quenched steels were published by Whitely,⁽⁹⁾ Robertson,⁽¹⁰⁾ Lucas⁽¹¹⁾, and Hanemann and Schrader⁽¹²⁾. Later work by Greninger and Troiano⁽¹³⁾ established that the morphology of martensite varied with the carbon concentration in the austenite from which it formed. In high carbon steels the martensite crystals



FIG.3 Athermal Martensite plates formed in
a 1.61% C steel. X1500.
(Habraken and De Brouwer.⁽¹⁷⁾)

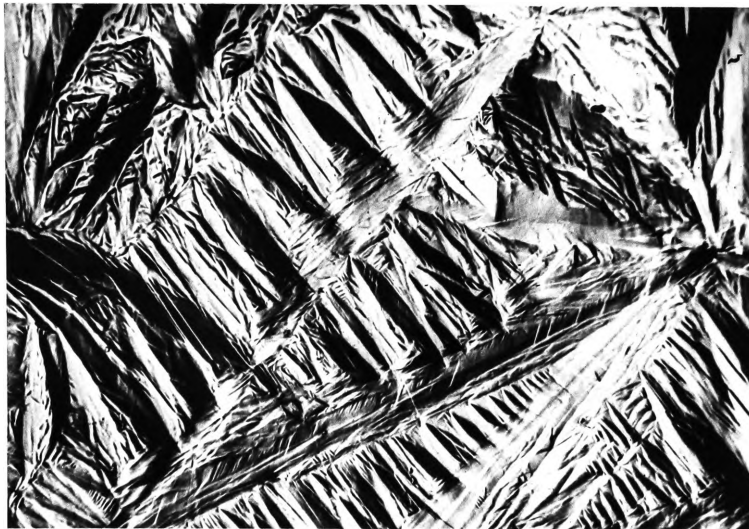


FIG.4 Surface relief effects accompanying the
formation of athermal martensite plates.
X500.

(Cohen.⁽¹⁸⁾)

appeared lenticular in polished and etched sections and were characterised by a straight mid-rib and zig-zag groupings of plates (Fig. 3). With decreasing carbon concentration the martensite crystals changed to laths in which the mid-rib could be revealed only with difficulty. Recent investigations^(14,15,16), using high alloy steels and iron-nitrogen alloys, have resulted in the identification of an additional product termed "massive" martensite which, in polished and etched specimens, appears as "packets" or "blocks" of parallel and sometimes interlacing plates.

The most fundamental characteristic of martensitic transformations is the accompanying change in shape, manifested as relief effects on a surface metallographically prepared prior to transformation.^(13,18) (Fig. 4). The significance of these surface relief effects will be considered in section 3.3.

With the development of thin foil techniques, for examining metals by transmission electron microscopy, it became possible to study the morphological features of the structure of martensite in detail. The first such study of the fine structure was reported by Kelly and Nutting⁽¹⁹⁾ who showed that the lenticular martensite crystals in high and medium carbon steels contained numerous narrow twins,

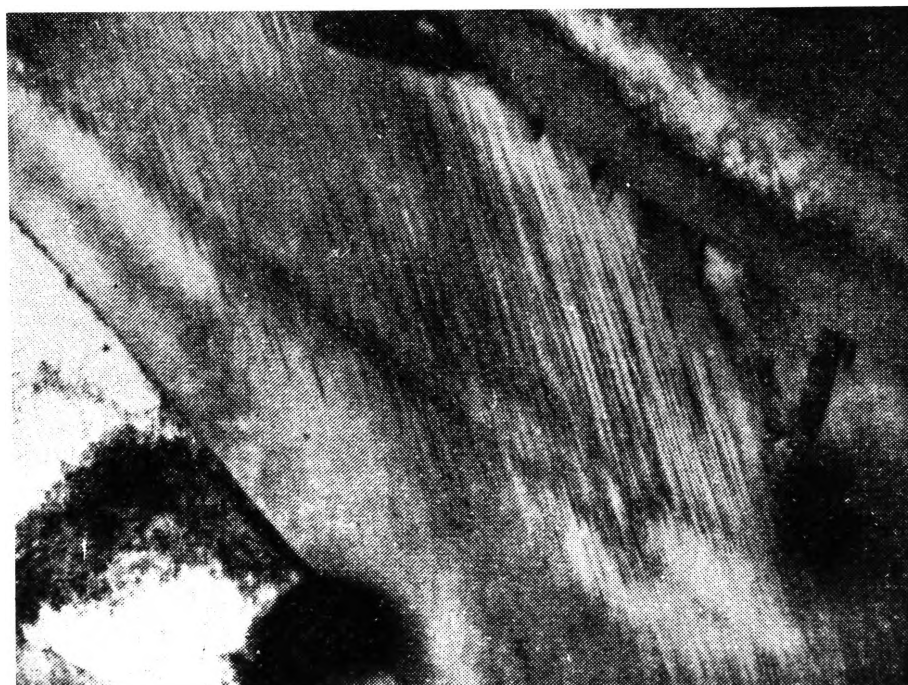


FIG.5 Transmission electron micrograph showing internally twinned martensite plates in an Fe-Ni-C steel quenched to -95°C . X15,000.
(Kelly and Nutting,⁽¹⁹⁾)

the spacing of which varied from 5 Å to 100 Å (Fig. 5). Martensite crystals in low carbon steels and martensite crystals in 18% Cr, 8% Ni stainless steels were shown to be composed of laths containing dense dislocation tangles. Recent work by Barton⁽²⁰⁾ demonstrated that internally twinned martensite may form in steels containing less than 0.2% carbon.

Although the mid-rib of a martensite plate is a well established morphological feature, very little is known about its origin. Greninger and Troiano⁽²¹⁾ described the martensite mid-rib as "the region of discontinuity in the lattice of a martensite crystal" where the transformation began. Their suggestion received support from Breedis and Wayman⁽²²⁾ who found that martensite mid-ribs were continuous across coherent annealing twin boundaries. Kelly and Nutting⁽¹⁹⁾, in transmission electron microscopical studies of martensite plates, were unable to find any discontinuity in the plates which might represent the mid-rib. However, they observed many instances of groups of two or more plates in contact and suggested that the mid-rib region may represent a junction plane between two parallel plates. The observations of high twin densities, near the central region of martensite plates in Fe-Ni alloys^(23,24), has been used⁽²⁵⁾ as evidence in support of the original hypothesis of Greninger and Troiano. According to Wayman⁽²⁵⁾

these observations suggest that the mid-rib is a high energy region where transformation nucleates and that growth of the plate occurs sideways from this volume. It was further proposed that, for a ferrous martensite plate in which the mid-rib is absent, transformation nucleates at the planar "mid-rib" but growth occurs in only one direction.

The morphological changes occurring during the tempering of ferrous martensites have been closely studied^(26,27,28,29,30,31) in recent years and are now well understood in terms of a three stage process. The first stage occurs in the temperature range 100-150°C and involves precipitation of carbon from the b.c.t., interstitial solid solution with an attendant decrease in the axial ratio of the tetragonal unit cell.^(32,33) X-ray and electron diffraction studies^(30,31,34,35,36,37) identified the carbide as hexagonal epsilon carbide, $\text{Fe}_{2.4}\text{C}$, which re-dissolves during the second stage of tempering. Jack⁽³⁰⁾ reported the orientation relationship between the lattices of the epsilon carbide and the ferrite as

$$(101)_{\alpha} \parallel (101)_{\epsilon}$$

$$(011)_{\alpha} \parallel (001)_{\epsilon}$$

$$[100]_{\alpha} \quad 5^{\circ} \text{ from } [110]_{\epsilon}$$

The observed increase in hardness, accompanying the initial stage of tempering high carbon martensites, has been attributed to the coherency of the small carbide

precipitates with the b.c.t. matrix (28).

The third stage of tempering, which occurs in the temperature range 200-300°C, involves the precipitation of carbon as orthorhombic cementite, Fe_3C . The orientation relationship between the lattices of the cementite and ferrite have been reported^(19,30) to be consistent with the relationship proposed by Pitsch and Schrader⁽³⁸⁾.

$$(211)_{\alpha} // (001)\text{Fe}_3\text{C}$$

$$[0\bar{1}1]_{\alpha} // [100]\text{Fe}_3\text{C}$$

$$[1\bar{1}\bar{1}]_{\alpha} // [010]\text{Fe}_3\text{C}$$

Recent investigations^(19,20) indicate that the tempering characteristics of martensite may be directly related to the morphology of the martensite and not only to the carbon concentration. Barton⁽²⁰⁾ and Kelly and Nutting⁽¹⁹⁾ showed that the main differences between the tempering of a high carbon and a low carbon steel arise from differences in the structural inhomogeneities. In high carbon steels the structural inhomogeneity is due to twinning and the twin interfaces provide sites for the nucleation of carbide particles which grow along the interfaces and also normal to them. Kelly and Nutting⁽¹⁹⁾ proposed that the absence of twins in low carbon martensites results in carbide precipitation in a Widmanstätten arrangement. However, the observation of

twins in low carbon martensite⁽²⁰⁾ does not support this proposal.

3.2 Transformation Kinetics

Greninger and Troiano⁽³⁹⁾ summarised the transformation kinetics of the martensite transformation.

- 1) Individual martensite plates form in a very short time.
- 2) Transformation during cooling begins at a temperature (M_s) and proceeds only during cooling. Transformation occurs by formation of new plates rather than by growth of existing plates.
- 3) Deformation may induce transformation above the M_s temperature. The highest temperature at which the transformation can be stress induced is termed the M_d temperature.

Quantitative evidence, demonstrating the rapidity with which individual martensite plates form, was first provided by Förster and Scheil⁽⁴⁰⁾ who found that each plate forms in less than 10^{-4} seconds. More recent work⁽⁴¹⁾ has shown that individual plates, in an Fe-Ni-C alloy, form in about 10^{-7} seconds and that the linear growth rate was approximately 10^5 cms/sec at all temperatures in the range -20°C to -200°C . Kulin and Cohen⁽⁴²⁾ showed that an Fe-Ni alloy transformed to martensite at temperatures as low as 4°K , at rates not appreciably different from those found

at much higher temperatures. These observations, that martensite plates form rapidly and at a rate which is not temperature dependent, indicate that the growth of martensite plates is not thermally activated.

Machlin and Cohen⁽⁴³⁾ observed, for an Fe-Ni alloy, that the formation of one martensite plate often nucleated a group of additional plates producing a characteristic "zig-zag" appearance. No further transformation occurred for a short cooling interval, after which a new burst appeared. This behaviour was termed the "burst phenomena" and indicated that the stresses produced by the formation of one martensite plate assisted in the nucleation of another such that the whole process was autocatalytic in nature. It was observed further that martensite plates formed by the burst phenomena were generally much wider than isolated plates formed in the same alloy. Christian⁽⁴⁴⁾ proposed that plates formed by the burst phenomena reduced the stresses in the matrix, thus forming a partially self accommodating stress system.

Cohen, Machlin, and Paranjpe⁽⁴⁵⁾ observed that the first plates to form were the largest, and as the martensite transformation proceeded, smaller and smaller plates must be produced since the plates could not intersect nor cross grain boundaries. They termed this

the "partitioning effect". Koistinen and Marburger⁽⁴⁶⁾ demonstrated that when the martensite transformation nears completion, the very small plates, which form according to the partitioning effect, require prohibitive surface and strain energy per unit volume. They suggested that it was highly improbable that martensite transformations ever reach completion.

3.3 Crystallography

3.31 Crystallographic Properties

The tetragonal crystal structure of martensite in steels was first detected by Fink and Campbell⁽⁴⁷⁾ who assumed that the iron atoms occupied the lattice points of a b.c.t. cell. More refined studies by Lipson and Parker⁽⁴⁸⁾ showed that the probable structure was one in which the iron atoms could undergo slight displacements in the direction of the C axis of the cell. Other studies^(32,33,49) demonstrated that the axial ratio of the b.c.t. cell was a linear function of carbon content, and varied between unity in pure iron to 1.08 in a 1.75% C alloy.

Martensite plates form on specific crystallographic habit planes of the parent austenite. Greninger and Troiano⁽¹³⁾ measured the traces of martensite plates in two non-parallel surfaces and showed that the habit plane changes discontinuously with carbon concentration (Fig. 13). This was subsequently verified by Smith and

Mehl⁽⁵⁰⁾ and Dornan and Hoffman⁽⁵¹⁾. The habit plane in steels containing more than 0.5% C is irrational being near $(259)_{\gamma}^*$, for carbon concentrations between 1.5% and 1.8%, and near $(225)_{\gamma}$ for carbon concentrations between 0.9% and 1.4%. Martensite plates in steels containing less than 0.5% carbon have habit planes near $(111)_{\gamma}$. In plain carbon steels the habit plane is independent of the temperature of formation and rate of cooling below the M_s temperature. In alloy steels, however, changes in the predominant habit plane with transformation temperature have been reported^(19,52).

Kelly and Nutting⁽¹⁹⁾ used single surface trace analysis and corresponding diffraction patterns from thin foils to show that the fine internal twinning of high carbon martensites occurred only on $\{112\}_{\alpha}$ planes. McDougall and Bowles,⁽⁵³⁾ in surface relief studies of martensite plates in 1.35 and 1.9% C steels, observed that some large martensite plates contained single systems of parallel bands within which the surface was tilted with respect to the rest of the plate. Two surface trace

* The bases α and γ refer respectively to the b.c.t. or b.c.c., and f.c.c. unit cells.

analyses of each plate showed that the transverse markings were parallel to a $\{112\}_{\alpha}$ martensite twinning plane.

The orientation relationship between the lattices of a martensite plate and the austenite from which it formed is composition dependent.⁽⁵⁴⁾ Three orientation relationships have been observed in steels;

- 1) the Kurdjumov-Sachs relationship⁽⁵⁵⁾

$$(111)_{\gamma} // (011)_{\alpha}$$

$$[0\bar{1}1]_{\gamma} // [1\bar{1}1]_{\alpha}$$

- 2) the Nishiyama relationship⁽⁵⁶⁾

$$(111)_{\gamma} // (011)_{\alpha}$$

$$[\bar{1}1\bar{2}]_{\gamma} // [0\bar{1}1]_{\alpha}, \text{ and}$$

- 3) the Greninger-Troiano relationship⁽²¹⁾

$$(111)_{\gamma} // (011)_{\alpha}$$

$$[5\bar{1}2\ 17]_{\gamma} // [7\bar{1}7\ 17]_{\alpha}$$

The Kurdjumov-Sachs relationship is found for carbon concentrations between 0.55 and 1.4%, i.e. for martensite plates having a $(225)_{\gamma}$ habit plane. The Nishiyama relationship has been reported for martensite plates formed in alloys containing 27-34% nickel,⁽⁵⁶⁾ but Christian and Bilby⁽⁵⁷⁾ suggested that reported instances are probably approximations to various irrational relationships, similar to that determined by Greninger and

Troiano⁽²¹⁾. Martensite plates with a $(259)_\gamma$ habit plane have the Greninger-Troiano orientation relationship.^(19,21) Kelly and Nutting⁽¹⁹⁾ demonstrated that the orientation relationship is dependent on the temperature of formation of the individual plates. They showed that, after quenching to -196°C , plates formed in a 20% Ni - 0.8% C alloy generally exhibited the Greninger-Troiano orientation relationship, whereas in specimens quenched to -95°C the Kurdjumov-Sachs orientation relationship predominated.

3.32 Crystallographic Theory

The phenomenological theories of martensitic transformations attempt to rationalise the crystallographic and geometrical features of a transformation in terms of the structures and lattice parameters of the parent and product phases, together with the structural inhomogeneities in the plates. The crystallographic theory takes account only of the initial and final structures of a transformation and can therefore provide no information about the detailed motion of atoms whereby these relationships are produced.

Several theories have been proposed for the martensite transformation.^(21,58,59,60,61,62) Greninger and troiano⁽²¹⁾ first realised the significance of surface relief effects accompanying the martensite transformation. From their studies on an Fe-Ni alloy it was concluded

that the surface relief closely resembled a homogeneous shear on the habit plane of the martensite plate. They proposed that the change in lattice, produced by the transformation, could be regarded as the result of two successive shears. The first of these occurred on the habit plane and was responsible for the change of shape, whilst the second was balanced by an equal and opposite slip shear so as to produce no observable macroscopic effects. The theory was incomplete in that it did not allow for a volume change in the transformation.

The most successful crystallographic theories, proposed by Bowles and MacKenzie^(60,61) and Wechsler, Lieberman and Read⁽⁶²⁾, are based on the principle of an approximately undistorted and unrotated habit plane. The total shape deformation is considered to comprise a pure lattice deformation together with a lattice invariant deformation, or inhomogeneous shear (complementary strain), and a rigid body rotation. In the Wechsler-Lieberman-Read theory different solutions for the crystallographic properties, i.e. habit plane, orientation relationship, etc., can be obtained by varying the lattice invariant shear system, maintaining the requirement that the interface is macroscopically undistorted. The Bowles-MacKenzie theory proposed that the interface (habit) plane

is unrotated but may undergo a small isotropic dilation. The general theory was developed from the hypothesis that the complementary strain occurred on the martensite twinning elements. Different solutions for the crystallographic features of the transformation can be obtained by assigning different values, close to unity, to the dilation parameter.

The hypothesis by Bowles and MacKenzie, that the complementary strain was part of the martensite twinning shear, is supported by electron microscopical observations of $\{112\}_{\gamma}$ twins in $(225)_{\gamma}$ martensite. However, theoretical considerations of the nature of the complementary strain,^(63,64) and recent observations, that the twins in Fe-Ni and Fe-Ni-C martensites do not completely cross the plates^(23,24,65), suggested that the twinning shear is only one component of the inhomogeneous (complementary) strain and an additional component can be described as a slip shear. Further evidence, that plastic deformation may constitute part of the complementary strain, was obtained by McDougall and Bowles⁽⁵³⁾ from studies of transverse markings on the relief surfaces of martensite plates. They observed striations, indicative of shear on the plane $(111)_{\gamma} // (101)_{\alpha}$, and concluded that a slip shear on this plane may be a component of the complementary strain. Their conclusion was subsequently verified by Morton and Wayman⁽⁶⁶⁾.

In all transformations, for which the predictions of the theory have been compared with experiment, the agreement was at least moderately satisfactory. Discrepancies have indicated that the theories, in their present form, are unable to account simultaneously for all of the geometrical properties of a martensitic transformation. However, apart from the discrepancies between theory and observations, sufficiently satisfactory agreement with experiment has been obtained to indicate that the assumptions on which the theories are based are tenable. The Wechsler-Lieberman-Read and Bowles-MacKenzie theories were first applied to transformation in steels but have since been used to interpret the crystallographic and geometrical properties of a number of other transformations which have martensitic characteristics.^(67, 68, 69, 70, 71, 72, 73) Discrepancies between experiment and predictions of the theory, indicate it has not yet been developed to its final form.

3.4 Nucleation and Transformation Mechanism

Classical, or thermally activated, nucleation theory was originally applied to the martensite transformation by Kurdjumov and Maximova⁽⁷⁴⁾ and later by Fisher, Holloman and Turnbull⁽⁷⁵⁾. The theory proposed that, although the formation of one phase from another

involves a decrease in chemical free energy at the temperature of transformation, the new phase must pass through a series of intermediate transition states before reaching the stable state. The transitional state that could spontaneously transform was that for which the free energy change was a maximum, the latter being referred to as the free energy for nucleation. Thus nucleation is considered to be thermally activated and compatibility with athermal behaviour can only be obtained by assuming extremely rapid nucleation at each temperature, and that barriers to further nucleation are established after the first plates are formed⁽⁷⁶⁾.

The classical theory predicts that nucleation should occur homogeneously but considerable evidence is available to suggest that martensite nuclei form at preferred sites in the parent austenite. Greninger and Mooradian⁽⁷⁷⁾ showed that, in many transformations which were reversible on heating, identical patterns of martensite plates were formed during each cooling cycle. Further, Cech and Turnbull⁽⁷⁸⁾ observed that, when very fine iron powders were quenched, a wide variation in the M_s temperature of individual particles, of the same size and composition, resulted and some particles did not transform even at the lowest temperatures investigated.

The observations of Greninger and Mooradian and Cech and Turnbull led to development of the strain nucleus theory. Early theories considered that embryos, which form in the austenite at high temperatures and are retained at the transformation temperature by quenching, provide preferred nucleation sites. The embryos were considered to have specific sizes and form either by compositional fluctuations or re-arrangement of arrays of defects. Since the critical size of embryo for nucleation decreased with decreasing temperature, a martensite plate would form spontaneously when the embryo became supercritical. Thus no thermal activation was required and the M_s temperature would be determined by the size of the largest embryo. This theory has difficulty in explaining observed⁽⁷⁹⁾ isothermal martensite formation at temperatures above the M_s temperature.

Christian⁽⁸⁰⁾ suggested that the condition for nucleation of martensite was not reached when the nucleus attained a critical size but rather, was connected with the establishment of conditions necessary to initiate the transformation. This suggestion, which implies the formation of an interface that is at least semi-coherent, led to the dislocation theories of nucleation.

The most detailed dislocation theory was developed by Knapp and Dehlinger⁽⁸¹⁾ who considered that a $(225)_\gamma$ martensite embryo was an oblate spheroid bounded by dislocation loops. Growth in the $[1\bar{1}0]_\gamma$ and $[225]_\gamma$ directions resulted from expansion of the loops and from generation of new loops in the $[55\bar{4}]_\gamma$ direction. When the driving force was sufficient to provide the energy for expansion of the interface, and to supply the elastic strain energy resulting from the formation of a martensite plate, spontaneous growth occurred. The driving force was considered to decrease with increasing embryo size. The theory proposed that, with decreasing temperature below the austenite-martensite equilibrium temperature, the driving force increased and at the M_s temperature the largest embryos expanded rapidly. At lower temperatures smaller embryos attained critical size and the transformation proceeded. This theory was applied only to the athermal mode of the martensite transformation but Kaufman and Cohen⁽⁷⁶⁾ developed it further to account for the kinetics of isothermal martensite formation in Fe-Ni-Mn alloys.

The modified theory is referred to as the "operational nucleation" theory and proposes that sub-critical embryos can grow as a result of thermal activation until they attain critical size, thus introducing some

isothermal characteristics to the original theory proposed for the athermal mode of transformation. Measured activation energies^(82,83) for isothermal nucleation in Fe-Ni-Mn alloys, were found to be in good agreement with the activation energies calculated from the model proposed by Kaufman and Cohen. However, Pati and Cohen⁽⁸²⁾ pointed out that the operational nucleation theory specifies a critical growth condition, and hence, the nucleation rate can only be inferred from the rate at which detectable changes occur.

The operational nucleation theory requires that the embryos existing in the austenite should be sufficiently large to be detectable by transmission electron microscopy of thin foils. Richman, Cohen and Wilsdorf⁽⁸⁴⁾ observed "plate like markings" in transmission studies of an Fe-Ni alloy and claimed that these were martensite embryos. Other attempts^(85,86) to detect the embryos predicted by the theory, were not successful. Pati and Cohen⁽⁸²⁾ calculated that the probability of finding the large embryos by this technique would be extremely small even should the embryos be sufficiently large to be resolved.

The operational nucleation theory has been applied⁽⁸⁷⁾ to the formation of thermolastic martensite,

stabilisation of austenite, the burst phenomena, and the isothermal mode of transformation. However, more experimental evidence is needed to establish the validity of the operational nucleation theory. Such evidence could be provided by a demonstration that the markings observed by Richman, Cohen and Wilsdorf, do in fact nucleate martensite plates at or below the M_s temperature.

It is known that the growth of martensite plates occurs by a regular co-operative re-arrangement of the atoms in which the relative displacements do not exceed the interatomic distance^(88,89). Very little work, concerned with the elucidation of a satisfactory growth mechanism, has been published. It is generally considered that the activation energy for growth is negligible and that nucleation is the controlling factor in the formation of a martensite plate.

Dislocation theories, for the formation of martensite, have been proposed by Christian⁽⁴⁴⁾ and by Cottrell and Bilby⁽⁹⁰⁾. These theories propose that regions of the austenite lattice can be transformed to martensite by the separation of suitable partial dislocations. In the treatment due to Cottrell and Bilby the interface is considered to move by the rotation of an imperfect transformation dislocation about a securely

anchored pole. The motion of the interface generates crystallographic relationships described by two shears, one of which produces an extended dislocation with a stacking fault of the martensite structure. Below the M_s temperature, the stacking fault is considered capable of rapid expansion to produce a martensite plate. Since no satisfactory explanation for thermal expansion of the stacking fault has been advanced, the theory in its present form is applicable only to the athermal mode of transformation.

After nucleation, growth of a martensite plate occurs by propagation of the interface, which must be at least semi-coherent with the austenite from which it forms. According to Wayman, ⁽²⁵⁾ growth in two directions from the nucleus produces martensite plates containing a central mid-rib, while for ferrous martensite plates, in which the mid-rib is absent, growth occurs in only one direction.

3.5 The Isothermal Transformation

The original concept, that martensite always forms athermally, is no longer valid since many instances of isothermal martensite formation have been reported ^(41,79, 82,91,92,93,94,95,96,97,98,99). Schmidtman, Vogt and Schenck ⁽⁹⁹⁾ concluded from their investigations, of

isothermal transformation in a number of ferrous alloys, that isothermal transformation most likely occurs in all iron alloys which undergo an athermal transformation. In all of those investigations either electrical resistivity measurements or optical metallography was used to identify the product of transformation.

3.51 Transformation Kinetics

Maximova and Kurdjumov⁽⁹¹⁾, who first reported the isothermal formation of martensite in an Fe-Ni-Mn alloy, showed that athermal transformation could be completely suppressed by rapid cooling to -180°C and that isothermal transformation then occurred on reheating to temperatures between -160°C and -80°C . The transformation kinetics were shown to be completely different from those for athermal transformation and normal C-curve behaviour was observed. These results were subsequently verified by Cech and Holloman⁽⁹²⁾. Shih, Averbach and Cohen⁽⁸³⁾ isothermally transformed Fe-Ni-Mn and Fe-Mn-C alloys at temperatures as low as -196°C and concluded from their investigations that a small volume fraction of athermal martensite may influence the form of the isothermal transformation curves. Existing athermal martensite was observed to provide nucleating sites for isothermal transformation thus decreasing the incubation period for

the transformation. It was suggested that the characteristics of the isothermal transformation can be studied only in samples in which the formation of athermal martensite has been completely suppressed. Raghaven and Entwisle⁽⁹⁸⁾ proposed that progress of the isothermal transformation could be quantitatively accounted for by assuming that, when a martensite plate forms, embryos are created in the surrounding austenite. These would then be capable of activation to give further transformation. On the other hand, Kulin and Speich⁽⁷⁹⁾ found that the presence of athermal martensite, in an Fe-Cr-Ni alloy, had no significant effect on the initial nucleation rate of isothermal martensite.

Maximova and Kurdjumov⁽⁹¹⁾, and Machlin and Cohen⁽⁹³⁾ concluded that individual plates form very rapidly and that the transformation proceeds by the nucleation of new plates rather than by growth of existing plates. From measurements of growth rates of martensite plates in an Fe-Ni-C alloy, Bunshah and Mehl⁽⁴¹⁾ showed that differences in the kinetic behaviour of the athermal and isothermal modes of transformation were not attributable to the growth mechanism. The time of formation of both athermal and isothermal martensite plates was of the order of 10^{-7} seconds and the linear growth rate was 10^5 cms/sec.

The measured growth rates were independent of temperature in the range -20 to -195°C .

Kulin and Speich⁽⁷⁹⁾ made electrical resistivity measurements, using an Fe-Cr-Ni-Mn alloy, and showed that isothermal transformation of austenite to martensite occurred at temperatures above the athermal M_s temperature. They concluded that the concept of the M_s temperature being independent of the cooling rate, except in instances where stabilisation effects occurred, was incorrect. Kulin and Speich suggested that the strong tendency, which existed for isothermal transformation, resulted in the measured M_s temperatures increasing with decreasing cooling rates. It was proposed that the true M_s temperature should be defined as the limiting temperature obtained with increasing cooling rates.

3.52 Effect of Austenite Grain Size

The effect of grain size on the formation of isothermal martensite has been studied by Pati and Cohen⁽⁸²⁾ and Raghaven and Entwisle⁽⁹⁸⁾. Raghaven and Entwisle found that the isothermal transformation curves, for an Fe-Ni-Mn alloy, were very sensitive to changes in austenite grain size, the incubation period for transformation varying inversely with the cube of the grain diameter. They proposed that pre-existing embryos

in the austenite were uniformly distributed and not located at preferred sites in the grain boundaries. Pati and Cohen⁽⁸²⁾ determined the nucleation rates, as a function of austenite grain size, for isothermal transformation in a series of Fe-Ni-Mn alloys. They established that the transformation time, required to produce 0.2% transformation product, increased with decreasing austenite grain size. However, since a small austenite grain size severely limits the martensite plate size, a larger number of nucleation events are necessary to produce 0.2% transformation in fine grained austenite than in coarse grained austenite. It was demonstrated that the initial rate of nucleation was independent of grain size so that, in the alloys studied, the austenite grain boundaries were not dominant nucleation sites for isothermal transformation.

3.53 Effect of Composition

A limited investigation of the effect of composition on the isothermal martensite transformation was carried out by Schmidtman, Vogt and Schenck⁽⁹⁹⁾ who used dilatometric methods to study Fe-Mn-C alloys in the temperature range 0 to -180°C. They found that increasing carbon concentration resulted in an approximately linear increase in the volume fraction of isothermally formed martensite at all temperatures, whilst the manganese/

carbon ratio, required to produce the same effect, was 12:1. Increasing concentrations of both manganese and carbon displaced the nose of the C-curve to lower temperatures.

Since the pioneering work of Maximova and Kurdjumov⁽⁹¹⁾, on the isothermal mode of the martensite transformation, was first published, many other investigations of the transformation have been reported for a number of ferrous alloys. However, these investigations have been concerned with the mechanism and kinetics of the transformation and consequently, very little is known about the morphology and crystallography of plates formed isothermally.

3.6 Thermodynamics of the Martensite Transformation

The thermodynamics of martensitic transformations have been reviewed by Borland and Walker⁽⁸⁷⁾. Martensitic transformations, being diffusionless, derive the driving force from the difference in free energy between the initial and final phases, these differing only in crystal structure. The latter implies that there is a temperature T_0 at which the bulk free energies of austenite and martensite are equal. The free energy of austenite is a minimum at temperatures above T_0 whilst free energy is available for the transformation to proceed at temperatures below T_0 . Although the change in free energy is favourable

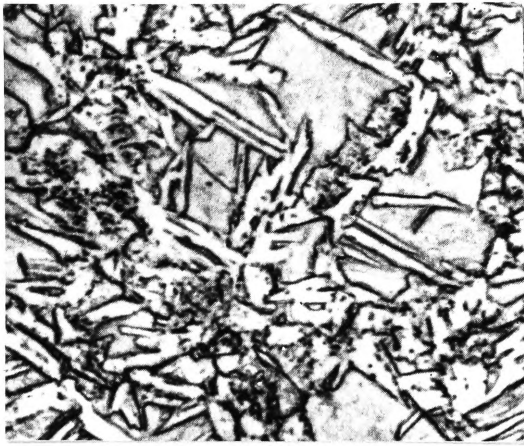
for martensite formation below T_0 , no transformation occurs until the alloy is cooled to the M_s temperature since energy is required to supply the non-chemical energies, such as interfacial energy and strain energy.

The chemical free energy for the martensitic transformation in Fe-C alloys has been calculated by Cohen, Machlin and Paranjpe⁽⁴⁵⁾ who reported a value of -290 cal/mole. This value was relatively independent of carbon concentration. For the transformation in Fe-Ni alloys, Kaufman and Cohen⁽¹⁰⁰⁾ reported -315 cal/mole at 30% nickel. They found that the free energy change decreased with decreasing nickel concentration. However, the more recent work of Clark⁽¹⁰¹⁾ suggested that the free energy change was independent of the nickel content.

The non-chemical contributions to the total free energy change, i.e. the interfacial and strain energies, have been calculated for assumed austenite-martensite interface structures. Fisher, Holloman and Turnbull⁽⁷⁵⁾ assumed that the interface was coherent and obtained 24 ergs/cm² for the surface energy contribution. Cohen, Machlin and Paranjpe⁽⁴⁵⁾ assumed a non-coherent, macroscopically matched boundary and obtained 1000 ergs/cm² for the surface energy. It was concluded, from this result, that the non-chemical factors contributed only

65 cal/mole and hence the martensite transformation should require only 50°C of undercooling below the equilibrium temperature and not the observed 200°C. Krisement, Houdremont and Wever⁽¹⁰²⁾ proposed that this discrepancy may result from the energy released during transformation causing local heating which would tend to raise the temperature of the austenite. Borland and Walker⁽⁸⁷⁾ suggested that this proposal would be plausible for transformations resulting in the formation of large martensite plates. However, Hillert⁽¹⁰³⁾ argued that the undercooling discrepancy could not be explained in terms of adiabatic effects. He proposed that it was more likely that barriers to nucleation increased the degree of undercooling required to initiate the transformation.

Owen and Gilbert⁽⁹⁵⁾ established a correlation between the morphology of martensite plates and the free energy change required to produce them. Poorly defined structures were formed in steels containing small concentrations of alloying elements, and therefore requiring only a small free energy change, whereas martensite, formed in carbon or highly alloyed steels, requires a large free energy change, and the plates generally had a well defined lenticular shape.



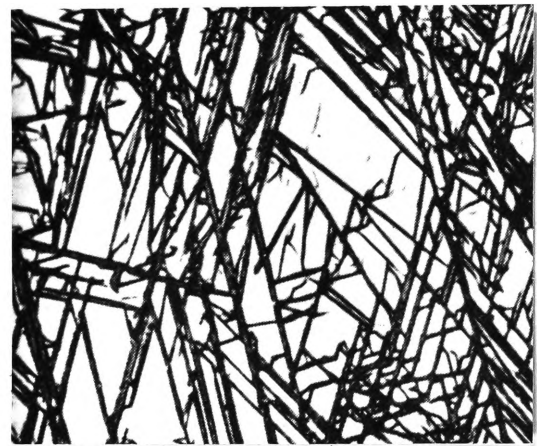
(a)



(b)



(c)



(d)

FIG.6 Photomicrographs of bainite formed at various transformation temperatures.

- a) The X-constituent, X500. (Mehl and Dube,⁽¹¹²⁾)
- b) Upper bainite formed in a eutectoid steel, X500. (Mehl and Dube,⁽¹¹²⁾)
- c) Lower bainite formed at 250°C in a 0.92%C steel, X250. (Greninger and Troiano,⁽¹³⁾)
- d) Lower bainite formed at 100°C in a 1.78%C steel, X500. (Greninger and Troiano,⁽¹³⁾)

4. THE BAINITE TRANSFORMATION

The term bainite, proposed in honour of E.C. Bain, refers to the microstructural constituent formed in steel by transformation of austenite at temperatures intermediate between the pearlite and martensite ranges. The transformation product was first reported by Davenport and Bain⁽⁵⁾ in their classical investigation of the transformation of austenite in a eutectoid steel. The transformation product was described as an aggregate of ferrite and cementite having a feathery appearance. Later studies, using different steels and transformation temperatures, demonstrated that the morphology of bainite could vary considerably.

In the following sections the properties of the bainite transformation will be reviewed with particular emphasis being placed on transformation at temperatures near M_s and factors and conditions which influence the transformation.

4.1 Morphology of Bainite

The temperature dependence of bainite morphology has led to the distinction between upper and lower bainite. Upper bainite (Fig. 6), formed above approximately 350°C , has a feathery appearance, usually nucleates at grain boundaries, and grows by the spreading of branches in towards the centres of the grains. Electron microscopical

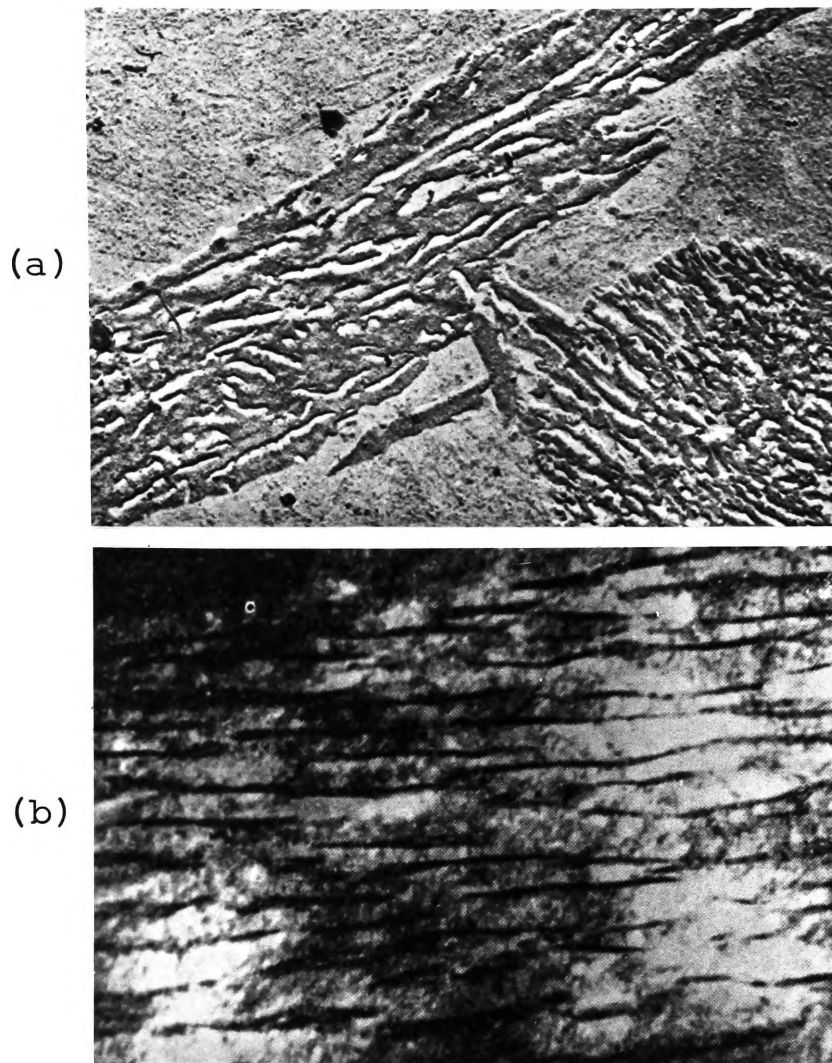
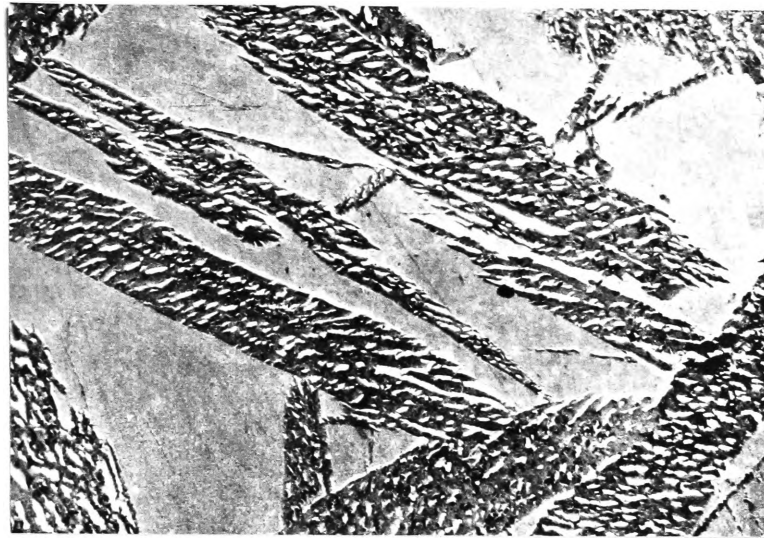


FIG.7 a) Electron micrograph of plastic replica showing upper bainite in a 0.87%C steel. X15,000.

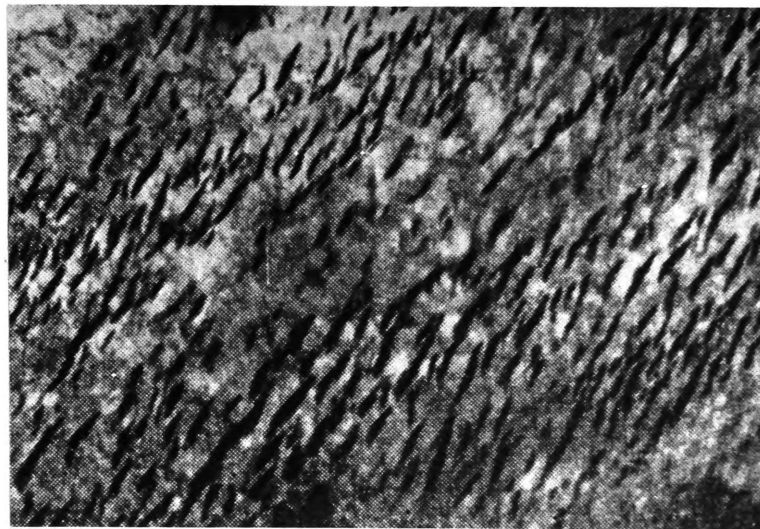
(Habraken and De Brouwer,⁽¹⁷⁾)

b) Transmission electron micrograph showing upper bainite in a 0.97%C steel. X30,000.

(Shackleton and Kelly,⁽¹⁰⁸⁾)



(a)



(b)

FIG.8 a) Electron micrograph of plastic replica showing lower bainite in a Ni-Cr steel. X10,000.

(Habracken and De Brouwer,⁽¹⁷⁾)

b) Transmission electron micrograph showing lower bainite in a 0.96%C steel. X30,000.

(Shackleton and Kelly,⁽¹⁰⁸⁾)

studies (104,105,106,107,108,109,110) have shown that upper bainite is composed of coarse plates of cementite aligned longitudinally in ferrite plates (Fig. 7). Irvine and Pickering⁽¹⁰⁹⁾ and Shackleton and Kelly⁽¹⁰⁸⁾ have observed carbide films surrounding the ferrite plates. The formation of films was attributed⁽¹⁰⁹⁾ to the rapid, side by side, nucleation of bainite plates entrapping carbon enriched austenite, from which carbide subsequently precipitated.

Below approximately 350°C the morphology of bainite changes to parallel and contiguous needles⁽¹³⁾ (Fig. 6). The similarity of lower bainite to tempered martensite presents some difficulties in differentiating the two structures. Lower bainite (Fig. 8), consists of ferrite plates delineated by relatively large cementite platelets, and containing very fine cementite platelets orientated at approximately 55° to the axis of the ferrite plate.^(104,107,108,109) Srinivasan and Wayman⁽¹¹¹⁾ reported, for an Fe-8% Cr - 1.1% C alloy, that additional carbides precipitated on striations parallel to the ferrite plate growth axis. These carbides could not be identified and it was suggested that the precipitation of carbides may have been complicated by the high alloy concentration of the steel.

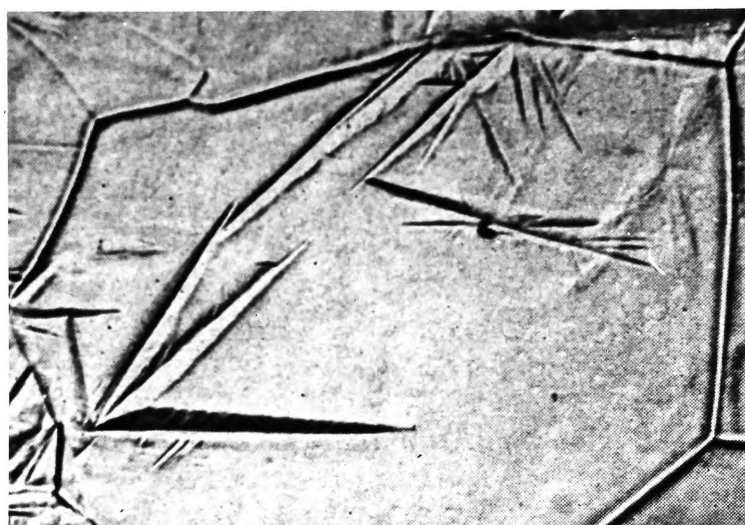


FIG.9 Surface relief effects accompanying
the formation of plates of lower
bainite. Oblique illumination. X500.
(Christian,⁽⁴⁴⁾)

The morphology of bainite is independent of composition in plain carbon steels⁽¹⁰⁹⁾, except that the volume fraction of carbides present within the ferrite increases with carbon concentration. Another bainite structure, referred to as acicular ferrite or the X-constituent, is sometimes formed in alloy steels.^(6,112) This structure (Fig. 6), differs from the other forms of bainite in that it consists of carbide free ferrite plates⁽¹¹³⁾.

The bainite transformation is accompanied by the formation of relief effects on surfaces metallographically prepared before transformation^(114,115,116) (Fig. 9). Ko and Cottrell⁽¹¹⁴⁾ reported that these relief effects were very similar to those which accompany the formation of martensite plates and concluded that the bainite transformation must proceed by the propagation of an interface which is, at least, semi-coherent with the two lattices.

4.2 Thermodynamics of the Bainite Transformation

The sharp upper temperature limit, B_s , for the bainite transformation, was examined thermodynamically by Zener⁽¹¹⁷⁾ who assumed that the ferrite of bainite inherited the carbon concentration of the austenite from which it formed, and that carbon partition, carbide precipitation, or both, were secondary processes. This

assumption led to the postulate that the B_s temperature was determined by the condition of zero free energy change for the transformation. Fisher⁽¹¹⁸⁾ used classical nucleation theory⁽⁷⁵⁾ to calculate the B_s temperature for 3% chromium steels, containing between .08% and 1.28%C. He found agreement with experiment provided it was assumed that the carbon concentration in the austenite, surrounding bainite nuclei, was increased approximately 0.4% by absorption.

The activation energies, reported for growth of both upper and lower bainite, vary considerably. Values of 2-8 K.cal/mole⁽¹¹⁹⁾ and 34 K.cal./mole⁽¹²⁰⁾ were determined for upper bainite, whereas corresponding activation energies for the growth of lower bainite were reported as 15-20 K.cal/mole and 14 K.cal/mole. Radcliffe and Rollason⁽¹²¹⁾ determined activation energies for the bainite transformation in a number of steels and showed that the overall activation energy for formation decreased with decreasing carbon concentration.

From thermodynamic considerations, Zener,⁽¹¹⁷⁾ Hillert⁽¹²²⁾, and Speich and Cohen⁽¹²³⁾ have developed models for the edgewise growth of a bainite plate. The Zener-Hillert model considers the growth rate to be controlled by diffusion of carbon through austenite, away from the tip of the advancing interface. The driving force

for carbon diffusion arises from the concentration gradient existing in the austenite as a result of local equilibrium at the ferrite-austenite interface. Whereas the Zener-Hillert model predicts an increase in carbon concentration of the austenite near the advancing edge, the model of Speich and Cohen considers the carbon to diffuse away into the surrounding austenite as the leading edge of the bainite plate advances. The surface relief accompanying the bainite transformation was explained by regarding the interface as being semi-coherent. Activation energies, calculated using this model, were found to decrease with increasing temperature, and were in good agreement with measured activation energies⁽¹²⁴⁾. Kaufman, Radcliffe and Cohen⁽¹²⁵⁾ proposed a model in which the basic characteristics of the bainite transformation were considered to be the propagation of a coherent ferrite-austenite interface as a leading edge, at a rate controlled by carbon diffusion through austenite. The precipitation of carbide was considered to be a secondary process which did not retard the rate of propagation.

4.3 Transformation Kinetics

Hehemann and Troiano⁽¹²⁶⁾ have summarised the transformation kinetics as follows:-

- 1) Transformation occurs isothermally in plain carbon

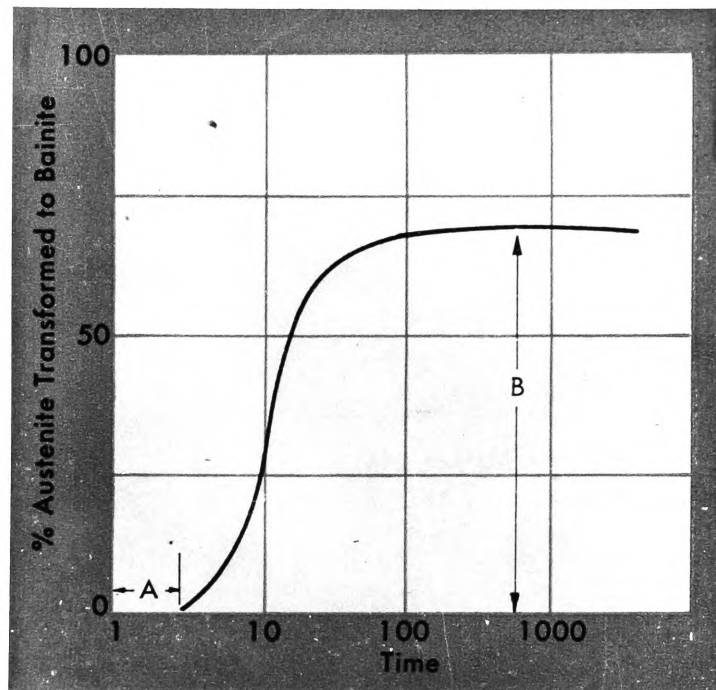


FIG.10 Progress of the isothermal
bainite transformation (Schematic).
(Hehemann and Troiano.⁽¹²⁶⁾)

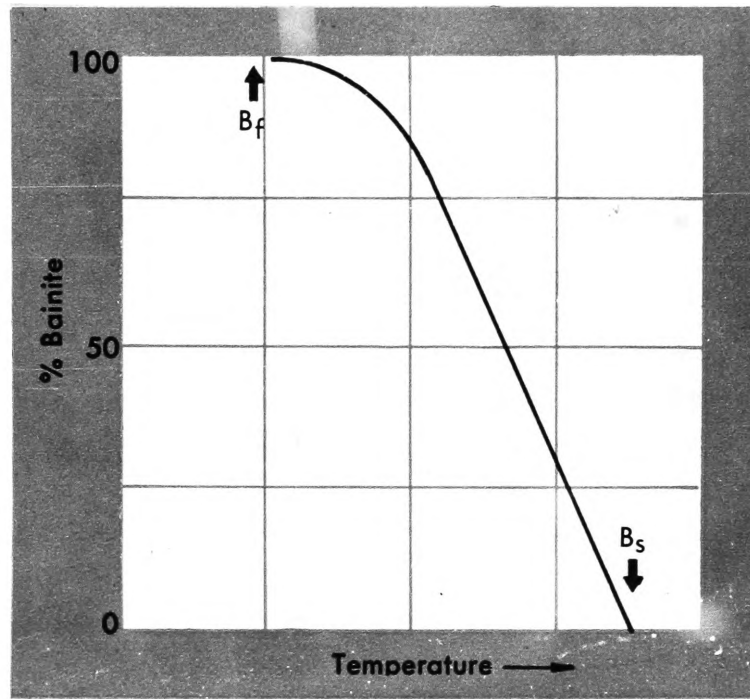


FIG.11 Influence of the transformation temperature on the volume fraction of bainite formed by the isothermal transformation. (Schematic).
(Hehemann and Troiano.⁽¹²⁶⁾)

steels and either isothermally or during continuous cooling in some alloy steels. An isothermal transformation curve is shown in Fig. 10.

The shape of the curve is typical of nucleation and growth processes i.e. transformation begins after an incubation period, proceeds for a short time and then ceases.

- 2) The curves for the transformation of austenite to bainite and to pearlite may either overlap or be separated, depending on the composition of the austenite (Figs. 1 and 2).
- 3) There exists a temperature, termed the bainite start temperature, B_s , above which bainite will not form.
- 4) Complete isothermal transformation of austenite to bainite is possible only below a certain limiting temperature, B_f (Fig. 11).
- 5) Partial transformation of austenite to bainite lowers the M_s temperature of the untransformed austenite and may therefore increase the amount of austenite retained at room temperature.

Recent work^(119,120,121,127) has shown that the transformation kinetics change at temperatures between 300 and 350°C. The change is usually considered to be the kinetic equivalent of the morphological distinction between

upper and lower bainite.

It has been suggested^(114,128) that diffusion of carbon in austenite is probably the rate controlling process in the formation of upper bainite. One measured activation energy of 34 K.cal./mole⁽¹²⁰⁾, for growth of upper bainite, is consistent with the activation energy of 32 K.cal./mole for diffusion of carbon in austenite⁽¹²¹⁾. However, this observation is not compatible with the lower activation energies also reported⁽¹¹⁹⁾ and the dependence of activation energy on carbon concentration⁽¹²¹⁾.

The measured activation energies for the bainite transformation, at temperatures below 300°C, were 14 K.cal./mole⁽¹²⁰⁾ and between 15 and 20 K.cal./mole⁽¹¹⁹⁾, indicating that the rate controlling process may be diffusion of carbon in supersaturated ferrite, for which the activation energy is 20 K.cal./mole⁽¹²¹⁾. However, Radcliffe and Rollason⁽¹²¹⁾ found that the activation energy depended on carbon concentration which seemed to preclude carbon diffusion as the rate controlling process. They suggested that the formation of bainite is not controlled by "any known diffusion process".

Kaufman, Radcliffe and Cohen⁽¹²⁵⁾ suggested that the observed change in kinetics, at temperatures between 300 and 350°C, may result from the mechanism of carbide

precipitation. They contended that, as far as the ferrite of bainite was concerned, there was no sharp kinetic division between upper and lower bainite.

4.4 Crystallography

4.41 Crystallographic Properties

Most of the crystallographic data for the bainite transformation relate to the ferrite phase. Only three orientation analyses have been reported for the carbides. (105,108,111). Plates of upper bainite have habit planes near $(111)_\gamma$ whereas the habit plane of lower bainite is irrational $(13,50,71)$, independent of carbon content, and changes gradually and continuously with transformation temperature. ⁽⁷¹⁾ (Fig. 14).

With decrease of transformation temperature the orientation relationship ⁽⁵⁰⁾, between the lattices of the ferrite and austenite, changes from the Nishiyama ⁽⁵⁶⁾ relationship,

$$(111)_\gamma // (110)_\alpha$$

$$[211]_\gamma // [011]_\alpha$$

to the Kurdjumov-Sachs ⁽⁵⁵⁾ relationship,

$$(111)_\gamma // (011)_\alpha$$

$$[0\bar{1}1]_\gamma // [1\bar{1}1]_\alpha.$$

Shackleton and Kelly ⁽¹⁰⁸⁾ and Srinivasan and Wayman ⁽¹¹¹⁾ found that the orientation relationship between

the lattices of the cementite and ferrite in lower bainite was

$$(001)\text{Fe}_3\text{C} \quad // \quad (211)_\alpha$$

$$[100]\text{Fe}_3\text{C} \quad // \quad [0\bar{1}1]_\alpha$$

$$[010]\text{Fe}_3\text{C} \quad // \quad [1\bar{1}\bar{1}]_\alpha$$

The relationship was also observed between the lattices of ferrite and cementite in tempered martensite⁽³⁸⁾.

Shackleton and Kelly⁽¹⁰⁸⁾ analysed 36 electron diffraction patterns from upper bainite and found 23 to be consistent with the above relationship. The other 13 indicated different relationships, with considerable variation between them. In all of these, the relationships between the lattices of the carbide and austenite phases were the same as found by Pitsch^(129,130) for pro-eutectoid cementite:

$$(001)\text{Fe}_3\text{C} \quad // \quad (\bar{2}25)_\gamma$$

$$[100]\text{Fe}_3\text{C} \quad // \quad [\bar{5}5\bar{4}]_\gamma$$

$$[010]\text{Fe}_3\text{C} \quad // \quad [\bar{1}\bar{1}0]_\gamma$$

The different ferrite-cementite orientation relationships were then explained in terms of different variants of the Kurdjumov-Sachs relationship between the lattices of the ferrite and austenite.

Shimizu, Ko and Nishiyama⁽¹⁰⁵⁾ reported the orientation relationship between the lattices of the cementite and ferrite in lower bainite as

$$(011)\text{Fe}_3\text{C} // (011)_\alpha$$

$$[100]\text{Fe}_3\text{C} // [01\bar{1}]_\alpha$$

The directional component of this relationship is identical with that subsequently reported.^(108,111) The planar component deviates $1^\circ 40'$ from the relationship found by Shackleton and Kelly and Srinivasan and Wayman. However, the deviation is within the accuracy limits of electron diffraction and therefore, it would seem probable that the results of Shimizu, Ko and Nishiyama are consistent with those reported by Shackleton and Kelly and Srinivasan and Wayman.

4.42 Crystallographic Theory

Investigations of the bainite transformation have provided evidence to suggest that the bainite and martensite transformations, in iron alloys, may be similar. The bainite transformation produces relief effects on polished surfaces,^(71,111,131) and from the nature of the surface tilt, the shape change accompanying the transformation has been shown to correspond approximately to an invariant plane strain.⁽⁴⁴⁾ The habit

plane of bainite is a high index austenite plane (Fig. 14) and the f.c.c. austenite and b.c.c. ferrite are related by an approximate Kurdjumov-Sachs orientation relationship^(13,50), indicating a unique lattice correspondence between the austenite and ferrite, similar to that associated with the formation of ferrous martensites.

Although the similarities between the martensite and bainite transformations in iron alloys are well established, few investigations concerning the crystallography of the bainite transformation, have been reported. The crystallographic theory of martensitic transformations^(60,61,62) has been applied to the bainite transformation in an Fe-1.35%C alloy by Bowles and Kennon⁽⁷¹⁾. They used the theory to examine the hypothesis that the crystallographic features of bainite arise during the formation, at or near the interface, of supersaturated ferrite. Bowles and Kennon attempted to account for their measured bainite habit planes by allowing the lattice invariant shear to occur on any plane containing the direction, in the b.c.c. phase, which was generated from $[1\bar{1}0]_{\gamma}$. Using the theory, habit planes, compatible with experiment, were obtained and the habit planes for lower bainite were probably consistent with the orientation relationships obtained using pole figure methods.

However, the habit planes for upper bainite were not in agreement with reported orientation relationships.

Srinivasan and Wayman⁽¹¹¹⁾ determined the specific habit plane indices of lower bainite plates in an Fe-8%Cr-1.1%C steel. They demonstrated that the measured habit plane and orientation relationship were not compatible with the hypothesis that the complementary strain occurred on the ferrite twinning elements, and proposed that the strain corresponds to a slip inhomogeneity involving shear on both the $(101)_\alpha$ and $(112)_\alpha$ planes, in the $[\overline{111}]_\alpha$ direction.

4.5 Factors which Influence the Transformation

4.51 Austenite Grain Size

The austenite grain size and austenitising temperature are closely related and it is therefore difficult to establish the independent effect of each variable on the bainite transformation. However, several attempts have been made to distinguish the individual effects.

Graham and Axon⁽¹³²⁾ reported that the bainite incubation period was shortened by increasing the austenite grain size. It was proposed that the first bainite plate to form must grow against the restraint imposed on it by the matrix and this restraint is greater the smaller the grain size. They also showed that the time required for

the completion of transformation was not sensitive to the austenite grain size.

On the other hand, Barford and Owen⁽¹³³⁾ showed that the rate of transformation was substantially reduced by increasing the austenite grain size. They attributed this effect to the reduction of available nucleation sites at grain boundaries, resulting from the increased austenite grain size.

The inconsistencies of these observations can only be resolved by consideration of the mechanisms of transformation. The effect observed by Barford and Owen would be expected if transformation proceeded by nucleation and diffusional growth, whereas if the transformation proceeded by a similar mechanism to martensitic transformations the observations of Graham and Axon can be explained.

4.52 Austenitising Temperature

Graham and Axon⁽¹³²⁾ showed that, for a particular carbon concentration, the incubation period for the transformation increased with austenitising temperature. The longer incubation period was attributed to the clustering of carbon atoms in austenite. The higher the austenitising temperature the smaller the degree of clustering and consequently, fewer nuclei would form and a longer incubation period would result. On the other

hand, Barford and Owen⁽¹³³⁾ suggested that the retardation in the rate of transformation, reported by Graham and Axon, is confined to the austenitising temperature between 900 and 1000°C. They proposed that the bainite nuclei were ferrite embryos in the austenite. The results of Barford and Owen showed that austenitising at temperatures above 1000°C increased the transformation rate at 370°C. In view of this, the explanation of the retardation in terms of the removal of carbon clusters by increased thermal agitation (accompanying an increase in austenitising temperature) is not tenable.

Cottrell and Ko⁽¹³⁴⁾ observed that the rate of transformation, in a Ni-Cr-Mo steel, was increased by high temperature austenitisation. They believed the increased rate of transformation to be due to the re-distribution of non-metallic inclusions. It is known⁽¹³⁵⁾ that the solubility of sulphur in austenite increases with austenitising temperature, and on cooling therefore, the sulphur will precipitate as a fine dispersion of sulphide particles, which are possibly coherent with the austenite lattice. Cottrell and Ko suggested that, on cooling below the temperature at which precipitation occurs, the coherency strains aid the nucleation of bainite.

4.53 Composition of Austenite

The bainite transformation is influenced by the presence of alloying elements in the austenite, most elements having essentially the same effects. Increasing amounts of carbon^(136,137), manganese⁽⁶⁾, nickel⁽¹³⁸⁾, chromium⁽¹³⁹⁾, molybdenum⁽¹⁴⁰⁾, tungsten⁽¹⁴¹⁾ and vanadium⁽⁴⁾, in solution in the austenite, increase the incubation period for the transformation and displace the nose of the C-curve to lower temperatures. The presence of cobalt, in solution in the austenite, has the reverse effect⁽¹⁴²⁾ and decreases the incubation period for the transformation.

With the exception of carbon and carbon-nickel steels, the time-temperature conditions for the bainite transformation are separated from those of the pearlite transformation when the alloying element is present in sufficient concentration. (See Fig. 2).

4.54 Influence of Other Transformations

There are two ways in which the bainite transformation may be influenced by the presence of other transformation products,

- 1) Change in the composition of the austenite, or
- 2) Changes in the nucleation rate by the presence of the first formed transformation product.

The change in composition, accompanying the formation of a pro-eutectoid constituent, is significant only if transformation produced an appreciable volume fraction of the constituents. However, the presence of a small amount of transformation product may change the features of the bainite transformation in other ways.

Generally the presence of small volume fractions of ferrite⁽¹⁴³⁾ increases the bainite transformation rate. This has been attributed to nucleation of the bainite transformation by the existing ferrite. However, while small amounts of pre-eutectoid ferrite can provide nucleating sites and thus increase the bainite transformation rate, the presence of large volume fractions of ferrite would cause carbon enrichment of the remaining austenite and displace the bainite transformation to longer times (See section 4.53).

Gordon, Cohen and Rose⁽⁴⁾ showed that large volume fractions of carbide can increase the bainite transformation rate and attributed the effect to depletion of the austenite in carbon and other elements by the precipitation of carbides. Lyman and Troiano^(137,139) found that the B_s temperature is raised by carbide precipitation.

The formation of pearlite does not alter the composition of the untransformed austenite, but it is not unreasonable to expect that the presence of pearlite may influence the nucleation of bainite, by reducing the number of available nucleation sites, and hence retard the formation of bainite. On the other hand it is possible that the interfaces created by the pearlite transformation may aid the nucleation of bainite. However, the work of Jolivet and Portevin⁽¹⁴⁴⁾ showed that the pearlite transformation does not alter the kinetics of the bainite transformation.

The influence of the martensite transformation on the formation of bainite is considered in section 7.

4.55 Influence of Stress

Cottrell⁽¹⁴⁵⁾, Birks⁽¹⁴⁶⁾ and Thompson and Jepson⁽¹⁴⁷⁾ found that applied tensile stresses increase the rate of transformation to bainite without affecting the nature of the transformation product. On the other hand, compressive stresses change the distribution of the transformation product⁽¹⁴⁷⁾ which shows a marked parallelism of the plates contained in any one austenite grain. Although compressive stresses changed the distribution of the plates, the time required for completion of the transformation remained unchanged. In grains containing the greatest volume fraction of product, the plates were inclined at about 45° to the stress axis.

4.6 Mechanism of Transformation

Since the original suggestion, by Davenport and Bain, that bainite was martensite which had rapidly tempered, numerous attempts have been made to account for the formation of bainite. Most of the proposed mechanisms are not compatible with experimental observation. The original idea of Davenport and Bain was extended by Vilella, Guelich and Bain⁽¹⁴⁸⁾, who claimed that bainite formed by the abrupt formation of supersaturated ferrite plates along definite crystallographic planes, followed by rejection of carbide particles at a temperature dependent rate. Wever and Jellinghaus⁽¹⁴⁹⁾ had previously suggested that bainite formed as supersaturated ferrite. Smith and Mehl⁽⁵⁰⁾ suggested that bainite was nucleated by ferrite and formed by a nucleation and growth process. Förster and Scheil⁽⁴⁰⁾ also believed that bainite formed by a slow growth process but was crystallographically similar to martensite.

Hultgren⁽⁶⁾, and Greninger and Troiano⁽¹³⁾, were first to suggest that bainite formed directly as an aggregate and not as single phase crystals. Klier and Lyman⁽¹⁵⁰⁾, and Wiester⁽¹⁵¹⁾ proposed that regions of low carbon concentration in the austenite transformed to martensite which immediately decomposed to bainite, thus reviving earlier views.

Most of the principles of the earlier suggestions are embodied in the hypotheses of Hultgren and Cottrell and Ko. Hultgren⁽⁶⁾ proposed that bainite formed as an aggregate of ferrite and carbide, while Cottrell and Ko⁽¹¹⁴⁾ suggested that austenite transformed to supersaturated ferrite by a mechanism similar to that of the martensite transformation, after which carbides were rejected by a diffusion controlled process.

4.61 The Hultgren Mechanism

The Hultgren mechanism⁽⁶⁾ was developed from observations of the structure and composition of bainite and involves the separate formation of ferrite and cementite from austenite. The transformation is considered to be nucleated by a special form of ferrite which, as it forms, enriches the surrounding austenite in carbon. The enrichment results in precipitation of cementite rods in juxtaposition to the ferrite. The ferrite is then considered to continue to grow around the cementite particles.

4.62 The Cottrell and Ko Mechanism

Cottrell and Ko⁽¹¹⁴⁾ suggested that bainite nucleates as supersaturated ferrite by a mechanism similar to that of the martensite transformation but growth of the coherent ferrite plate is diffusion controlled. The free

energy change for the transformation is supplied by the low carbon concentration of the ferrite, which results either by diffusion of carbon into the surrounding austenite, or by precipitation of carbides within the ferrite. As a result, the bainite plate will stop growing when:

- i) the interface loses coherency
- ii) the carbon concentration in the ferrite, at the interface, can no longer be reduced sufficiently rapidly, or
- iii) some obstacle to growth is encountered.

The Cottrell and Ko mechanism was derived partly from observation of surface relief effects, similar to those accompanying the martensite transformation.

4.63 Comments on the Mechanisms

A thermally activated controlled process for the bainite transformation is suggested by, i) progress of the transformation occurs by growth of individual plates, ii) transformation can occur isothermally, iii) the bainite transformation starts after an incubation period, and iv) the shape of the isothermal transformation diagram. Thermal activation implies that long range diffusion must accompany the formation of bainite plates.

However, the irrational habit plane, and the shape change accompanying the transformation, indicates that bainite may form by a mechanism similar to that of the martensite transformation. The effect of stress (see section 4.55) on the kinetics of the transformation, and on the distribution of bainite plates, also favours a mechanism of this kind. However, since lenticular structures usually result only from transformations producing a single phase,⁽⁵⁰⁾ the structure of bainite can be explained in terms of the Cottrell and Ko mechanism only if it is assumed that transformation at the interface produces supersaturated ferrite which later rejects the carbides.

4.64 Nucleation

It is generally agreed that bainite is nucleated by ferrite. Zener⁽¹⁵²⁾ suggested that the composition of the nucleus is inherited directly from the austenite, while Fisher⁽¹¹⁸⁾ claimed that during quenching into the bainite transformation range of temperatures, carbon free regions in the austenite become non-coherent ferrite nuclei, which grow slowly during isothermal transformation. When the critical size for coherent growth is reached, (the critical size for non-coherent growth is less than that for coherent growth assuming reasonable interfacial tensions⁽¹¹⁸⁾), these nuclei grow rapidly to form a bainite plate. This

theory, however, is not compatible with the transformation kinetics. (See section 4.3).

Irvine and Pickering⁽¹¹³⁾ believed that the bainite nuclei were "quenched in carbon fluctuations". As the transformation temperature decreases, the critical size of nucleus for growth will also decrease and hence the number of available nuclei will increase. Hehemann and Troiano⁽¹⁵³⁾ proposed that the bainite transformation would not be completed at high temperatures because of the limited number of available supercritical nuclei.

The results obtained by Ko⁽¹¹⁵⁾ indicate that ferrite and bainite are formed from different kinds of nuclei, the ferrite nuclei being non-coherent and the bainite nuclei being coherent with the austenite lattice. Ko suggested that the coherent nuclei become stable at the Bs temperature and transformation to bainite then occurs in preference to the slow formation of non-coherent ferrite.

The proposal by Irvine and Pickering⁽¹⁰⁹⁾ and Krisement and Wever⁽¹⁵⁴⁾, that in high carbon steels bainite is nucleated by carbide, precipitated directly from the austenite, does not seem tenable since the orientation relationship of carbide, in bainite, is not the same as that for pro-eutectoid carbide, which nucleates directly from austenite.

5. STABILISATION OF AUSTENITE

It is well established^(44,155,156,157) that stabilisation of austenite retards the martensite transformation. If austenite is cooled to below the M_s temperature, held isothermally for a short time, then cooled again, athermal transformation does not begin immediately and at all lower temperatures the volume fraction of transformation product is less than that produced by direct cooling. The degree of stabilisation increases with the time for which the austenite is held isothermally. When cooling is arrested above the M_s temperature there is no general agreement as to whether or not stabilisation occurs, although it is known that the M_s temperatures of high carbon and chromium steels are depressed by arrested cooling above M_s ^(137,158).

The influence of austenite stabilisation on the bainite transformation has not been satisfactorily investigated. Jaffe⁽¹⁴³⁾ observed a stabilisation effect when both hypo- and hyper-eutectoid, low alloy steels were held isothermally for times less than the incubation period, and then cooled to a lower temperature within the bainite transformation range. This treatment retarded transformation at the lower temperature. Previously, however, Jaffe, Holloman and Norton⁽¹⁵⁹⁾ had observed appreciably

shorter incubation periods when quenching was interrupted briefly in the pro-eutectoid ferrite temperature range. Their observations were later confirmed by Moore⁽¹⁶⁰⁾.

Hehemann and Troiano^(126,153) found stabilisation effects as follows:

- 1) Partial transformation to bainite at a high temperature results in longer incubation periods at lower temperatures.
- 2) The incubation periods at lower temperatures are reduced by isothermal holding at higher temperatures for times shorter than the incubation periods.
- 3) At a particular transformation temperature, the retardation of transformation increases as the isothermal holding temperature is decreased.

All results described above were obtained using low alloy steels. Owen and White⁽¹⁶¹⁾ claimed that the morphology of the bainite in these steels is not the same as in plain carbon steels and therefore the conclusions may not be generally relevant. Owen and White investigated the effects of up quenching on the kinetics of the bainite transformation in a 0.8% carbon steel. They found that partial transformation at 258°C did not affect the transformation rate at temperatures between 258°C and 320°C, but caused a slight retardation in the

rate of transformation to upper bainite after up quenching to temperatures between 350°C and 400°C.

The mechanisms which have been proposed to account for stabilisation, are of two kinds. Firstly, processes which take place within the austenite or secondly, to some change which occurs as a result of the influence that prior transformation products have on subsequent transformation. Theories of the first kind are based on experimental evidence obtained from the martensite transformation in steels. Machlin and Cohen⁽⁴³⁾ showed that deformation of the austenite matrix, which accompanies the formation of a martensite plate, favours nucleation of other martensite plates. Glover and Smith⁽¹⁶²⁾ postulated that relaxation of elastic stresses destroys the favoured nucleation sites for further martensite formation, thus necessitating a decrease in temperature to increase the free energy difference between the two phases sufficiently for transformation to take place in the less favoured regions. Theories of the second kind have been proposed by Morgan and Ko⁽¹⁵⁶⁾, and by Cech and Holloman⁽¹⁶³⁾, and can possibly account for stabilisation that occurs in the absence of pre-existing transformation product but have difficulty in explaining the characteristics of stabilisation after partial transformation has occurred.

6. ISOTHERMAL TRANSFORMATION JUST ABOVE M_s

There have been few investigations of the isothermal transformation of austenite, at temperatures just above M_s , and considerable doubt exists as to the identity of the transformation product and the nature of the isothermal transformation diagram in this range of temperatures. Investigations of the isothermal transformation of austenite, above the M_s temperature, generally report bainite as the product phase, but the techniques used to identify the product have not been sufficiently accurate to substantiate the conclusions.

In isothermal transformation diagrams the rate of transformation, below the nose of the C-curves, usually decreases with decreasing temperature. However, for high purity Fe-1.16%C⁽¹⁶⁴⁾ and Fe-1.35%C⁽¹⁶⁵⁾ alloys, the transformation incubation period was observed to decrease at temperatures just above M_s . Howard and Cohen⁽¹⁶⁵⁾ attributed this behaviour to the formation of a "new", thin, plate-like product which was not bainite. Radcliffe and Rollason⁽¹²¹⁾ attempted to explain the reported decreased incubation period, with decreasing temperature near M_s , by proposing that the bainite transformation may be preceded by the formation of another product. No attempt was made to identify the product. Schaaber⁽¹⁶⁶⁾

observed a transformation, which preceded the bainite transformation at temperatures just above M_s , and suggested that it might be the isothermal martensite transformation.

Smith, Speich and Cohen⁽¹⁶⁴⁾ used hot stage microscopy and a double quenching technique to show that the unusual kinetics of the transformation, just above M_s , may be attributed to "stress induced" martensite generated isothermally by the start of the bainite transformation. They contended that, in previous investigations, isothermal martensite was mistakenly identified as lower bainite with consequent error in the description of the isothermal transformation diagram above M_s . Kulin and Speich⁽⁷⁹⁾ concluded that austenite transforms isothermally to martensite at temperatures above M_s . However, they used electrical resistivity measurements in their investigations and, as was the case for all reported investigations of the isothermal transformation above M_s , the identity of the transformation product was not unequivocally established.

7. ISOTHERMAL TRANSFORMATION JUST BELOW M_s

The possibility of isothermal austenite transformation, and the nature and mechanism of formation of the product, have been subject to considerable discussion for many years. It was established in section 3.5 that austenite may transform isothermally to martensite below M_s in Fe-Ni-Mn, Fe-Ni-C, and Fe-Mn-C steels, but the possibility also exists that austenite may transform isothermally to bainite below M_s . This possibility has not been satisfactorily investigated.

Many investigations of the isothermal transformation below M_s (114,126,164,165,167) have reported the product of transformation to be bainite, but Thompson and Jepson (147) considered that the product formed initially as martensite which changed to acicular bainite on tempering. However, it is well established (121) that even after prolonged tempering, martensite retains a tetragonal structure, and since no evidence of tetragonality has been obtained for the structure of the isothermal product, this suggestion would not appear to be tenable.

An observed increase in the isothermal transformation rate, below M_s , has been interpreted as the isothermal formation of bainite. (4,114,165,167,168) Since formation of martensite does not alter the composition of the untransformed austenite, any explanation of the

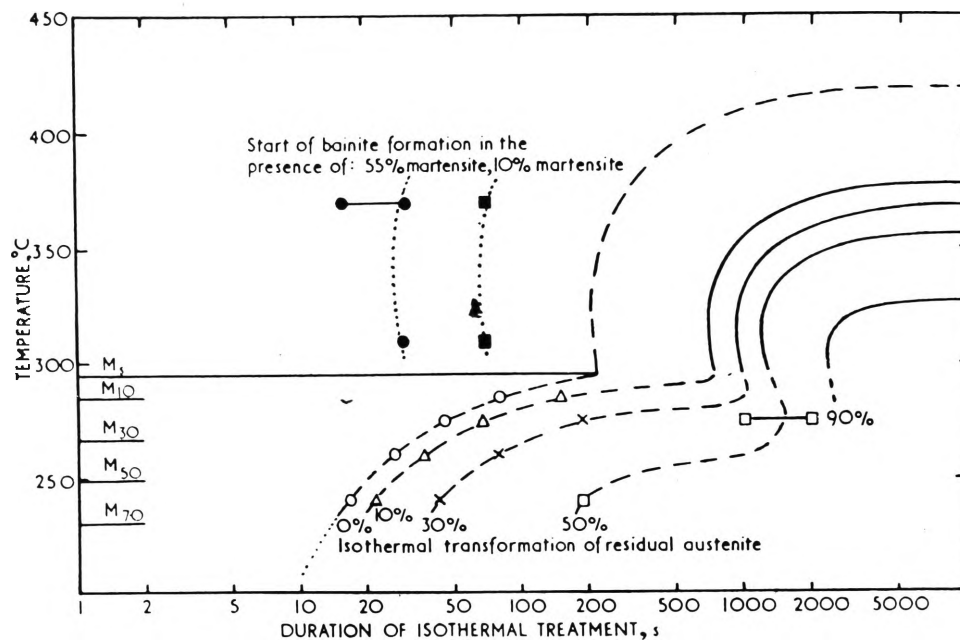


FIG.12 Diagram showing the influence of athermal martensite on the isothermal transformation of austenite below M_s . (Steven and Haynes. (167))

increased rate of transformation must involve nucleation of the isothermal transformation product by existing martensite plates. If the isothermal transformation product is bainite, it seems reasonable that the existing martensite plates may provide sites for nucleation as the lattices of both martensite and bainite have similar orientation relationships with that of austenite⁽⁵⁰⁾. However, Howard and Cohen⁽¹⁶⁵⁾ observed that many of the isothermally formed plates were not associated with the martensite plates and suggested that deformation of the austenite by formation of the martensite plates may aid nucleation. They also observed that, at low transformation temperatures, the large volume fraction of martensite appeared to have little effect on the kinetics of isothermal transformation.

Steven and Haynes⁽¹⁶⁷⁾ used lineal analysis to investigate the effect of existing martensite plates on the rate of isothermal transformation below M_s in a number of steels. They found that the presence of martensite decreased the incubation period for isothermal transformation from about 200 seconds at the M_s temperature to 30 seconds at 30°C below M_s . (Fig. 12). Steven and Haynes assumed that the product of isothermal transformation below M_s was bainite.

8. EXPERIMENTAL PROCEDURES FOR DISTINGUISHING BETWEEN MARTENSITE AND BAINITE

In the preceding sections the similarity of tempered martensite and lower bainite, formed in the same steel, have been clearly established. This section surveys the features of lower bainite and martensite which may possibly be used to distinguish the two transformation products in the same steel.

The transformations of austenite to martensite and bainite both result in volume expansion, similar changes in electrical resistivity and a ferro-magnetic product. Thus measurement of changes in volume, electrical resistivity, or magnetic susceptibility would not be capable of distinguishing between martensite and lower bainite. Information, concerning other physical properties, of the two constituents, is not available.

It should be possible to distinguish the b.c.t. crystal structure of quenched or lightly tempered martensite from the b.c.c. crystal structure of the ferrite of lower bainite, by X-ray methods. However, this technique is limited by line broadening, resulting from the lattice strain produced by both transformations, and by the relatively small volume fractions of products formed.

The activation energy for the martensite transformation is less than 500 cal./mole^(45,100) whereas, for the formation of lower bainite, the activation energy exceeds 14,000 cal./mole^(119,120,121). It should therefore be possible to distinguish the two transformations by thermodynamic measurements, but as the experimental techniques are generally complex and time consuming, it is desirable to establish a simpler criterion for differentiating the two transformation products.

In section 3.1 it was shown that martensite and bainite are morphologically similar in polished and etched metallographic sections. However, transmission electron microscopy of thin foils generally reveals morphological features peculiar to each transformation product. Untempered martensite consists of internally twinned plates whilst lower bainite is composed of ferrite plates containing precipitated carbides. No internal twinning has ever been observed in either upper or lower bainite. Thus the presence of internal twinning should be a distinguishing characteristic of martensite. However, the precipitation of carbides, during light tempering, has been shown to almost completely destroy all evidence of internal twinning^(19,20). Further since

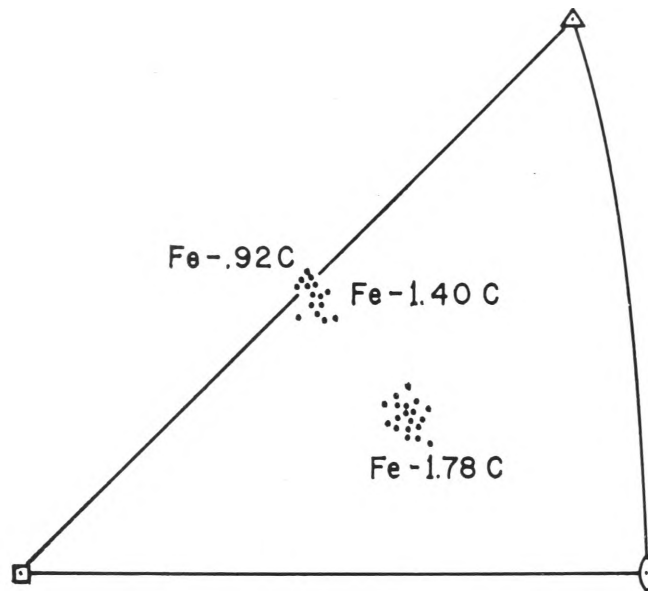


FIG.13 Martensite habit planes for medium and high carbon steels.
(Wayman. (25))

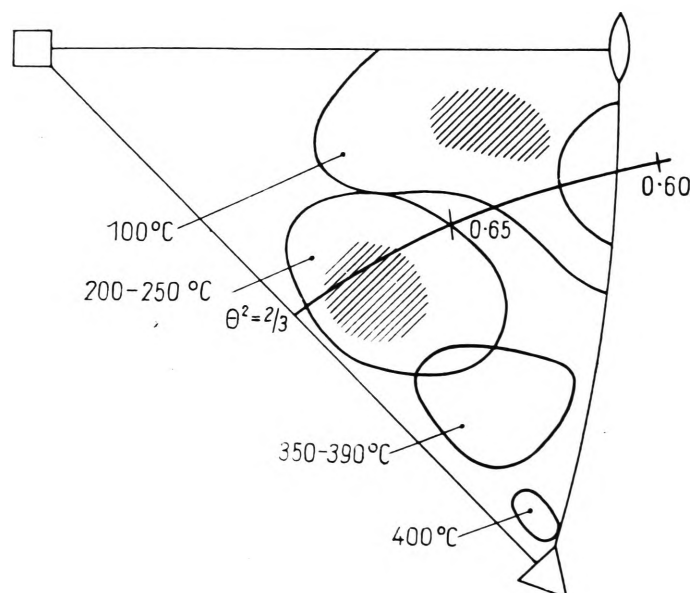


FIG.14 Showing variation of bainite habit planes with transformation temperature.
(Christian. (44))

the appearance of twins in transmission electron microscopy of foils is dependent on the orientation of the plate, with respect to the electron beam, twinning is normally observed in only approximately 20% of the plates. Consequently, high resolution electron microscopy, would not be capable of unambiguously distinguishing lightly tempered martensite from lower bainite.

It is clear therefore that bainite and tempered martensite cannot be readily distinguished by any of these means. However, since the two transformations have different crystallographic properties, determination of these properties should provide the means for distinguishing between the transformation products.

In sections 3.31 and 4.41 it was established that the habit plane of martensite in high carbon steels, is near $(259)_\gamma$, near $(225)_\gamma$ in medium carbon steels and near $(111)_\gamma$ in very low carbon steels (Fig. 13). On the other hand, the habit plane of bainite seems to be independent of carbon concentration but changes gradually and continuously with transformation temperature (Fig. 14). Consequently, habit plane measurements appear to offer the best experimental means for distinguishing between the two transformation products in high carbon steels, at low transformation temperatures.

The following sections of this thesis describe the isothermal transformation of a 1.44%C steel at temperatures near M_s . The habit planes of the transformation products, formed isothermally just above and just below the M_s temperature, are determined using quantitative metallographic techniques, and optical and transmission electron microscopical methods are used to determine the morphology and structural inhomogeneities of the products. Transformation kinetics are studied to obtain detailed information concerning the isothermal transformation diagram, in the range of temperatures near M_s .

PART B

EXPERIMENTAL WORK

9. INTRODUCTION

The investigations, which were described in sections 6 and 7, have established that austenite does transform isothermally at temperatures just above and just below M_s . It is generally agreed that one product of transformation above M_s is lower bainite but it is uncertain whether one (or more) additional products also form.

At temperatures below M_s the possibility exists that austenite may isothermally transform to lower bainite and/or martensite. The identity of the product, or products, of isothermal transformation below M_s has not been unequivocally established. Evidence for isothermal transformation below M_s has been obtained either by indirect methods, or by optical metallography in which the product of transformation has been assumed to be either martensite or bainite. In view of the uncertainty, concerning the identity of the products of isothermal transformation above and below the M_s temperature, the true form of the isothermal transformation diagram in this temperature range is not known.

In the following sections the experimental techniques used in the investigation are described and the results of habit plane determinations and morphological studies are shown to provide an unequivocal identification

of the products of isothermal transformation of austenite, at temperatures near M_s . The results of the kinetic study are used to establish the detailed form of the TTT diagram for the range of temperatures near M_s .

10. MATERIALS AND TECHNIQUES

10.1 Material

The material selected for study was a commercial hot rolled hyper-eutectoid steel available as 2.5 cm x .64 cm bar and with composition given in Table 1.

TABLE 1

Composition of Steel used in the Investigation							
C	P	Mn	Si	S	Ni	Cr	Mo
1.44	.035	.38	.12	.035	.020	.165	.005

To remove the effects of decarburisation, which may have occurred during production, 0.16 cm was ground from each surface producing a 2.2 cm x .32 cm bar.

Specimens approximately 1.25 cm x .64 cm x .32 cm in size were sectioned transversely from the bar and heat treated as described in section 10.2.

10.2 Heat Treatment

10.21 Austenitisation

The specimens, sealed in silica capsules evacuated to 10^{-5} mm Hg using a mercury diffusion pump, were austenitised at $1240^{\circ}\text{C} \pm 10^{\circ}\text{C}$ in a "Kanthal" wound horizontal tube furnace. Specimens used for habit plane determinations were austenitised for 8 hours to produce a large austenite grain size, while specimens used for

transformation studies, and determination of the Ms temperature of the steel, were austenitised for 4 hours. Specimens used for preparation of electron microscope transmission specimens were austenitised at $1000^{\circ}\text{C} \pm 10^{\circ}\text{C}$ for 30 minutes to avoid excessive grain coarsening of the austenite.

The microstructures of specimens austenitised for 4 and 8 hours and air cooled, consisted of fine pearlite and pro-eutectoid cementite, both at the edges of the specimens and within the specimens, indicating that no significant decarburisation had occurred. However, microscopical examination of quenched specimens showed a smaller volume fraction of retained austenite at the specimen edges than within the specimens. It was concluded therefore that some decarburisation had occurred and the maximum observed depth was .002" after austenitising at 1240°C for 8 hours. The decarburised layer was removed during the preparation of all specimens used for metallographic studies.

10.22 Determination of the Ms Temperature

The Ms temperature of the steel was determined using the "quench and temper" technique described by Greninger and Troiano⁽¹³⁾. Specimens were austenitised, the silica capsules broken in air, and the specimens quenched into an oil bath, held at temperatures between 50°C and 120°C. The specimens were maintained in the bath for 90 seconds to ensure attainment of the bath temperature and then rapidly transferred to molten salt* and maintained at 250°C for 2 minutes to temper any martensite present. The specimens were then quenched to room temperature. The Ms temperature was determined from metallographic estimation of the volume fraction of tempered martensite present in the specimens. The lowest temperature at which no tempered martensite was present in the specimens was taken as the Ms temperature.

The oil bath, into which the specimens were quenched, was heated electrically by an immersion heater and the temperature controlled to within $\pm 1/2^\circ\text{C}$ by a "Sunvic" TS1 bi-metallic strip. Temperature gradients within the bath were minimised by mechanical stirring.

* 50% NaNO_2 50% KNO_3

10.23 Quenching and Isothermal Transformation

Specimens for isothermal transformation studies were removed from the austenitising furnace, the capsules broken in air, and the specimens rapidly transferred to the oil bath maintained at the required temperature. Specimens for crystallographic and morphological studies were quenched to temperatures between 70°C and 130°C and isothermally transformed for times between 50 and 200 hours. Kinetic studies were made using groups of specimens isothermally transformed at temperatures between 70°C and 130°C for times between 30 minutes and 350 hours.

When necessary, specimens were quenched directly to room temperature by breaking the silica capsuled under oil.

10.3 Metallographic Technique

10.31 Optical Metallography

Specimens for metallographic study were mounted in "Epirez" cold setting resin to prevent tempering of any martensite formed during quenching to room temperature, and also to avoid transformation of any retained austenite present. To minimise rounding of the specimen surface during metallographic preparation, the hardness of the resin was increased by impregnation with 0-1 μ alumina powder.

The mounted specimens were wet ground on silicon carbide papers, to remove .025 cm from the surface, and polished to a 1 μ diamond finish.

All specimens were etched in 3% HNO₃ in ethyl alcohol (3% nital) and optical microscopy carried out using a Reichert MeF metallurgical microscope.

Surface relief effects were studied using specimens metallographically polished prior to sealing in the evacuated silica capsules. To minimise deterioration of the prepared surfaces the capsules were broken, after austenitisation, under oil maintained at the required transformation temperature. The surface relief effects were studied using oblique illumination. Some specimens were lightly polished and etched so that the features observed in relief could be correlated with the micro-structure in normal bright field illumination.

10.32 Habit Plane Analysis

Experimental determinations of habit planes requires measurement of the austenite planes on which the plates of transformation product form, together with a measurement of the orientation of the lattice of the austenite grain, within which the plates are formed.

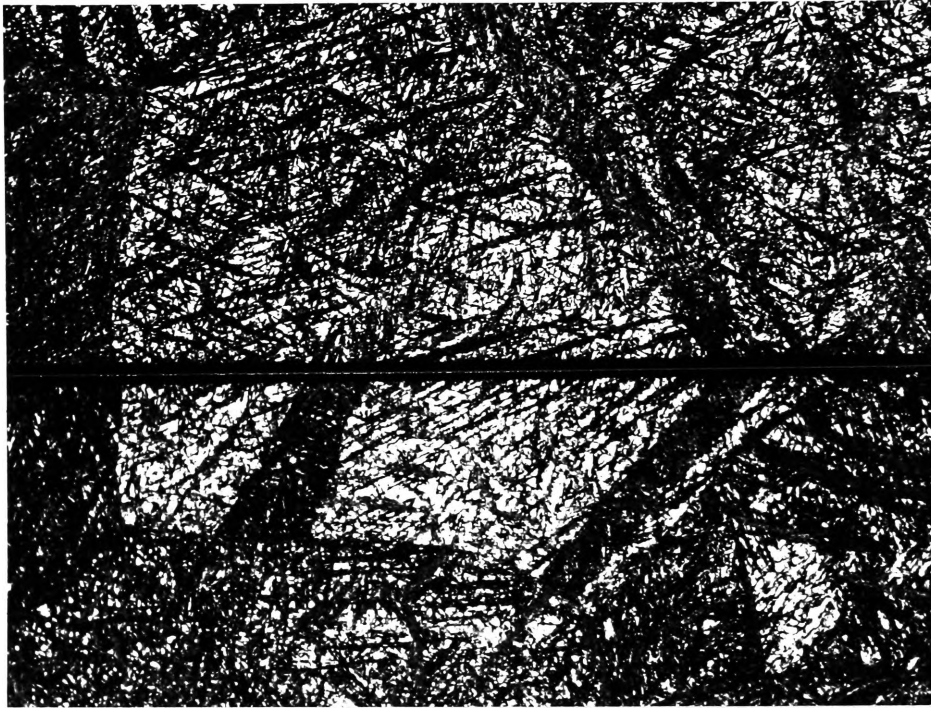


FIG.15 Composite photomicrograph showing twin vestiges in two normal surfaces through a grain in a 1.44%C steel, transformed at 120°C for 168 hours. X100.
Etchant 3% nital.

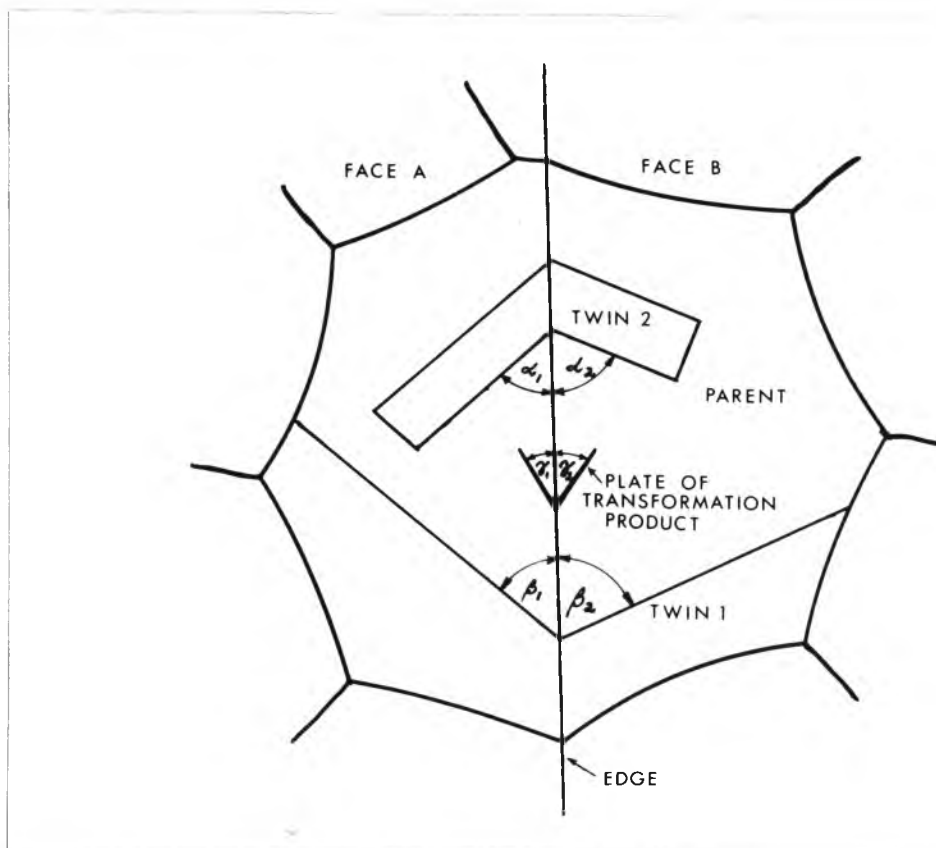


FIG.16 Diagrammatic representation of a specimen prepared for habit plane analysis. Surface A is the original polished surface. Surface B, approximately normal to A, was polished to facilitate measurement of the orientations of the twin planes and plates of transformation product.

The orientation of the lattice of the parent austenite was determined from measurement of twin vestiges⁽¹³⁾ in two non-parallel surfaces (See Appendix A). Each specimen was searched for grains containing two or more non-parallel twin vestiges. When a suitable grain was located, a second polished surface was prepared normal to the original surface through the grain, thus exposing the features to be examined in two surfaces as shown in Fig. 15.

The twin vestiges are traces of $\{111\}_\gamma$ annealing twins in the austenite and measurement of the angles $\alpha_1, \alpha_2, \beta_1, \beta_2$, (Fig. 16), specifies the orientations of two non-parallel $\{111\}_\gamma$ planes of the austenite and so uniquely defines the orientation of the austenite lattice, relative to the external geometry of the specimen.

The angles γ_1, γ_2 , (Fig. 16), subtended by a plate of transformation product appearing in both polished surfaces, uniquely specify the plane of the plate relative to the specimen geometry and thus to the austenite lattice. The angles were measured from plates matched in photomicrographs of the two surfaces, A and B (Fig. 16), taken at a magnification of 1000X (See Fig. 50).

Measurements of the angles $\alpha_1, \alpha_2, \beta_1, \beta_2$, (Fig. 16), were made using the rotating stage of a Reichert MeF metallurgical microscope. The angle between the two

surfaces, A and B (Fig. 16), was determined using a Unicam S25 single crystal goniometer.

Plates of transformation product, formed at temperatures near M_s , were small ($\sim 50\mu$ x $\sim 3\mu$) so that accurate measurements of the angles γ_1 and γ_2 required the preparation of an extremely sharp edge between the surfaces A and B (Fig. 16). Appendix B describes the polishing technique used to attain the sharp edge.

10.33 Electron Metallography

The structural inhomogeneities in the plates of isothermal transformation products, formed above and below the M_s temperature, were examined using high resolution electron microscopy of thin foils. An AEI EM6G electron microscope was used for the transmission studies and the technique used for the preparation of transmission specimens is described in Appendix C.

Electron diffraction patterns were obtained from thin foils containing the products of isothermal transformation at 120°C and 89°C and from foils containing untempered martensite and martensite tempered at 100°C for 5 hours and at 300°C for 2 minutes. An accelerating voltage of 100 KV was used to obtain the patterns.

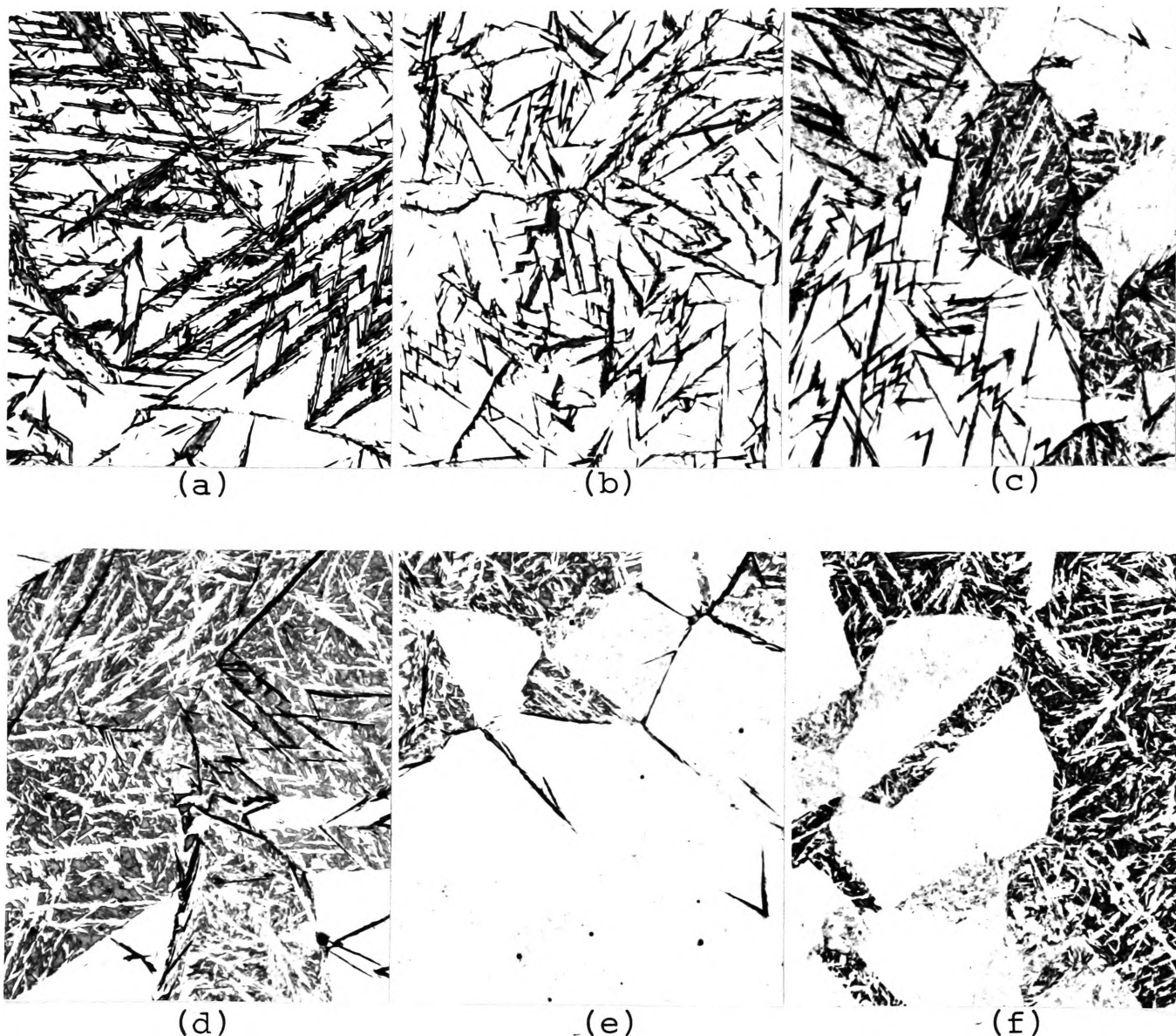


FIG.17 Photomicrographs showing the decrease in volume fraction, "f", of tempered martensite with increased temperature of the quenching bath.

a)	Quenched	55°C,	tempered	200°C	for	2 mins.	$f = \sim 0.40$
b)	"	70°C,	"	"	"	"	$f = \sim 0.20$
c)	"	80°C,	"	"	"	"	$f = \sim 0.10$
d)	"	90°C,	"	"	"	"	$f = \sim 0.03$
e)	"	92°C,	"	"	"	"	$f = \sim 0.01$
f)	"	94°C,	"	"	"	"	$f = \sim 0$

Etchant 3% nital

Magnification X100

11. RESULTS

11.1 The Ms Temperature

Metallographic examination of the specimens, heat treated as described in section 10.23, showed that the volume fraction, "f", of tempered martensite decreased as the quenching temperature was increased from 50°C to 92°C. Specimens quenched to 92°C contained only isolated plates of tempered martensite, confined mainly to the prior austenite grain boundaries, while no tempered martensite plates could be found in specimens quenched to 94°C (Fig. 17). It was therefore concluded that the Ms temperature of the steel was $93 \pm 1^\circ\text{C}$.

The measured Ms temperature of $93 \pm 1^\circ\text{C}$, for the 1.44%C steel used, is similar to the Ms temperature of 105°C, measured for a 1.35%C steel by Howard and Cohen⁽¹⁶⁵⁾, using the lineal analysis technique.

Several empirical equations, relating chemical composition and Ms temperature, have been proposed. Using the information given in Table 1, and the relationships developed by Payson and Savage⁽¹⁶⁹⁾ and Carapella⁽¹⁷⁰⁾ gives Ms temperatures of 27°C and 37°C respectively. The more recent relationship proposed by Nehrenburg⁽¹⁷¹⁾ gives an Ms temperature of 51°C. The discrepancies between calculated and measured Ms temperatures suggest that the empirical relationships are suitable only for low and medium carbon steels.

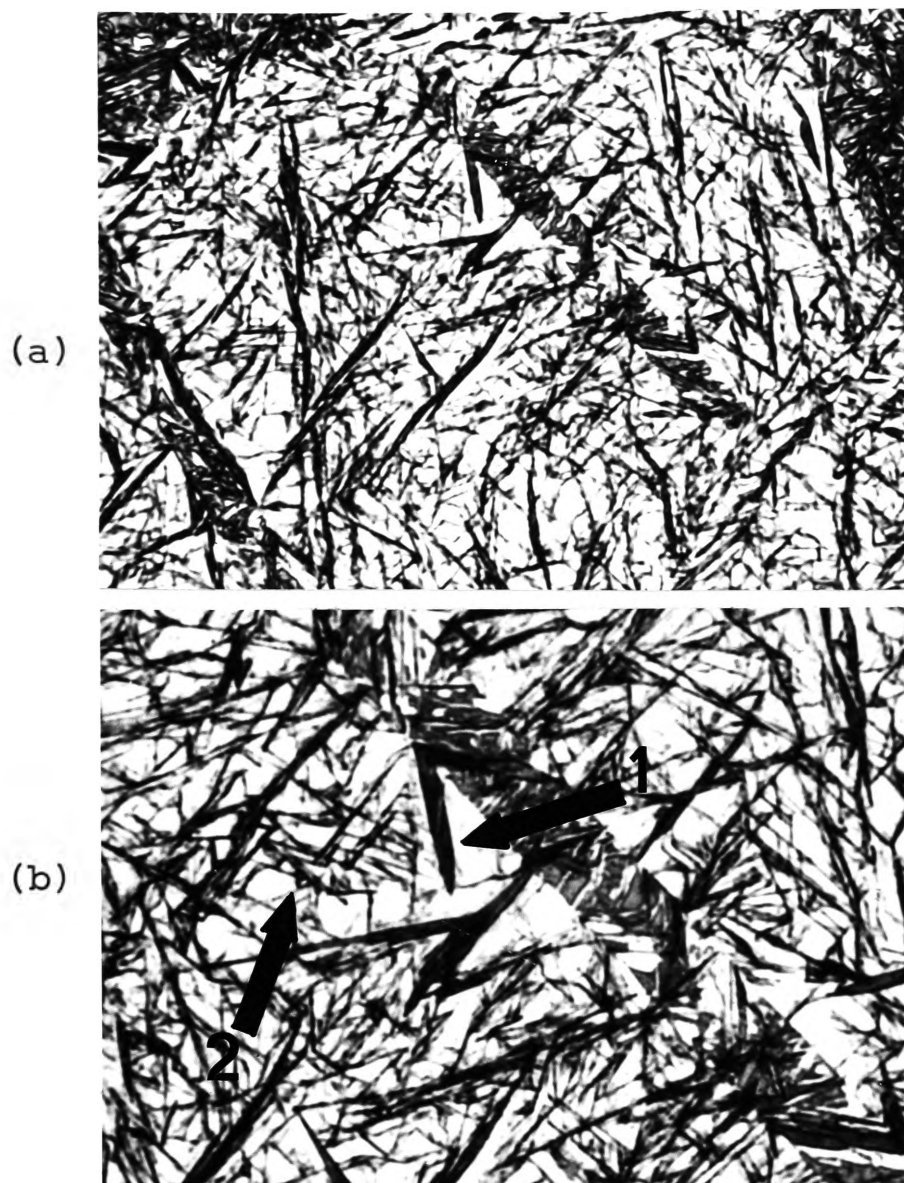


FIG.18 Photomicrographs showing plates of type 1 and type 2 transformation product formed by isothermal transformation at 105°C for 137 hours.

a) X100.

b) X500.

Etchant 3% nital.



(a)



(b)

FIG.19 Photomicrographs showing coarse athermal martensite plates formed during quenching to 88°C , and smaller plates of type 1 product formed by isothermal transformation at 88°C for 143 hours.

a) X100.

b) X500.

Etchant 3% nital.

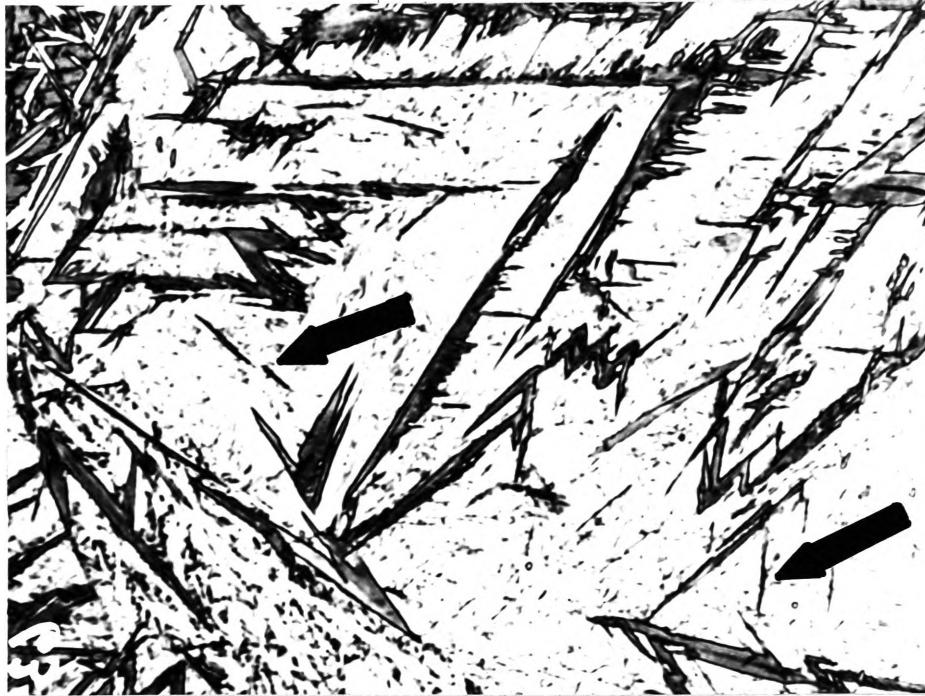


FIG.20 Photomicrograph showing athermal martensite plates and plates of type 1 transformation product (Arrowed), in a specimen isothermally transformed at 75°C for 22 hours. X500.

Etchant 3% nital.

11.2 Products of Isothermal Transformation Above Ms

The isothermal decomposition of austenite, at temperatures just above Ms, resulted in the formation of two transformation products, both having a lenticular morphology in metallographically prepared sections.

(Fig. 18). The transformation products will be referred to as type 1 product and type 2 product. The plates of type 1 transformation product were approximately 50 μ long and 4 μ wide. Type 2 transformation product was characterised by groupings of plates which were approximately 70 μ long and less than 1 μ wide.

11.3 Products of Isothermal Transformation Below Ms

The microstructures of specimens, transformed at 89°C for times between 50 and 170 hours, consisted of plates of the type 1 product and coarse tempered athermal martensite (formed during quenching to the transformation temperature) in a light etching matrix of untempered martensite and retained austenite (Fig. 19). The presence of small plates, contiguous with the large plates of tempered martensite (Fig. 20), was also observed in specimens which were quenched to room temperature and then tempered at 300°C for 60 seconds. These small plates were therefore formed during quenching. The other small plates (type 1 product, arrowed, Fig. 20) were not associated with

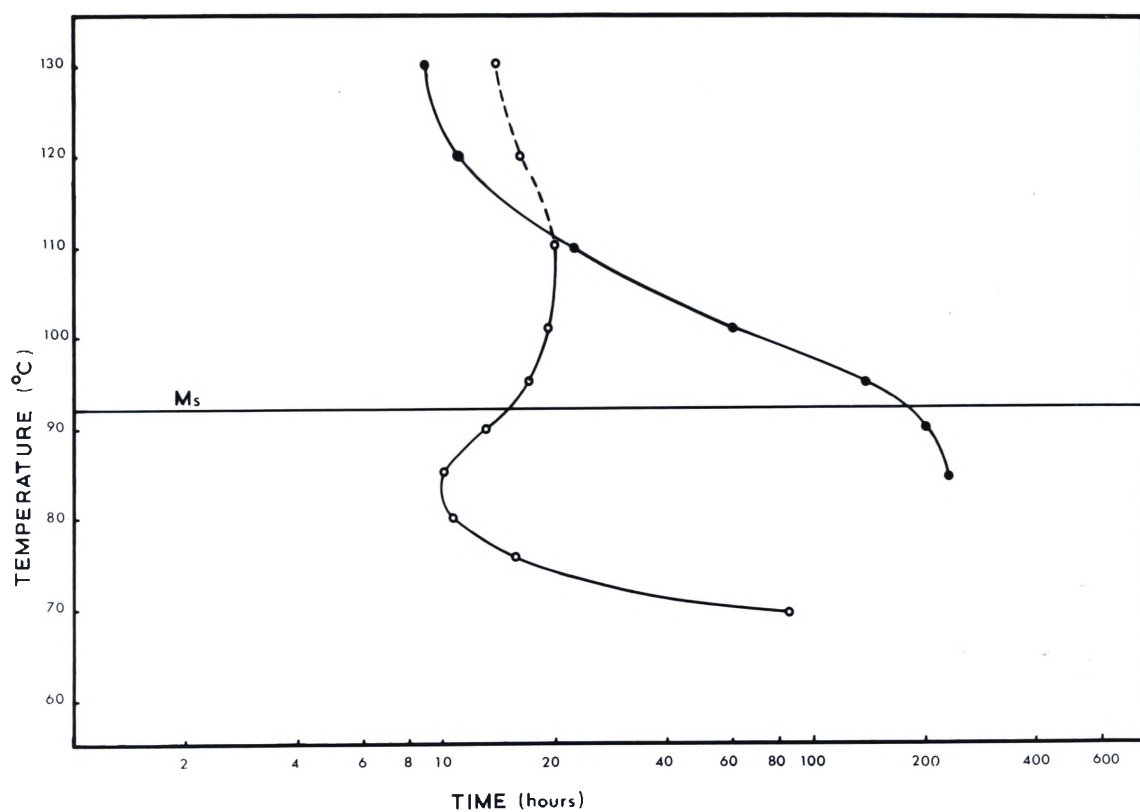


FIG.21 Isothermal transformation curves for type 1 and type 2 products, determined for 1% transformation.

○ TYPE 1

● TYPE 2

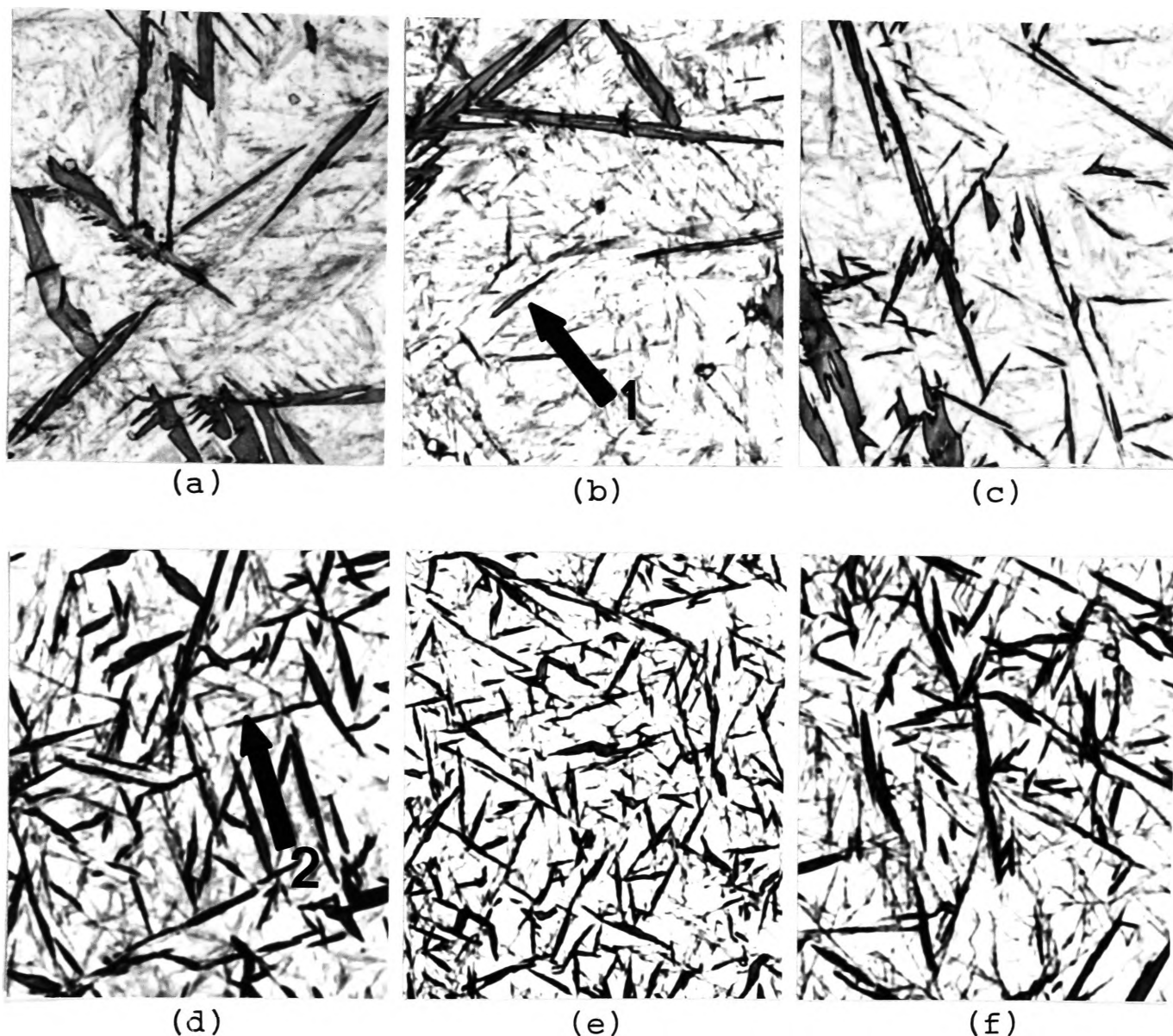


FIG.22 Photomicrographs showing the progress of isothermal transformation at 90°C.

a)	Transformed	8 hours,	X 500.	Athermal martensite.
b)	"	15 "	, X 500.	Type 1 product.
c)	"	69 "	, X 500.	" " "
d)	"	206 "	, X1000.	Type 1 and 2 Products.
e)	"	224 "	, X 500.	" " " " "
f)	"	224 "	, X1000.	" " " " "

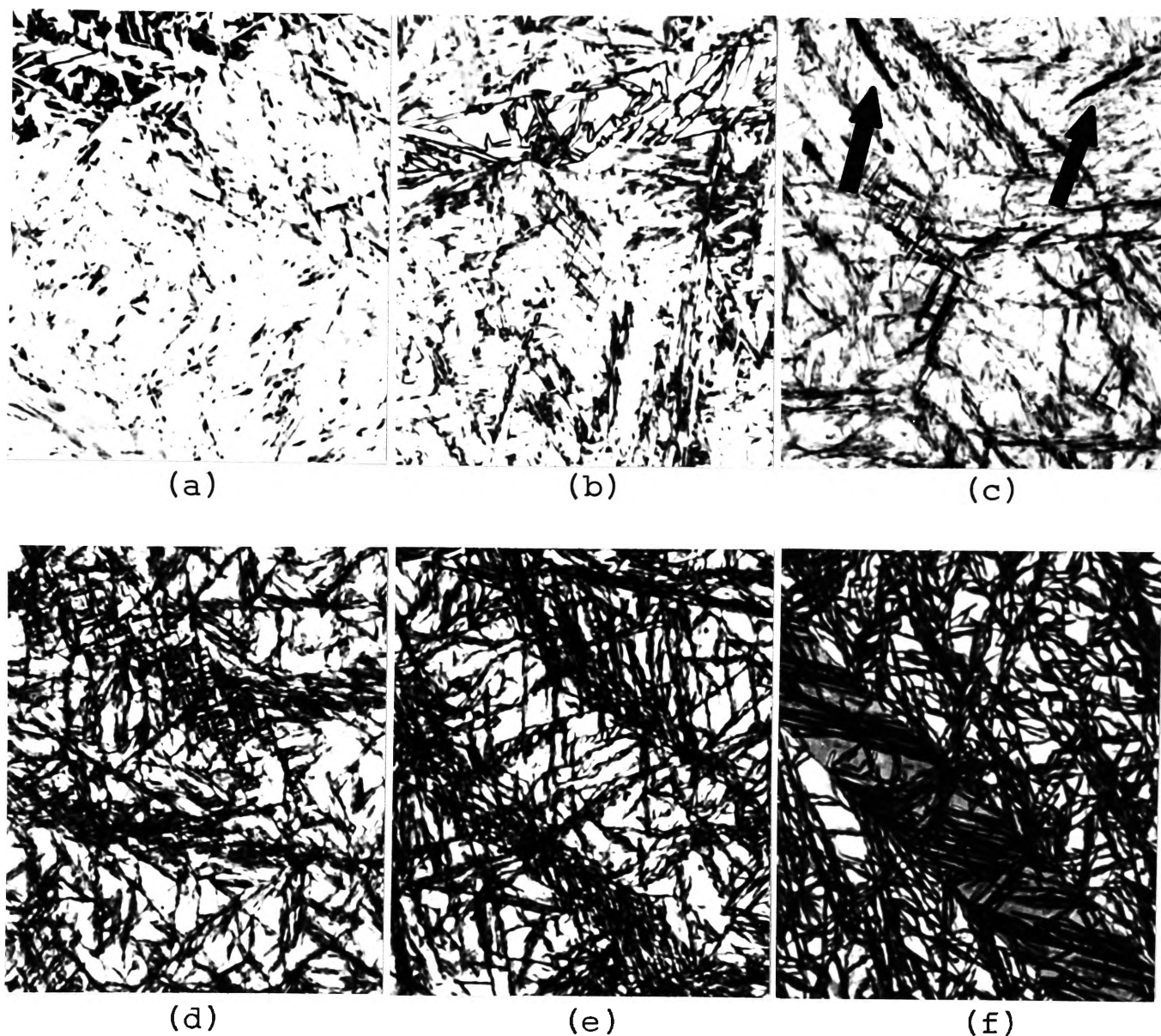


FIG.23 Photomicrographs showing the formation of type 2 transformation product by isothermal transformation at 120°C. Type 1 product formed in one specimen only (arrowed).

a)	Isothermally transformed for 8 hours.			
b)	"	"	"	10 "
c)	"	"	"	16 $\frac{1}{4}$ "
d)	"	"	"	27 $\frac{1}{4}$ "
e)	"	"	"	69 $\frac{1}{2}$ "
f)	"	"	"	166 "

Etchant 3% Nital. Magnification X500.

athermal plates and it was therefore concluded that nucleation of type 1 transformation product, by pre-existing martensite plates, had not occurred.

Plates of type 2 transformation product were observed in the microstructures of specimens isothermally transformed for times exceeding 200 hours (See fig. 22).

11.4 Transformation Kinetics

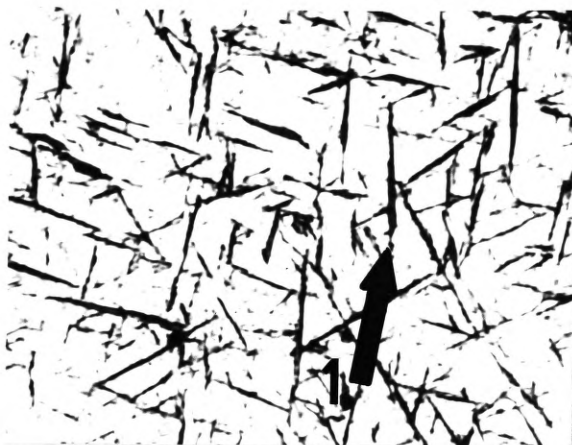
Estimation of the volume fractions of transformation products was made from metallographic examination of the specimens and 1% volume fraction was adopted as the criterion for establishing the start of isothermal transformation. The isothermal transformation curves, determined by these means, are shown in Fig. 21.

At temperatures below M_s both transformation products were formed, after transformation times exceeding the incubation periods, and the volume fraction of each product increased with time at the transformation temperature (Fig. 22). The incubation period for the transformation of austenite to type 1 product was a minimum at 84°C .

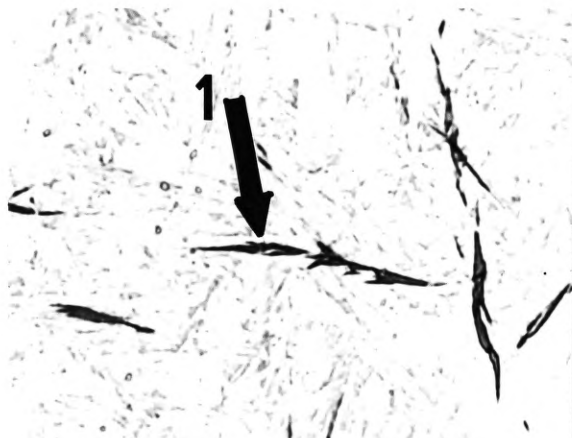
At approximately 112°C , both transformations had the same incubation periods. At 120°C plates of type 1 product were detected after 16 hours transformation but were not present in specimens isothermally transformed for longer periods at the same temperature. (Fig. 23). Similar



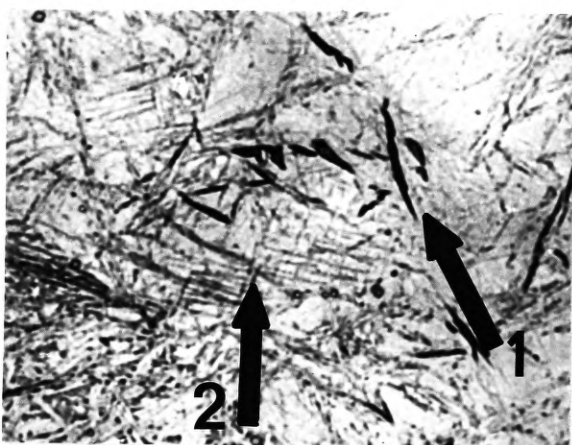
(a)



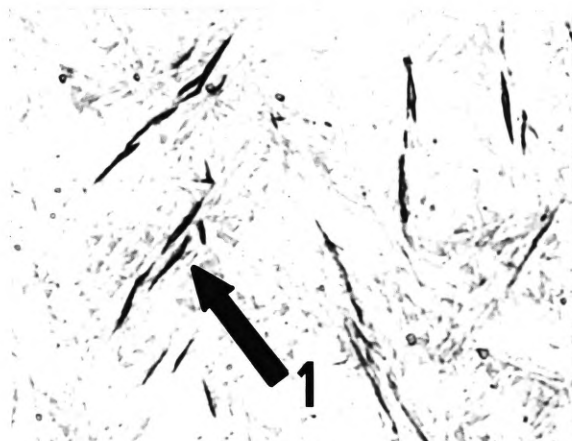
(b)



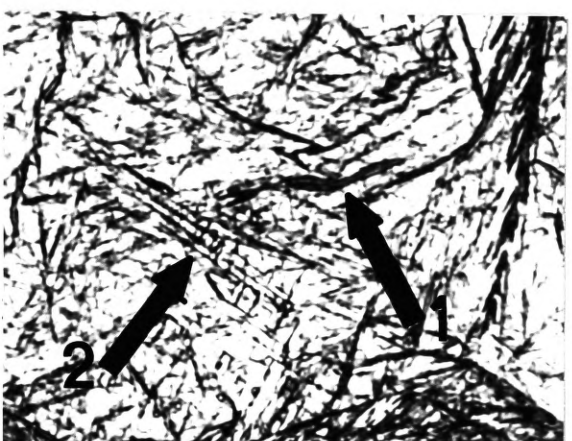
(c)



(d)



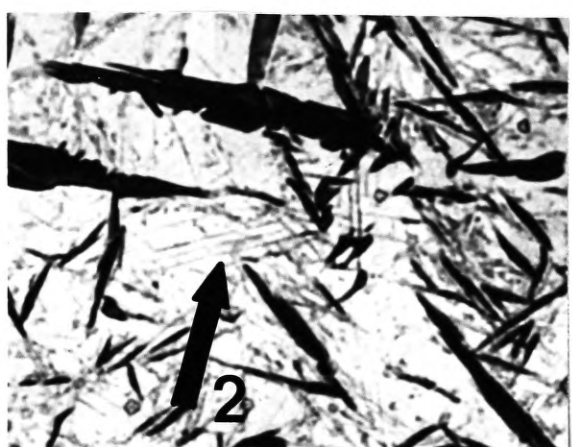
(e)



(f)



(g)



(h)



FIG.24 Photomicrographs showing the start of the isothermal transformations producing type 1 and type 2 products.

a)	Isothermally transformed	9¼ hours at 130°C	X500.
b)	"	"	X500.
c)	"	"	X500.
d)	"	"	X500.
e)	"	"	X500.
f)	"	"	X500.
g)	"	"	X500.
h)	"	"	X1000.
i)	"	"	X500.
j)	"	"	X500.

Etchant 3% Nital.

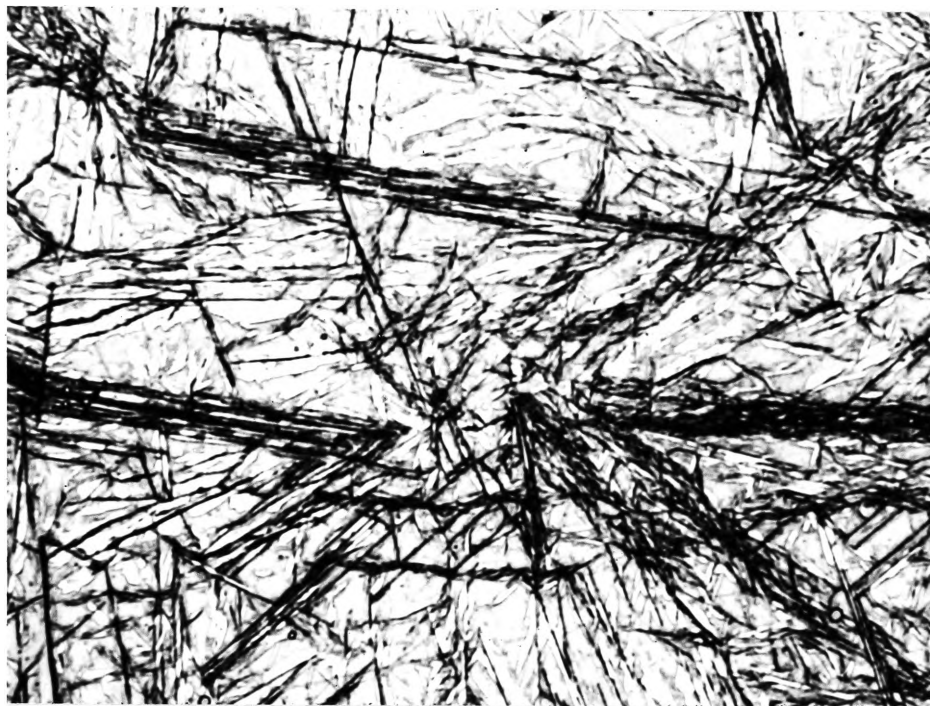


FIG.25 Photomicrograph showing plates of type 2 transformation product only, in a matrix of light etching martensite and retained austenite. Specimen isothermally transformed at 130°C for 23 hours. X500.

Etchant 3% nital.

results were observed at 130°C, at which temperature, plates of type 1 product were present in one end of a specimen isothermally transformed for 16 hours (Fig. 24). However, the product could not be found in two other identical specimens or in specimens transformed for longer times (Fig. 25). It was therefore concluded that incomplete removal of the decarburised layer, from one end of the surface of one specimen examined, may have resulted in the presence of the plates of type 1 product.

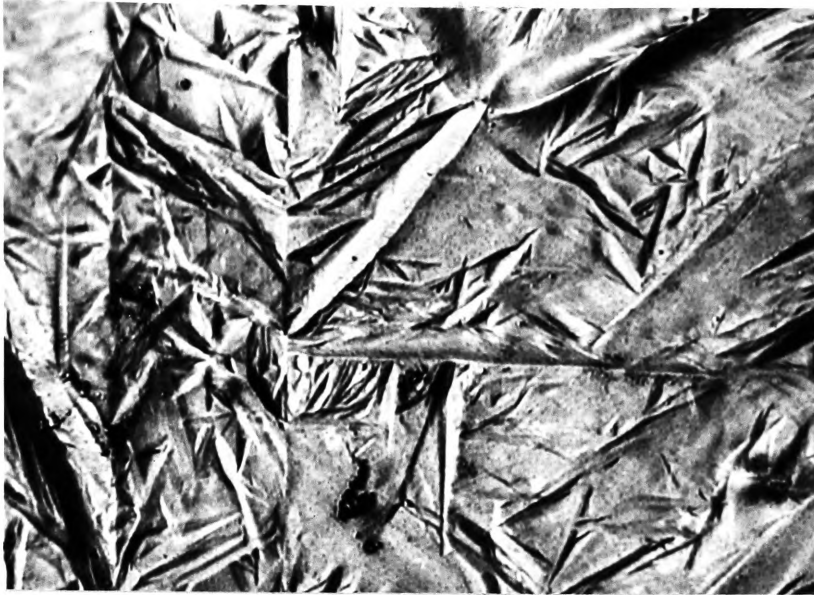
The incubation period for the transformation to type 2 product was longer than 200 hours over the temperature range examined below M_s . However, the slope of the transformation curve increased at temperatures just below M_s , suggesting the possibility of nucleation by existing plates of type 1 product and/or athermal martensite plates.

Type 2 transformation product was found at all temperatures investigated above M_s and the volume fraction of product increased with transformation time at all temperatures.

11.5 Morphology of Transformation Products

Optical microscopy of polished and etched metallographic sections established that both type 1 and type 2 transformation products form as plates. The plates

(a)



(b)



FIG.26 a) Photomicrograph showing surface relief effects accompanying the formation of plates of type 1 transformation product. Specimen isothermally transformed at 87.5°C for 137 hours. Oblique illumination.

b) Photomicrograph showing corresponding field to that shown in a) after light polishing, and etching in 3% nital.

Magnification X750.



FIG.27 Photomicrograph showing surface relief effects accompanying the formation of plates of type 2 transformation product. Specimen isothermally transformed at 115°C for 214 hours. Oblique illumination. X750.

(a)



(b)

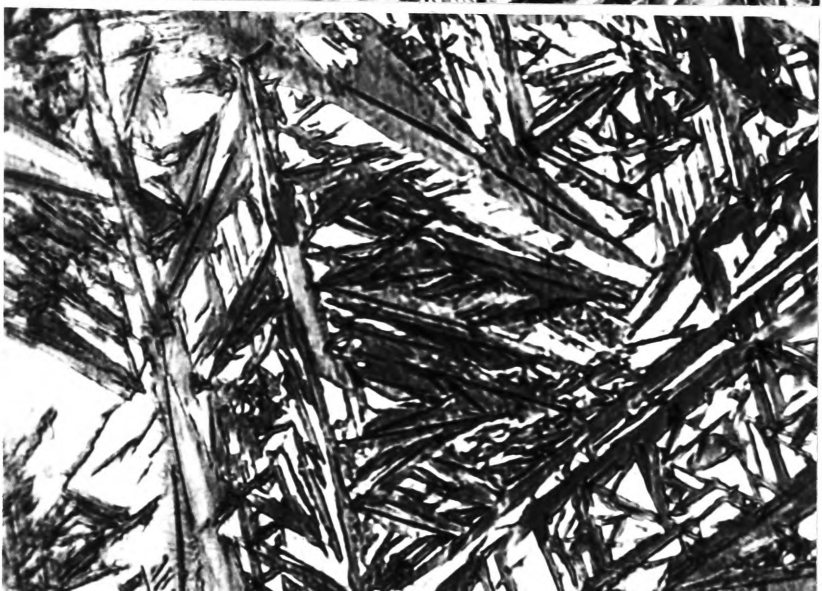


FIG.28 Photomicrographs showing a) surface relief effects accompanying the formation of athermal martensite plates (oblique illumination) and, b) the corresponding field after light polishing, and etching in 3% nital.

Magnification X750.

of type 1 product were usually lens shaped but, in some specimens, distorted or irregularly shaped plates were observed, particularly in specimens transformed at temperatures higher than 110°C (See Fig. 24). Plates of type 1 product formed at these higher temperatures were also generally larger than those formed at temperatures below M_s . The plates of type 2 product were long and thin ($\sim 70\mu \times \sim 1\mu$) and the plate shape did not appear to be influenced by transformation temperature.

Examination, using oblique illumination, of specimens metallographically polished before transformation, showed that surface relief effects were produced by both isothermal transformations and the surface relief effects accompanying the formation of type 1 product and type 2 product are shown in Figs. 26 and 27 respectively. The distribution and dimensions of the relief effects were consistent with the distribution and dimensions of the plates, observed in polished and etched sections.

Surface relief effects, accompanying the formation of athermal martensite plates, are shown in Fig. 28. These effects were very much larger than either of those produced by plates of type 1 or type 2 transformation products.

Transmission electron microscopical studies showed that the type 2 transformation product was composed of

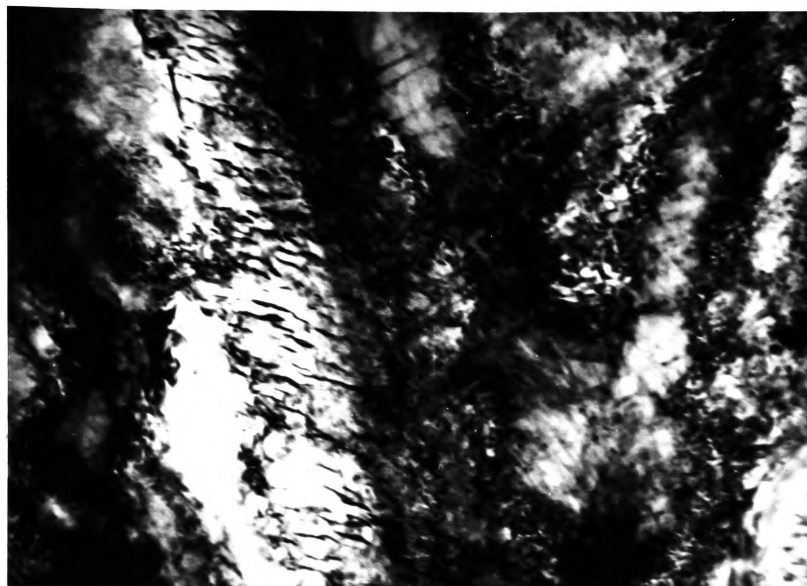


FIG.29 Transmission electron micrograph showing carbide distribution in a plate of type 2 transformation product formed during transformation at 120°C for 150 hours. X40,000.

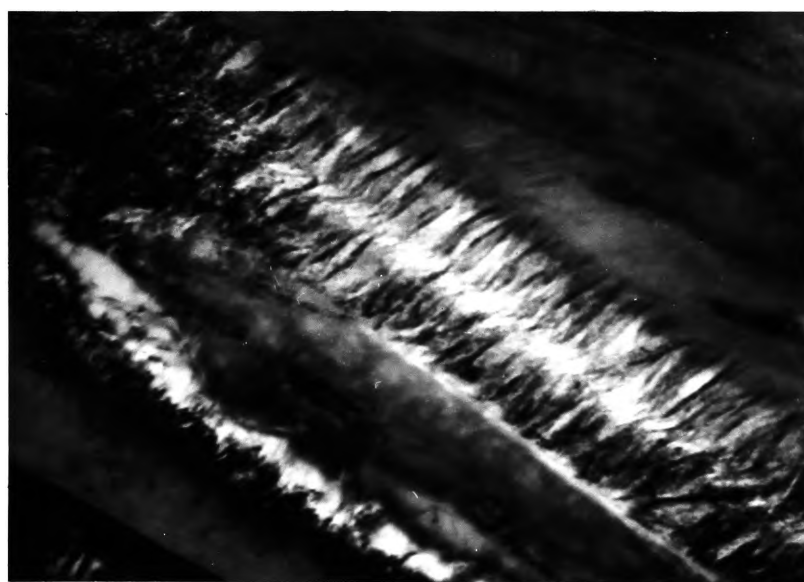


FIG.30 Transmission electron micrograph showing carbide platelets nucleated at the ferrite plate edges. Specimen transformed at 120°C for 150 hours. X55,000.



FIG.31 Transmission electron micrograph showing dislocations in a plate of type 1 transformation product. Specimen transformed at 89°C for 140 hours. X55,000.

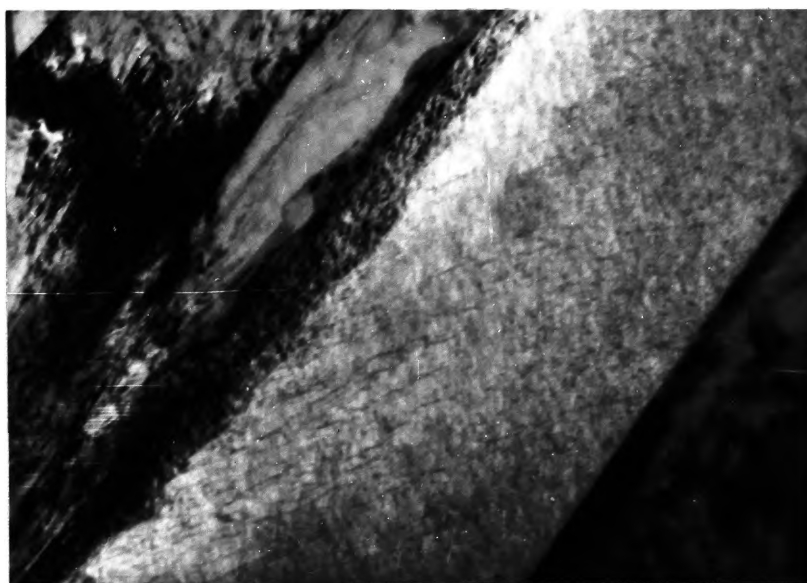


FIG.32 Transmission electron micrograph showing almost complete absence of internal inhomogeneities in a plate of type 1 product. Specimen transformed at 89°C for 140 hours. X55,000.

(a)



(b)

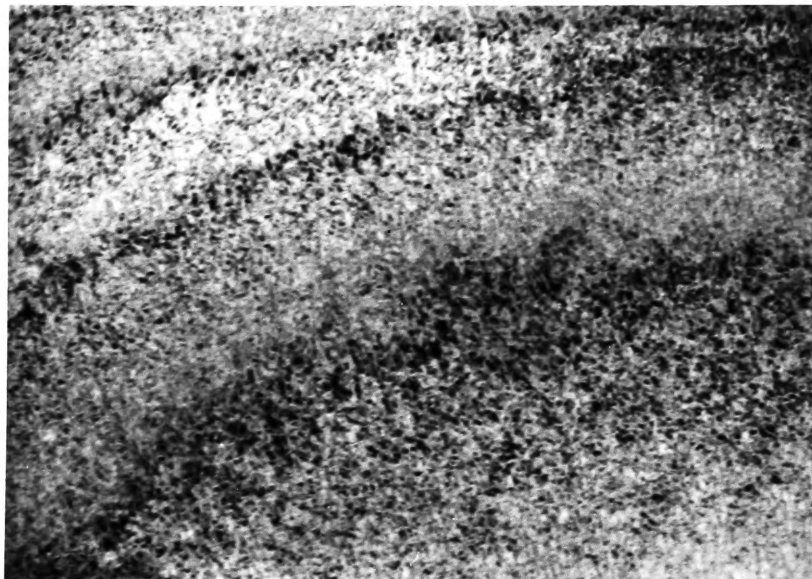


FIG.33 Transmission electron micrographs showing precipitates in a plate of type 1 transformation product. Specimen transformed isothermally at 89°C for 140 hours.

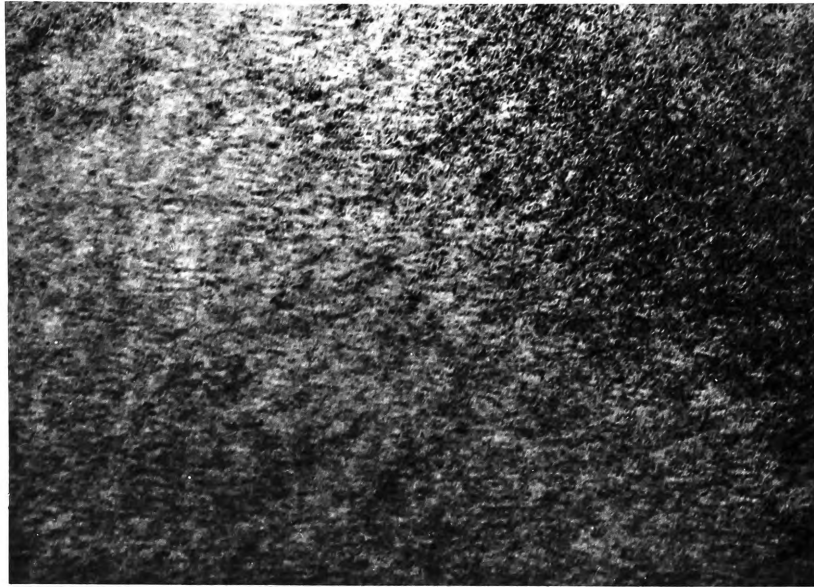
a) X30,000.

b) X55,000.



FIG.34 Transmission electron micrograph showing twins in an athermal martensite plate, formed by quenching to room temperature. X71,000.

(a)



(b)

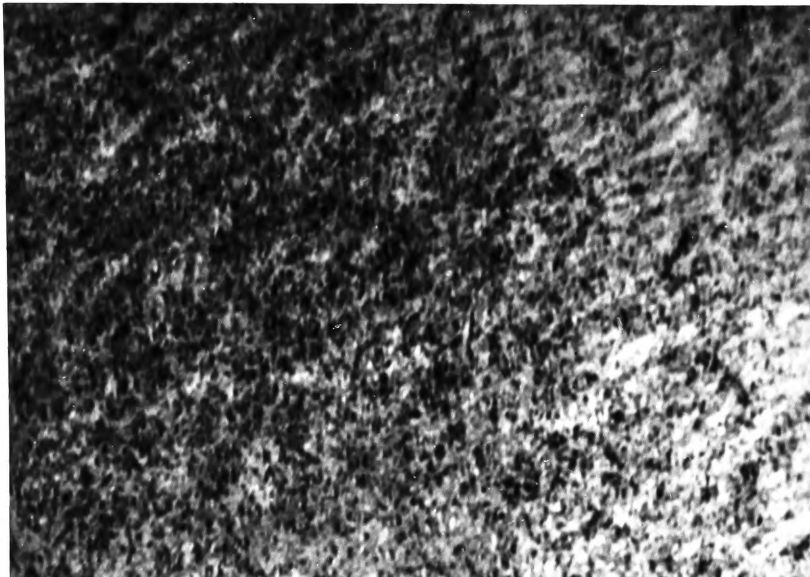


FIG.35 Transmission electron micrographs showing carbides precipitated in athermal martensite plates tempered at 100°C for 5 hours.

a) X55,000.

b) X100,000.

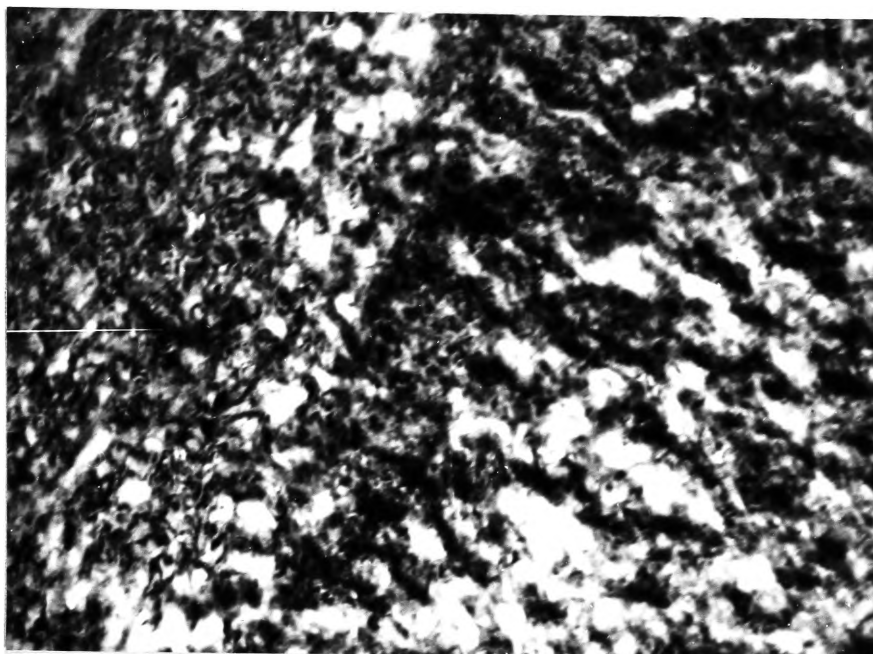
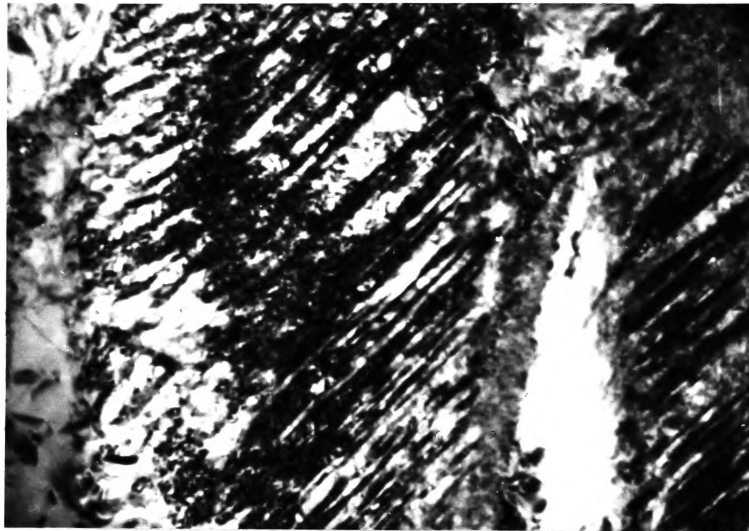


FIG.36 Transmission electron micrograph showing carbide platelets precipitated in an athermal martensite plate during tempering at 300°C for 2 minutes. X71,000.

(a)



(b)

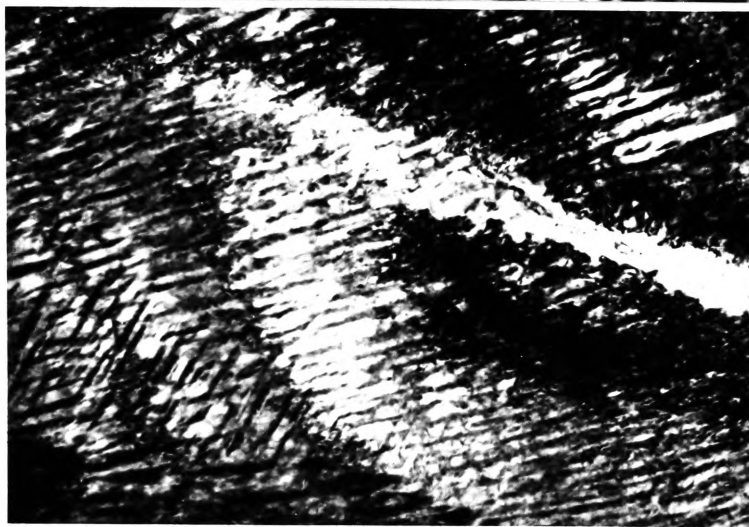


FIG.37 Transmission electron micrographs showing carbides precipitated in athermal martensite plates during tempering at 300°C for 2 minutes.

- a) Precipitation on twin planes. X55,000.
- b) Precipitation on and across the twin planes. X55,000.

ferrite plates containing carbide platelets oriented at approximately 55° to the ferrite plate axis (Fig. 29). In some plates, the carbide platelets had nucleated at the ferrite-austenite interface and grown into the ferrite, giving the appearance of a central mid-rib. (Fig. 30).

The structural inhomogeneities varied considerably within the plates of type 1 transformation product. Some plates contained a high density of dislocations, which were aligned in approximately perpendicular directions (Fig. 31), whereas other plates contained few internal inhomogeneities (Fig. 32). The majority of plates contained a dense dispersion of small spherical precipitates approximately 75\AA in diameter. (Fig. 33).

Athermal martensite plates were either internally twinned (Fig. 34) or appeared to contain no internal inhomogeneities (See section 3.1). Plates tempered at 100°C for 5 hours contained a dense dispersion of precipitates, approximately 40\AA in diameter (Fig. 35). The precipitate morphology was similar to that observed in some plates of type 1 product (Fig. 33). Tempering of athermal martensite plates at 300°C for 2 minutes resulted in the precipitation of carbide platelets (Fig. 36). In internally twinned plates, the carbides precipitated on the twin planes, and in some plates, across the twin planes (Fig. 37).

(a)



(b)

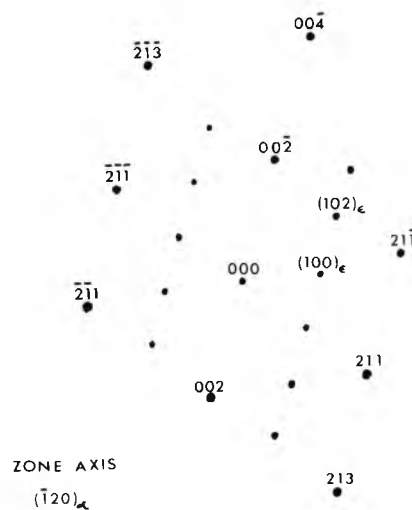


FIG.38 a) Electron diffraction pattern from a plate of type 1 transformation product formed during isothermal transformation at 89°C for 140 hours.

b) Strong reflections in the pattern (a) indexed according to the b.c.c. ferrite unit cell and the streaked reflections indexed according to the hexagonal unit cell of epsilon carbide.

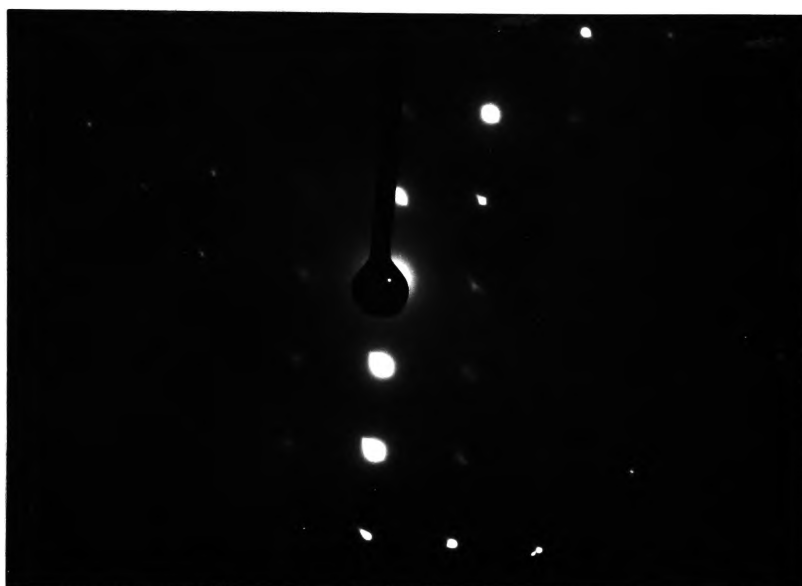


FIG.39 Electron diffraction pattern from a plate of type 1 transformation product showing streaking of the b.c.c. reflections. Specimen isothermally transformed at 88.5°C for 139 hours.

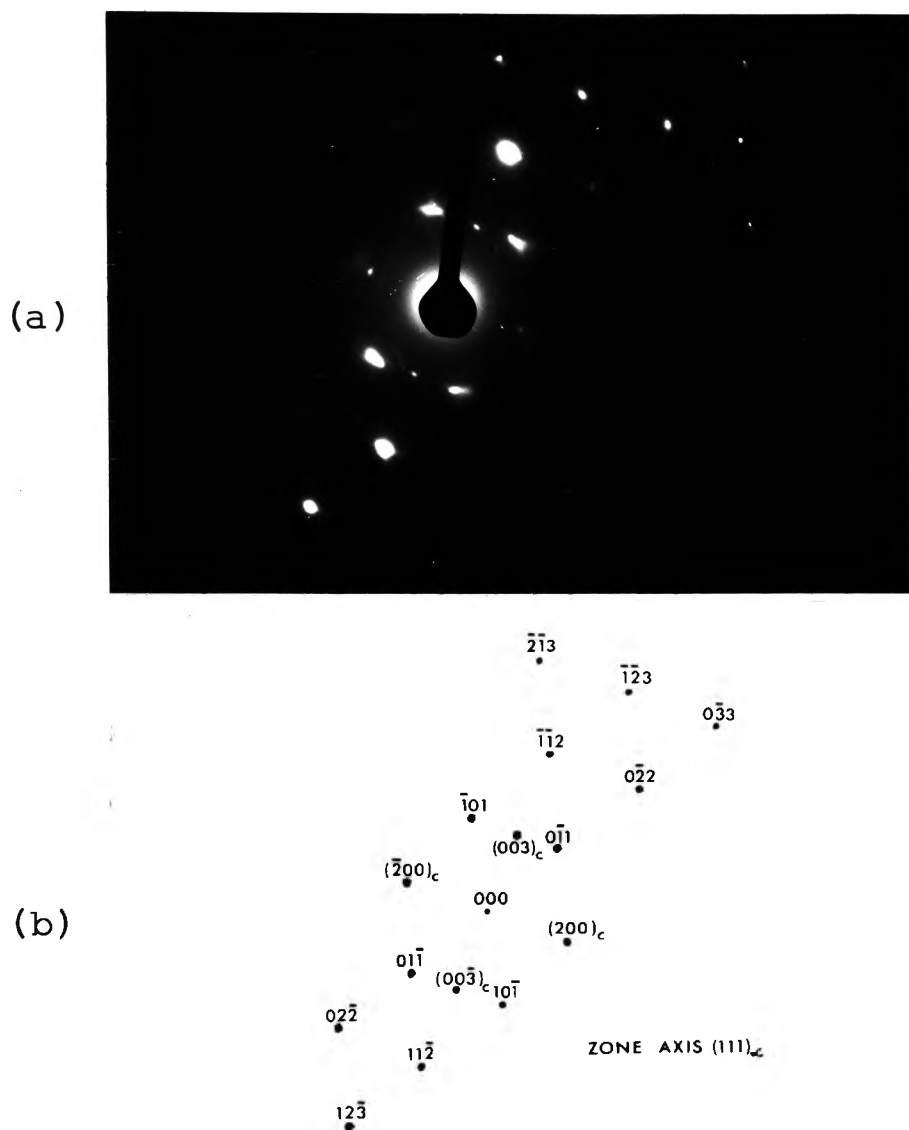


FIG.40 a) Electron diffraction pattern from a plate of type 2 product formed during isothermal transformation at 120°C for 150 hours.

b) Strong reflections in the pattern (a) indexed according to the b.c.c. ferrite unit cell and the weak reflections indexed according to the orthorhombic unit cell of cementite.

11.6 Electron Diffraction

The electron diffraction patterns obtained from plates of the type 1 product contained strong b.c.c. reflections from ferrite and weaker reflections from the carbide precipitate (Fig. 38). The interplanar spacings, obtained from the weak precipitate reflections (See Appendix D), were consistent with the structure of epsilon carbide, $\text{Fe}_{2.4}\text{C}$. Streaking of the carbide reflections, in two directions, was observed in a number of patterns (Fig. 38). However, it was not possible to determine the directions of reduced periodicity resulting in streaking, nor to determine the orientation relationships between the lattices of the epsilon carbide and the ferrite because insufficient diffraction patterns were obtained.

In two of the electron diffraction patterns, from plates of type 1 product, the b.c.c. reflections contained streaks (Fig. 39), which implied reduced periodicity of the reciprocal lattice in at least two $\langle 100 \rangle_{\alpha}$ directions. The significance of this streaking is not understood.

Diffraction patterns from type 2 plates also contained b.c.c. reflections and weaker reflections from the carbide platelets (Fig. 40). The interplanar spacings for the carbide phase (See Appendix D) agreed with published data for cementite, Fe_3C . The carbide reflections

(a)



(b)

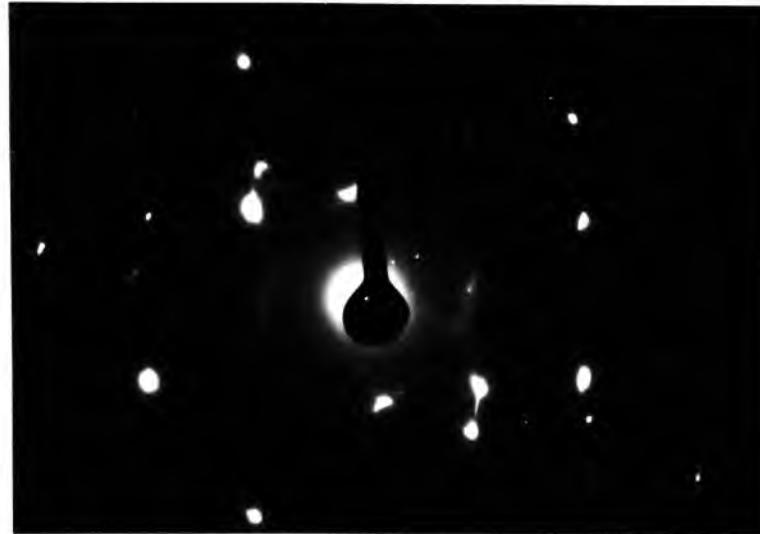


FIG.41 Transmission electron micrograph (a) and corresponding electron diffraction pattern (b) from an athermal martensite plate, showing streaking parallel to the twin traces. X55,000.



(a)



(b)

FIG.42 a) Electron diffraction pattern from an athermal martensite plate tempered at 100°C for 5 hours.

b) Strong reflections in a) indexed according to the b.c.c. ferrite unit cell and the weak reflections indexed according to the hexagonal unit cell of epsilon carbide.

(a)



(b)

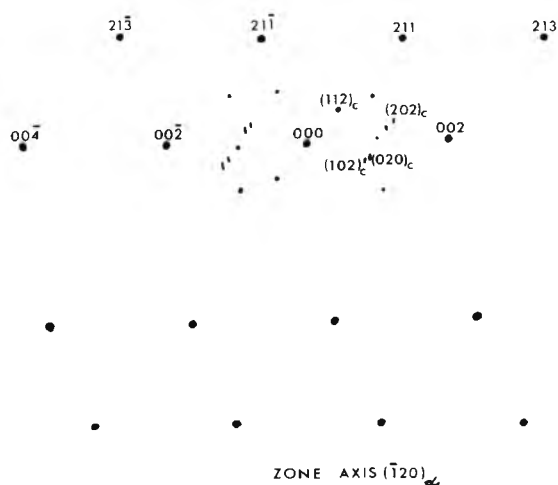


FIG.43 a) Electron diffraction pattern from an athermal martensite plate tempered at 300°C for 2 minutes.
b) Strong reflections in a) indexed according to the b.c.c. ferrite unit cell and the weak reflections indexed according to the orthorhombic unit cell of cementite.

were streaked in two directions but it was not possible to determine the directions of streaking from the limited number of patterns available. Streaks through the b.c.c. reflections were not observed in any of these patterns.

The directional component of the orientation relationship, between the lattices of the ferrite and cementite, was determined from the pattern shown in Fig. 40 and found to be

$$[0\bar{1}0]\text{Fe}_3\text{C} \quad // \quad [111]_{\alpha}$$

which is consistent with the results of Shackleton and Kelly⁽¹⁰⁸⁾ for the carbide of lower bainite.

Reflections obtained from plates of untempered martensite were indexed according to a b.c.c. unit cell. Faint streaking, parallel to the traces of the internal twins, was present in several patterns (Fig. 41), and suggests the possibility that carbide precipitation occurred on the twin planes during preparation of the foils.

Patterns obtained from martensite plates tempered at 100°C for 5 hours contained, in addition to the b.c.c. reflections, streaked reflections from epsilon carbide (Fig. 42). Martensite plates, tempered at 300°C for 2 minutes, produced b.c.c. reflections and reflections from cementite (Fig. 43).

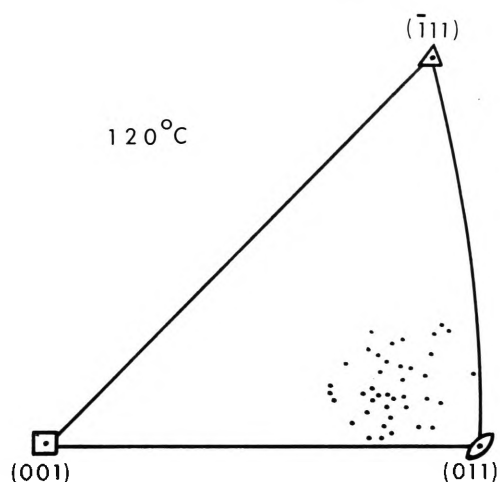
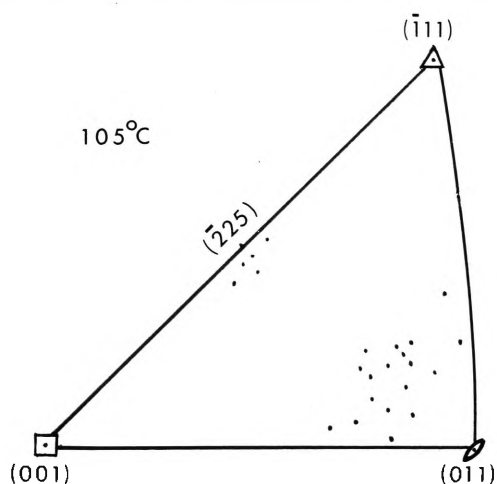
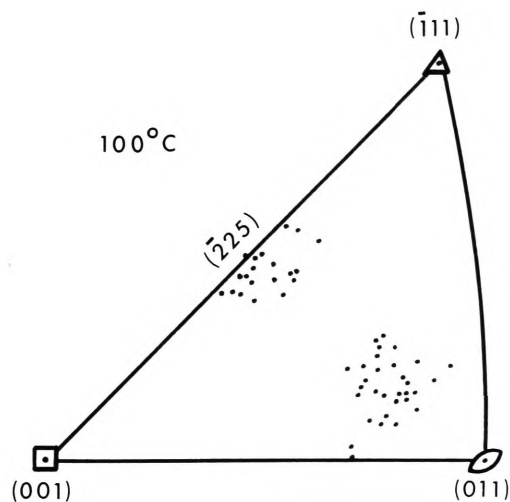
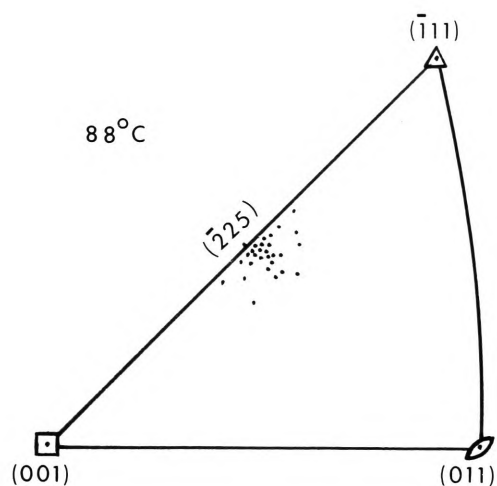


FIG.44 Stereographic projections showing measured habit planes from plates of transformation products, formed isothermally at 88°C , 100°C , 105°C and 120°C .

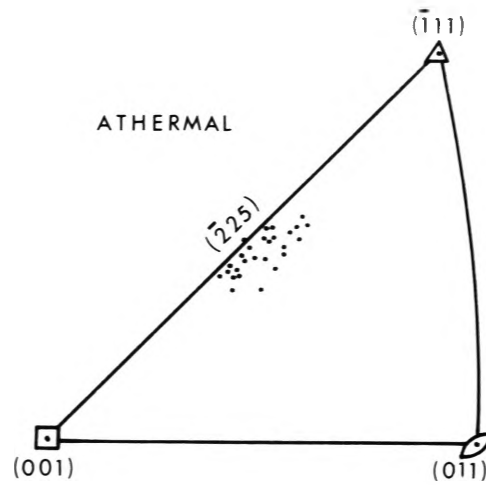


FIG.45 Stereographic projection showing habit planes determined from athermal martensite plates formed by quenching to 55°C and tempering at 300°C for 2 minutes.

11.7 The Habit Planes

The measured habit planes of plates of the isothermal transformation products, formed at 88°C, 100°C, 105°C and 120°C, are shown in Fig. 44 and the habit planes of athermal martensite plates are shown in Fig. 45.

The habit planes of the type 1 plates were independent of transformation temperature (in the temperature range studied) and, for the standard stereographic triangle used, were located within 10° of $(\bar{2}25)_\gamma$.

The habit planes of the type 2 plates, although subject to considerable scatter, were located within approximately 15° of $(011)_\gamma$ and appeared to be independent of transformation temperature.

The habit planes, near $(\bar{2}25)_\gamma$, of the athermal martensite plates agree with previous measurements. (13,19)

Errors associated with the technique used to measure the habit planes have been analysed by Kennon, (116) who attributes scatter in the habit plane results to the following:

- 1) Error associated with the measurement of the angles $\alpha_1, \alpha_2, \beta_1, \beta_2$, (Fig. 16), subtended by the twin vestiges, and the variation of the austenite orientation within the austenite grain.

- 2) Error associated with the measurement of the angles γ_1 , γ_2 (Fig. 16), subtended by the plates of transformation product. This error is significant for irregularly shaped plates.
- 3) The mis-matching of plates in the surfaces A and B.
- 4) Errors in the stereographic net used to analyse the measurements.

Error associated with the stereographic net used is approximately 1° and the use of a photographic technique to match plates in the two surfaces greatly reduces the error arising from 3). However, significant error would arise from the difficulty in establishing the twin vestiges and since the plates of transformation products were very small, and often irregular in shape, large errors could exist in measurements of the angles γ_1 and γ_2 .

The accuracy of the method used was estimated to be $\pm 3^\circ$ for plates of type 1 product and $\pm 5^\circ$ for plates of type 2 product, these being the average deviations of the angular measurements of the plates.

12. DISCUSSION

In sections 6 and 7 it was established that the possible products of isothermal transformation of austenite, at temperatures near M_s , are bainite and martensite. The results described in section 11 showed that two different products are formed isothermally at temperatures both above and below the M_s temperature. It will now be demonstrated that the measured habit planes unequivocally identify the two transformation products and that the observed morphological features of the products are consistent with this identification. The identification then enables the detailed form of the TTT diagram, in the range of temperatures examined, to be specified.

12.1 The Habit Planes

The measured habit planes of plates of the type 1 product were near $(\bar{2}25)_\gamma$ (Fig. 44). The plates of athermal martensite also had habit planes near $(\bar{2}25)_\gamma$ (Fig. 45), consistent with the reported habit planes in steels of similar chemical composition to that used in the present investigation. For the estimated experimental error of $\pm 3^\circ$ the measured habit planes of the type 1 product are clearly compatible with the habit planes of athermal martensite and cannot be confused with the habit planes of any other transformation product. Consequently

the type 1 transformation product can be described as being crystallographically equivalent to athermal martensite and will hereafter be referred to as isothermal martensite.

The present investigation is the first in which the habit planes of isothermal martensite plates have been measured.

The habit planes of the plates of type 2 transformation product, although subject to considerable scatter, were located within 15° of $(011)\gamma$ (Fig. 44), and therefore compatible with the habit planes of lower bainite, formed at similar transformation temperatures in high carbon steels. Hence type 2 transformation product can be described as being crystallographically similar to lower bainite and will hereafter be referred to as lower bainite.

The habit plane measurements have clearly shown that both transformation products are formed at temperatures above M_s . The habit planes of bainite plates, formed below M_s , were not measured. However, since the habit planes of lower bainite appear to be independent of transformation temperature, there is no reason to believe that the habit planes of the plates of type 2 product, formed below M_s , do not also lie within 15° of $(011)\gamma$, and therefore this product would also be lower bainite. The



FIG.46 Isothermal martensite formed in an Fe-Ni-Mn alloy during transformation at -196°C for 100 minutes. X100.

(Shih, Averbach and Cohen.⁽⁸³⁾)

formation of lower bainite and isothermal martensite, at temperatures both above and below the M_s temperature, is compatible with the TTT curves established for the range of temperatures examined.

12.2 Morphology

The plate morphology of the isothermal transformation products is perfectly compatible with the plate morphology of martensite and lower bainite.

The distribution of isothermal martensite plates was consistent with the distribution of plates observed by Shih, Averbach and Cohen⁽⁸³⁾ in an Fe-Ni-Mn alloy (Fig. 46). However, the size of the plates formed in the 1.44%C steel (Fig. 19), were smaller than those formed in the Fe-Ni-Mn alloy. Plates of athermal martensite in plain carbon steels are also generally smaller than athermal martensite plates in alloy steels, implying that the factors which limit the growth of athermal martensite plates also limit the growth of isothermal martensite plates.

Electron microscopical studies showed that, except for the absence of internal twinning, the isothermal martensite plates were morphologically similar to the athermal martensite plates. The isothermal martensite plates, containing dislocations aligned in perpendicular

directions (Fig. 31), were structurally similar to the reported (173) morphology of athermal martensite plates in Fe-Mn-Cu alloys.

The morphology suggests that isothermal martensite plates, containing the dislocation arrays, and the plates which appeared to contain few internal inhomogeneities, probably formed just prior to completion of isothermal transformation. The short time at the transformation temperature would preclude the precipitation of epsilon carbide. On the other hand, plates of isothermal martensite, containing a dense precipitate dispersion of epsilon carbide (Fig. 33), probably formed during the initial stages of isothermal transformation and hence would have been tempered for sufficient time to facilitate precipitation of the carbide.

The observed morphology of the lower bainite plates was compatible with the morphology of ferrite plates containing carbide platelets oriented at 55° to the ferrite needle axis, described in section 4.1. However, the appearance of a mid-rib in some plates (Fig. 30), has not been reported previously and may result from carbide nucleation at the ferrite-austenite interface and subsequent growth towards the central regions of the ferrite plates.

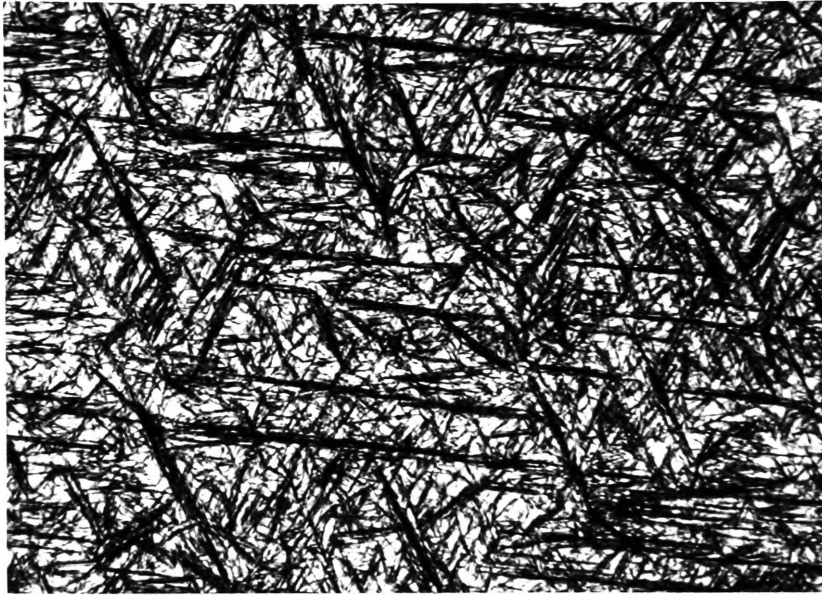


FIG.47 Photomicrograph showing lower bainite formed by isothermal transformation at 120°C for 72 hours. X100.

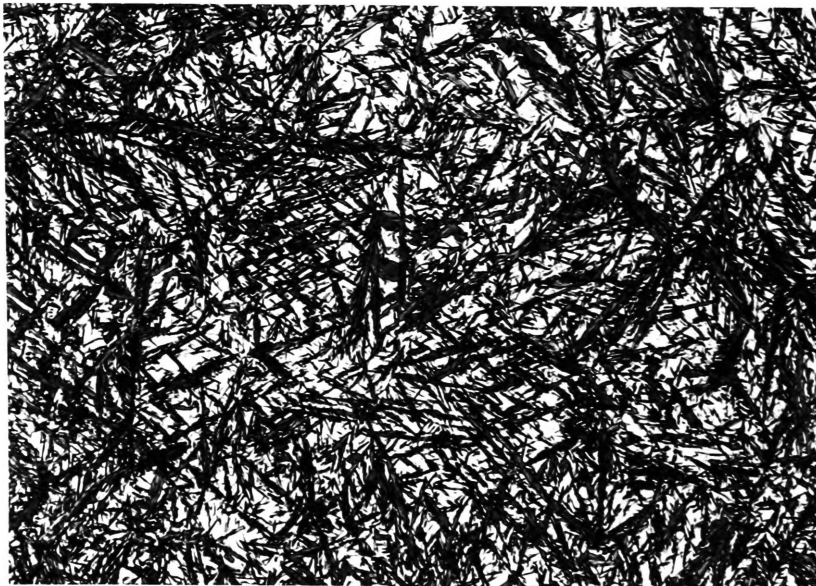


FIG.48 Photomicrograph showing athermal martensite formed by quenching to room temperature and tempering at 300°C for 2 minutes. X100.

The observed carbide distributions in plates of tempered athermal martensite, and the structural inhomogeneities in the untempered martensite plates, were consistent with those described in section 3.1. The precipitation of cementite plates on and normal to the twin planes, in the tempered martensite plates, supports the suggestion of Kelly and Nutting⁽¹⁹⁾ that the martensite twin interfaces act as sites for the nucleation of cementite.

The morphological studies clearly demonstrated the ease with which the identities of the products of isothermal transformation of austenite, at temperatures near M_s , can be confused. Optical microscopy was not capable of distinguishing lower bainite from tempered martensite as the appearance of both constituents is similar in polished and etched metallographic sections. (Figs. 47 and 48). The appearances of athermal and isothermal martensite plates is also similar in polished and etched sections but when both products are present in the one specimen, the smaller size of the isothermal martensite plates distinguishes them from the larger athermal martensite plates.

Although the detection of internal inhomogeneities in the plates of transformation products was dependent on

the orientation of the plates, with respect to the electron beam, electron microscopical studies provided sufficient evidence to suggest that the isothermal martensite and lightly tempered athermal martensite plates were morphologically similar, but different from the plates of lower bainite. The carbide platelets, precipitated in the athermal martensite plates during tempering at 300°C for 2 minutes, were coarser than the carbide platelets in the plates of lower bainite and were not oriented at 55° to the ferrite plate axis.

Electron diffraction studies identified the carbides, in the plates of isothermal martensite and lightly tempered athermal martensite, as epsilon carbide, whereas the carbides of lower bainite and athermal martensite plates tempered at 300°C were shown to be cementite.

These conclusions, regarding the morphological inhomogeneities, were facilitated by prior knowledge of the identities of the products. Electron microscopical studies alone were not capable of unequivocally distinguishing the products.

12.3 Surface Relief

The surface relief effects, which accompanied the formation of plates of both isothermal martensite and lower

bainite, were similar to the relief effects which accompany the formation of athermal martensite and indicate, that for both transformations, the initial and final lattices are at least semi-coherent during growth. Relief effects of this kind imply that both transformations are accompanied by a shape change which corresponds to a homogeneous strain. Consequently, both transformations can be termed martensitic and the crystallographic properties should be related by the crystallographic theory of martensitic transformations. (See sections 3.32 and 4.32).

The athermal martensite and lower bainite transformations in plain carbon steels have been shown to be at least approximately consistent with the theory but, as yet, no crystallographic analysis of the isothermal martensite transformation has been made. There is no reason to believe that this transformation would not also be consistent with the theory, since it has been shown that the isothermal plates form on habit planes near $(\bar{2}25)_\gamma$, similar to athermal martensite plates. However, the complementary strain for this transformation may not have as a component, a shear on the martensite twinning elements, since twins were not observed in the plates.

The dislocation arrays are compatible with a slip shear on some other elements. An analysis of the crystallography, similar to that made for lower bainite,⁽⁷¹⁾ may be necessary in the absence of information concerning the possible slip shear systems. However, before such an analysis is possible, determination of the orientation relationship, between the lattices of the isothermal martensite and austenite, is necessary.

The surface relief effects, accompanying the lower bainite transformation, imply that lower bainite forms by a mechanism of the kind proposed by Cottrell and Ko.⁽¹¹⁴⁾ (See section 4.62).

12.4 Transformation Kinetics

The results of the kinetic study showed that isothermal transformation of austenite occurs both above and below the M_s temperature and that two products are formed. Using the criterion of 1% transformation product, the transformation start curve was determined for both products.

For isothermal martensite, the transformation curve was similar to a normal C-curve at temperatures below 110°C , suggesting that the transformation is thermally activated. (Fig. 21). At higher transformation temperatures the TTT curve was not satisfactorily established

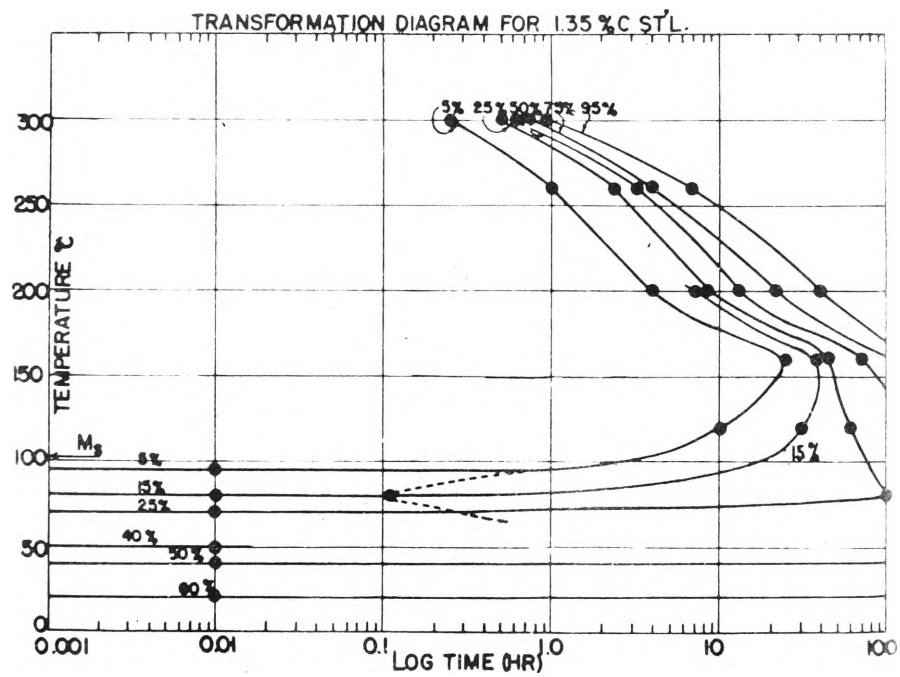


FIG.49 Isothermal transformation diagram for a 1.35%C steel.

(Howard and Cohen.⁽¹⁶⁵⁾)

although the results obtained suggested a change in slope of the curve at about 112°C . Since the change in slope occurred at the point of intersection of the isothermal martensite and lower bainite transformation curves, it is possible that the apparent shorter incubation periods for the isothermal martensite transformation resulted from the influence of lower bainite in aiding the nucleation of isothermal martensite. However, it is more probable that, for austenite containing 1.44% C, the TTT curve for isothermal martensite is a true C-curve and the atypical behaviour resulted from depletion of carbon in the austenite by decarburisation.

Howard and Cohen⁽¹⁶⁵⁾ isothermally transformed a 1.35% C steel, at temperatures between 80°C and 300°C , and reported a change in the slope of the TTT curve at temperatures just above M_s . (Fig. 49). The change in kinetics was attributed to the formation of an acicular product which was not identified. The observed kinetics can be interpreted in terms of the present results if the isothermal martensite and lower bainite transformation curves are combined to give a single transformation curve. In view of this it is probable that the "new" product, observed by Howard and Cohen, was isothermal martensite.

The incubation period for the bainite transformation increased with decreasing temperature over the temperature range investigated. The change in slope of the bainite transformation curve, at the M_s temperature, indicates that lower bainite may be nucleated by martensite plates, formed during quenching to the transformation temperature. However, since no bainite plates were observed to be associated with martensite plates, it is probable that nucleation of lower bainite is aided only by deformation of the austenite during formation of the athermal martensite plates, as suggested by Howard and Cohen⁽¹⁶⁵⁾. This is compatible with the observations of Cottrell,⁽¹⁴⁵⁾ Birks,⁽¹⁴⁶⁾ and Jepson and Thompson⁽¹⁴⁷⁾ that tensile stresses aid the nucleation of lower bainite. (See section 4.55).

The bainite transformation was not influenced by the presence of isothermal martensite plates, between the M_s temperature and 110°C . It is probable that the stresses produced in the austenite by the formation of the isothermal martensite plates were not sufficient to significantly influence the nucleation of the lower bainite.

In sections 6 and 7 the uncertainty in the shape of the isothermal transformation diagram, at temperatures

near M_s , was demonstrated. The confusion arises because of the uncertainty in the identity of the products of isothermal transformation, uncertainty as to whether or not bainite forms below M_s , and the possibility of simultaneous formation of lower bainite and isothermal martensite. TTT diagrams usually show the bainite transformation curves terminating abruptly at M_s . However, Christian⁽⁴⁴⁾ suggested that isothermal formation of bainite may continue below the M_s temperature after athermal martensite has ceased to form and it is considered (4,167) that shorter incubation periods, below M_s , would result from the influence of athermal martensite in aiding the nucleation of lower bainite.

The results of the present kinetic study have shown that the bainite transformation curve does project below the M_s temperature but the incubation period is not shortened considerably by the presence of athermal martensite. The isothermal transformation of austenite to martensite has been shown to occur both above and below the M_s temperature and to adequately describe the transformation behaviour of austenite, at temperatures near M_s , it is proposed that transformation curves for lower bainite, isothermal martensite and athermal martensite are necessary.

It is also evident from the kinetic studies that, for medium and high carbon steels, the results of measured changes in physical properties, accompanying the isothermal transformation of austenite at temperatures near M_s , must be interpreted in terms of the formation of two products, isothermal martensite and lower bainite, and not a single product as was previously thought.

13. CONCLUSIONS

The results of metallographic, crystallographic and kinetic studies of the isothermal transformation of austenite, at temperatures near M_s , can be summarised as follows:-

- 1) At temperatures just above and just below the M_s temperature, austenite transforms isothermally to two morphologically and crystallographically different products.
- 2) The morphology of the products appears to be independent of the temperature of formation.
- 3) The results of surface relief studies imply that both transformations are accompanied by a shape change, which can be described at least approximately as a homogeneous strain, and hence the transformations can be termed martensitic.
- 4) Habit plane measurements showed that one of the transformation products is crystallographically similar to martensite, and that the other is crystallographically similar to lower bainite.
- 5) Transmission electron microscopy showed that the morphology of the products was consistent with the identifications as isothermal martensite and lower bainite.

- 6) Kinetic studies of the transformations indicated that, to properly describe the transformation of austenite at temperatures near M_s , at least in medium carbon steels, three transformation curves are required:
- i) isothermal martensite
 - ii) lower bainite and
 - iii) athermal martensite. Thus at temperatures near M_s all previously determined TTT curves are incomplete.

From these results it is concluded that austenite transforms isothermally to martensite and lower bainite at temperatures both just above and just below M_s . It is further concluded that to satisfactorily describe the isothermal transformation of austenite, over the range of temperatures near M_s , transformation curves for the isothermal martensite, athermal martensite and lower bainite transformations are necessary.

14. APPENDICES

A. Twin Vestiges

Habit plane measurements necessitate determination of the orientation of the lattice of the initial austenite relative to the external geometry of the specimen. The orientation of the austenite was determined by the method of twin vestiges reported by Greninger and Troiano⁽¹³⁾.

Almost all austenite grains contain at least one twin band in which the differing lattice orientations produce differing spatial arrays of the transformation products. Suitable etching methods distinguish between these arrays and therefore define the traces. The traces were best defined in grains containing about 75% of retained austenite and martensite and suitable etching achieved by immersion for 15 seconds in 3% nital.

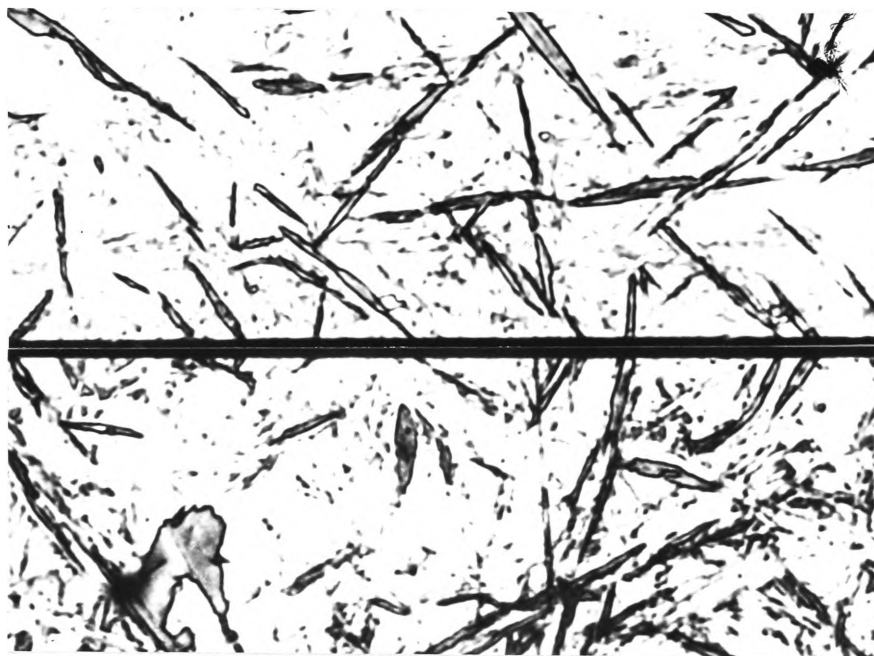


FIG.50 Composite photomicrograph showing plates of type 1 transformation product in two surfaces. X1000.

Etchant 3% nital.

B. Metallographic Preparation of Specimens for Habit Plane Analyses

The metallographic preparation of specimens for habit plane analyses required that a sharp edge be maintained between the two polished surfaces. The use of napped cloths for final polishing was precluded due to the edge rounding which resulted.

In the method adopted, the specimens were held in a grinding jig and initially ground on silicon carbide papers and a napless cloth impregnated with 4-8 μ diamond powder. Final polishing was effected using 1 μ diamond abrasives on a napless cloth with kerosine lubricant. The sharpness was preserved by "trailing" the edge during all the preparation steps and the quality of the edge obtained is shown in Fig. 50.

The method did not produce a high quality metallographic finish. However, at high magnifications the sharpness of the edge is not impaired and the plates of transformation product are exposed without distortion in both surfaces.

C. Preparation of Transmission Specimens for Electron Microscopy

Thin foils for electron microscopical studies were prepared from 0.016 cm. thick discs, sawn from a 0.23 cm diameter cylinder of the 1.44%C steel, then sealed in evacuated silica capsules and heat treated as required.

The discs were ground to a thickness of 0.002 cm and then jet profiled in a 10% perchloric acid - 90% glacial acetic acid electrolyte with a potential of 100 volts D.C. The profiled discs, held with stainless steel tweezers, were then electro-polished to perforation at 37 volts D.C. using an electrolyte of the following composition:

25 gms chromium trioxide

133 mls glacial acetic acid

7 mls water.

The foils were washed in alcohol prior to examination.

D. Identification of Carbide Precipitates from Measured Interplanar Spacings

1) Carbides in Isothermal Martensite

<u>Measured "d" Spacing (Å°)</u>	<u>"d" Spacing for ε-carbide (Å°)⁽¹⁷²⁾</u>	<u>h k l</u>
2.35	2.38	100
2.08	2.08	101
1.59	1.60	102
1.23	1.24	103
1.15	1.16	112, 201

2) Carbides in Lower Bainite

<u>Measured "d" Spacing (Å°)</u>	<u>"d" Spacing for Cementite (Å°)⁽¹⁷²⁾</u>	<u>h k l</u>
2.79	2.81	012
2.27	2.26	200
2.24	2.25	003
1.98	1.98	211
1.85	1.85	122

3) Carbides in Athermal Martensite, Tempered at 100°C for 5 Hours

<u>Measured "d" Spacing (Å°)</u>	<u>"d" Spacing for ε-carbide (Å°)⁽¹⁷²⁾</u>	<u>h k l</u>
2.37	2.38	100
2.07	2.08	101
1.60	1.60	102
1.24	1.24	103
1.17	1.16	112, 201

4) Carbides in Athermal Martensite, Tempered at 300°C for 2 Minutes

<u>Measured "d" Spacing (Å°)</u>	<u>"d" Spacing for Cementite (Å°) (172)</u>	<u>h k l</u>
4.47	4.52	100
4.09	4.06	011
3.73	3.76	101
2.68	2.70	102
2.56	2.54	020
2.41	2.39	112
2.26	2.25	003
2.07	2.06	013
2.03	2.03	022
1.99	1.98	211
1.88	1.88	202
1.54	1.55	131

15. REFERENCES

1. COHEN M., Trans. A.S.M., 1940, 28, 537.
2. SAUNDERS E.R. and KAHLES J.T., Trans. A.S.M., 1942, 30, 1139.
3. FLINN R.A., COOK E. and FELLOWS J.A., Trans. A.S.M., 1943, 31, 41.
4. GORDEN P., COHEN M. and ROSE R.S., Trans. A.S.M., 1943, 31, 161.
5. DAVENPORT E.S. and BAIN E.C., Trans. A.I.M.E., 1930, 90, 117.
6. HULTGREN A., Trans. A.S.M., 1947, 39, 915.
7. MEHL R., J.I.S.I., 1948, 159, 113.
8. MEHL R., and HAGEL W.C., in "Progress in Metal Physics", 1956, 6, 74.
9. WHITELEY J., J.I.S.I., 1925, 3, 315.
10. ROBERTSON J., Iron and Steel Inst. Carnegie Schol. Mem., 1931, 20, 1.
11. LUCAS F., Trans. Amer. Soc. Steel Treat., 1924, 6, 1.
12. HANEMANN H., and SCHRADER A., Trans. Amer. Soc. Steel. Treat., 1926, 9, 169.
13. GRENINGER A.B., and TROIANO A.R., Trans. A.I.M.E., 1940, 140, 307.
14. YEO R.B.G., Trans. A.S.M., 1964, 57, 48.
15. SPEICH G.R., and SWAN P.R., J.I.S.I., 1965, 203, 480.

16. OWEN W.S., and WILSON E.A., Iron and Steel Inst. Spec. Rept. No.93, 1965, 53.
17. HABRAKEN L., and DeBROUWER J.L., in "De Ferri Metallographia", Lond., W.B. SAUNDERS, 1966, 172,181.
18. COHEN M., Trans. A.I.M.E., 1962, 224, 638.
19. KELLY P.M., and NUTTING J., J.I.S.I., 1961, 197, 199.
20. BARTON C.J., Acta Met., 1969, 17, 1085.
21. GRENINGER A.B., and TROIANO A.R., Trans A.I.M.E., 1949, 185, 590.
22. BREEDIS J.F., and WAYMAN C.M., Trans. A.I.M.E., 1962, 224, 1128.
23. WARLIMONT H., Proc. 5th Intl. Conf. on Electron Microscopy, Acedemic Press, 1962, 1, HH6.
24. SHIMIZU K., J. PHYS. Soc. Japan, 1962, 17, 508.
25. WAYMAN C.M., in "Intro to the Cryst. of Martensitic Transformations", N.Y. MacMILLAN, 1964, 166.
26. ROBERTS C.S., AVERBACH B.L., and COHEN M., Trans. A.S.M., 1953, 45, 576.
27. LEMENT B.S., AVERBACH B.L., and COHEN M., Trans. A.S.M., 1955, 47, 291.
28. LEMENT B.S., AVERBACH B.L. and COHEN M., Trans. A.S.M., 1954, 46, 851.
29. KERLINS V., and ALTSTETTER C., Trans. A.I.M.E., 1963, 227, 94.
30. JACK K.H., J.I.S.I., 1951, 169, 26.

31. JACKSON M.R. and KRAUSS G., A.S.T.M., 1965, STP396, 6, 62.
32. OHMAN E., J.I.S.I., 1931, 123, 445.
33. HAGG G., J.I.S.I., 1934, 130, 439.
34. MODIN S., Metal Treatment, 1960, 133, 177.
35. WELLS M.G.H., Acta Met., 1964, 12, 389.
36. KING H.W., and GLOVER S.G., J.I.S.I., 1959, 193, 123.
37. McGRATH J., and RAWLINGS R., Acta. Met., 1964, 12, 958.
38. PITSCH W., and SCHRADER A., Arch. Eisen., 1958, 29, 485.
39. GRENINGER A.B. and TROIANO A.R., Metal Progress, 1946, 50, 303.
40. FÖRSTER F., and SCHEIL E., Z. Metallkunde, 1940, 32, 165.
41. BUNSHAH R.F., and MEHL R.F., Trans. A.I.M.E., 1953, 197, 1251.
42. KULIN S.A., and COHEN M., Trans. A.I.M.E., 1950, 188, 1139.
43. MACHLIN E.S., and COHEN M., Trans. A.I.M.E., 1951, 191, 744.
44. CHRISTIAN J.W., in "The Theory of Transf. in Metals and Alloys". Lond., Pergamon Press, 1965, 675, 822, 856.
45. COHEN M., MACHLIN E.S., and PARANJPE V.G., in "Thermodynamics in Phys. Met."., Ohio, A.S.M., 1950, 201.
46. KOISTINEN D.P., and MARBURGER R.E., Acta Met., 1959, 7, 59.

47. FINK W., and CAMPBELL E., Trans. Amer. Soc. Steel Treat., 1926, 9, 717.
48. LIPSON H., and PARKER A.M.B., J.I.S.I., 1944, 149, 123.
49. KURDJUMOV G.V., J.I.S.I., 1960, 195, 26.
50. SMITH G.V., and MEHL R.F., Trans. A.I.M.E., 1942, 150, 211.
51. DORNEN P., and HOFFMAN W., Arch. Eisen., 1959, 30, 627.
52. MEHL R.F., and VAN WINKLE D.M., Rev. Met., 1953, 50, 465.
53. McDOUGALL P.G., and BOWLES J.S., Acta Met., 1964, 12, 779.
54. BOWLES J.S., and BARRETT C.S., in "Progress in Metal Physics", Lond., Pergamon Press, 1952, 3, 1.
55. KURDJUMOV G., and SACHS G., Z. Physik., 1930, 64, 325.
56. NISHIYAMA Z., SCI. Rep. Tohoku Imp. Uni., 1934, 23, 637.
57. CHRISTIAN J.W., and BILBY B.A., Inst. of Metals Monograph and Report Series, No.18, 1956, 129.
58. HIBBARD W.R., and YEN M.K., Trans. A.I.M.E., 1948, 175, 126.
59. BARRETT C.S., and STEADMAN F.W., Trans. A.I.M.E., 1942, 147, 57.
60. BOWLES J.S., and MacKENZIE J.K., Acta Met., 1954, 2, 129.
61. MacKENZIE J.K., and BOWLES J.S., Acta Met., 1954, 2, 138.

62. WECHSLER M.S., LIEBERMAN D.S., and READ T.A, Trans. A.I.M.E., 1953, 197, 1503.
63. BOWLES J.S., AND MacKENZIE J.K., Acta Met., 1962, 10, 625.
64. BOWLES J.S., and MORTON A.J., Acta Met., 1964, 12, 629.
65. NISHIYAMA Z., and SHIMIZU K., Mem. Inst. Sci. and Ind. Res., 1962, 19, 213.
66. MORTON A.J., and WAYMAN C.M., Acta Met., 1966, 14, 1567.
67. BOWLES J.S., and MacKENZIE J.K., Acta Met., 1957, 5, 137.
68. LIEBERMAN D.S., WECHSLER M.S., and READ T.A., J. Appl. Phys., 1955, 26, 473.
69. GAUNT P., and CHRISTIAN J.W., Acta Met., 1959, 7, 534.
70. BOWLES J.S., and McG-TEGART W.J., Acta Met., 1955, 3, 590.
71. BOWLES J.S., and KENNON N.F., J. Aust. Inst. Metals, 1960, 5, 106.
72. KENNON N.F., and BOWLES J.S., Acta Met., 1969, 17, 373.
73. EFSIC E.J., and WAYMAN C.M., Trans. A.I.M.E., 1967, 239, 873.
74. KURDJUMOV G.V., and MAXIMOVA O.P., U.S.S.R. Academy of Sciences Report, 1948, 61, 53.
75. FISHER J.C., HOLLOMAN J.M., and TURNBULL D., Trans. A.I.M.E., 1949, 185, 691.

76. KAUFMAN L., and COHEN M., in "Progress in Metal Physics"., Lond., Pergamon Press, 1958, 7, 165.
77. GRENINGER A.B., and MOORADIAN V.C., Trans. A.I.M.E., 1938, 128, 337.
78. CECHE R.E., and TURNBULL D., Trans. A.I.M.E., 1951, 189, 47.
79. KULIN S.A., and SPEICH G.R., Trans. A.I.M.E., 1952, 194, 258.
80. CHRISTIAN J.W., in "Physical Metallurgy" Cahn R.W., Ed., North-Holland, Amsterdam, 1965, 509.
81. KNAPP H., and DEHLINGER U., Acta Met., 1956, 4, 289.
82. PATI S.R., and COHEN M., Acta Met., 1969, 17, 189.
83. SHIH C.H., AVERBACH B.L., and COHEN M., Trans. A.I.M.E., 1955, 203, 183.
84. RICHMAN M.H., COHEN M., and WILSDORF H.G.F., Acta Met., 1959, 7, 819.
85. GRAGGERO J., and HULL D., Acta Met., 1962, 10, 995.
86. NISHIYAMA Z., and SHIMIZU K., Acta Met., 1961, 9, 980.
87. BORLAND D.W., and WALKER D.G., J. Aust., Inst. Metals, 1960, 5, 75.
88. KURDJUMOV G.V., ZHUR. Tekhn. Fiz., 1948, 18, 999.
89. ISAICHEV I.V., Trans. A.I.M.E., 1938, 128, 361.
90. COTTRELL A.H., and BILBY B.A., Phil. Mag., 1951, 42, 573.

91. MAXIMOVA O.P., and KURDJUMOV G.V., Dokl. Akad. Nauk. S.S.S.R., 1948, 61, 83.
92. CECIL R.E., and HOLLOMAN J.H., Trans. A.I.M.E., 1953, 197, 685.
93. MACHLIN E.S., and COHEN M., Trans. A.I.M.E., 1952, 194, 489.
94. DAS GUPTA S.C., and LEMENT B.S., Trans. A.I.M.E., 1951, 191, 727.
95. OWEN W.S., and GILBERT A., J.I.S.I., 1960, 196, 142.
96. PHILIBERT J., and CRUSSARD C., J.I.S.I., 1955, 180, 39.
97. RAGHAVEN V., Acta Met., 1969, 17, 1299.
98. RAGHAVEN V., and ENTWISLE A.R., Iron and Steel Inst. Spec. Rept. No.93, 1965, 30.
99. SCHMIDTMAN E., VOGT K., and SCHENCK H., Arch. Eisen, 1967, 38, 639.
100. KAUFMAN L., and COHEN M., Trans. A.I.M.E., 1956, 206, 1393.
101. CLARK C.A., J.I.S.I., 1959, 193, 11.
102. KRISEMENT O., HOUDREMONT E., and WEVER F., Rev. Met., 1954, 51, 401.
103. HILLERT M., Acta Met., 1958, 6, 122.
104. Report by Sub-Committee, Proc. A.S.T.M., 1952, 52, 543.
105. SHIMIZU K., KO T., and NISHIYAMA Z., Trans. J.I.M. 1964, 5, 225.

106. MATAS S.J., and HEHEMANN R.F., Trans. A.I.M.E.,
1961, 221, 179.
107. Report by Sub-Committee Proc. A.S.T.M., 1950, 50, 444.
108. SHACKLETON D.N. and KELLY P.M., Iron and Steel Inst.
Spec. Rept. No.93, 1965, 126.
109. IRVINE K.J., and PICKERING F.B., Iron and Steel Inst.
Spec. Rept. No.93, 1965, 110.
110. PICKERING F.B., in "Trans. and Hardenability in Steels",
Chicago, Climax Molyb. Co., 1967, 109.
111. SRINIVASAN G.R., and WAYMAN C.M., Acta Met., 1968,
16, 609.
112. MEHL R.F., and DUBE A., in "Phase Trans. in Solids",
N.Y., J. Wiley & Sons, 1951, 545.
113. IRVINE K.J., and PICKERING F.B., J.I.S.I., 1958,
188, 101.
114. Ko T., and COTTRELL S.A., J.I.S.I., 1952, 172, 307.
115. Ko T., J.I.S.I., 1953, 175, 16.
116. KENNON N.F., MSc. Thesis, Uni. N.S.W., 1960.
117. ZENER C., Trans. A.I.M.E., 1946, 167, 550.
118. FISHER J.C., in "Thermodynamics in Phys. Met.," A.S.M.
Cleveland Ohio, 1950, 201.
119. GOODENOW R.H., MATAS S.J. and HEHEMANN R.F., Trans.
A.I.M.E. 1963, 227, 651.
120. VASUDEVAN P., GRAHAM L.W., and AXON H.J., J.I.S.I.,
1958, 190, 386.
121. RADCLIFFE S.V., and ROLLASON E.C., J.I.S.I., 1959,
191, 56.

122. HILLERT M., Jern. Ann., 1957, 141, 757.
123. SPEICH G.R., and COHEN M., Trans. A.I.M.E., 1960, 218, 1050.
124. TSUYA K., and MITSUHASHI T., J. Mech. Lab. of Japan, 1955, 1, 42.
125. KAUFMAN L., RADCLIFFE S.V., and COHEN M., in "The Decomp. of Austenite by Diff. Processes", Interscience 1962, 313.
126. HEHEMANN R.F., and TROIANO A.R., Metal Progress, 1956, 70, 97.
127. WHITE J.S., and OWEN W.S., J.I.S.I., 1960, 195, 79.
128. KRISEMENT O., and WEVER F., Arch. Eisen, 1954, 25, 489.
129. PITSCH W., Acta Met., 1962, 10, 897.
130. PITSCH W., Arch. Eisen, 1963, 34, 381.
131. SPEICH G.R., in "The Decomp. of Austenite by Diff. Processes", Interscience, 1962, 361.
132. GRAHAM T.W., and AXON H.J., J.I.S.I., 1959, 191, 361.
133. BARFORD J., and OWEN W.S., J.I.S.I., 1961, 197, 146.
134. COTTRELL S.A., and Ko T., J.I.S.I., 1953, 173, 224.
135. HANSEN M., in "Constitution of Binary Alloys" N.Y., McGraw-Hill, 1958, 705.
136. GUELICH E., Arch. Eisen, 1951, 20, 245.
137. LYMAN T., and TROIANO A.R., Trans. A.S.M. 1946, 37, 402.

138. SHEEHAN J.P., JULIEN C.A., and TROIANO A.R., Trans. A.I.M.E., 1949, 41, 1165.
139. LYMAN T., and TROIANO A.R., Trans. A.I.M.E., 1945, 162, 196.
140. SCOTT R.A., ARMSTRONG W.M., and FORWARD F.A., Trans. A.I.M.E., 1949, 41, 1145.
141. BISCHOF W., Arch. Eisen, 1949, 20, 13.
142. BAIN E.C., and PAXTON H.W., in "Alloying Elements in Steel", Ohio, A.S.M., 1961, 152.
143. JAFFE L.D., Trans. A.I.M.E., 1948, 176, 363.
144. JOLIVET H., and PORTEVIN A., Compt. Rend. 1939, 209, 376.
145. COTTRELL A.H., J.I.S.I., 1945, 151, 93.
146. BIRKS L.S., J. Metals, 1956, Aug., 989.
147. THOMPSON F.C., and JEPSON M.D., J.I.S.I., 1949, 162, 49.
148. VILELLA J.R., GUELICH G.E., and BAIN E.C., J.I.S.I., 1936, 24, 225.
149. WEVER F., and JELLINGHAUS W., J.I.S.I., 1932, 14, 85.
150. KLIER E.P., and LYMAN T., Trans. A.I.M.E. 1944, 158, 394.
151. WIESTER H.J., Arch. Eisen, 1944, 18, 97.
152. ZENER C., Metals Tech., 1946, 13, T.P. 1925.
153. HEHEMANN R.F., and TROIANO A.R., Trans. A.I.M.E., 1954, 200, 1272.

154. KRISEMENT O., and WEVER F., Inst. of Metals Monograph and Report Series, No.18, 1955, 258.
155. PRIESTNER R., and GLOVER S.G., Iron and Steel Inst. Spec. Rept., No.93, 1965, 38.
156. MORGAN E.R., and Ko T., Acta Met., 1953, 1, 36.
157. HARRIS W.J. and COHEN M., Trans. A.I.M.E., 1949, 180, 447.
158. KLIER E.P., and TROIANO A.R., Trans. A.I.M.E., 1945, 162, 175.
159. JAFFE L.D., HOLLOMAN J.H., and NORTON M.R., Trans. A.I.M.E., 1946, 167, 419.
160. MOORE P.T., J.I.S.I., 1954, 177, 305.
161. OWEN W.S., and WHITE J.S., J.I.S.I., 1961, 197, 241.
162. GLOVER S.G., and SMITH T.B., Inst. of Metals Monograph and Report Series No.18, 1956, 265.
163. CECH R.E., and HOLLOMAN J.H., Trans. A.I.M.E., 1954, 200, 682.
164. SMITH M.F., SPEICH G.R., and COHEN M., Trans. A.I.M.E., 1959, 215, 528.
165. HOWARD R.T., and COHEN M., Trans. A.I.M.E., 1949, 176, 384.
166. SCHAABER O., Trans. A.I.M.E., 1955, 203, 559.
167. STEVEN W., and HAYNES A.G., J.I.S.I., 1956, 183, 349.
168. ELMENDORF H., Trans. A.S.M., 1944, 33, 236.
169. PAYSON P., and SAVAGE C.H., Trans. A.I.M.E., 1944, 33, 261.

- 170. CARAPELLA L.A., Metal Progress, 1944, 46, 108.
- 171. NEHRENBURG A.E., Trans. A.I.M.E., 1946, 167, 494.
- 172. Powder Diffraction File, 1966, A.S.T.M. Phila.
- 173. COX A.R., J.I.S.I., 1969, 207, 358.